

18/000/198/2016

M. Phil 92.

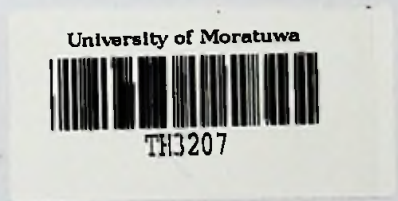
# STABILITY AND SECURITY ANALYSIS OF INDIA-SRI LANKA HVDC INTERCONNECTION

Ampegama Gamage Chenuka Uppalani Perera

(118076J)

LIBRARY  
UNIVERSITY OF MORATUWA SRI LANKA  
MORATUWA

Thesis submitted in partial fulfillment of the requirements for the degree  
Master of Philosophy



Department of Electrical Engineering

University of Moratuwa  
Sri Lanka

621.3<sup>16</sup>"  
-----  
621.3 (043)



TH 3207  
+ CD-ROM

TH 3207

## Declaration

I declare that this is my own work and this thesis does not incorporate without acknowledgement any material previously submitted for a Degree or Diploma in any other University or institute of higher learning and to the best of my knowledge and belief it does not contain any material previously published or written by another person except where the acknowledgement is made in the text.

Also, I hereby grant to University of Moratuwa the non-exclusive right to reproduce and distribute my thesis, in whole or in part in print, electronic or other medium. I retain the right to use this content in whole or part in future works (such as articles or books).

Name of Candidate                      A.G.C.U Perera

Date    10

The above candidate has carried out research for the MPhil thesis              under              our supervision.              /

*UOM Verified Signature* ..

Signature of the Supervisor  
(Dr W.D.A.S Rodrigo)

10/05/2016

Date

*UOM Verified Signature*

Signature of the co-supervisor  
( Eng W.D.A.S Wijayapala)

10/05/2016

Date

Dedicated to my Family

My parents, my husband Shami Mudunkotuwa and my baby girl Yanuli

## **Acknowledgments**

I acknowledge with gratitude my advisor Dr. W.D.A.S Rodrigo for his excellent guidance, supervision and the encouragement during my entire period of study.

I would also like to express gratitude towards Eng. W.D.A.S Wijayapala for the assistance and support for this work.

Special thanks to Isuru Pasan Dasanayake and Supun De Silva for the great help given me during the study during their busy schedules.

I would like to thanks my husband Shami Mudunkotuwa for the support he gave me during this whole period of study.

## Abstract

This thesis concentrates on the stability performance of HVDC-HVAC interaction of the transnational HVDC interconnection between Sri Lanka and India. This transmission line was under consideration since mid-1970 and the prefeasibility study was done by India in cooperated with Sri Lanka together. In this study it was focused on modeling the HVDC link between Indian and Sri Lankan power grids with the basic control system and studying the transient stability performance of the HVDC interconnection under the Sri Lankan transmission network perturbed conditions. The complete system was modeled on PSCAD/EMTDC software. The complete system was divided into five subsystems while modeling as, rectifier side AC source, converter transformers and converters, DC transmission line, HVDC control system and inverter side detailed Sri Lankan network. The simulations were done for steady state conditions, for system accuracy verification and for different system perturbed conditions. The analysis was done based upon the maximum power curve, Short circuit ratio (SCR) and time domain analysis. It was found that; modeled Sri Lankan network is a strong network for the proposed HVDC interconnection in steady state condition. However, there is a considerable impact on the stability of HVDC-HVAC interaction under different perturbed scenarios of Sri Lankan AC network. This study discusses the results obtained from the qualitative and quantitative analysis.

The results obtained from this study can be taken as guidance during the planning and designing stage of the proposed DC interconnection to have an idea on stability of the AC-DC interaction. The DC power operating curve, maximum DC power in-feed to inverter side Sri Lankan network, AC system strength behavior during different disturbances, time domain faults behavior, impact of AC system impedance on the stability are the facts which are discussing in this thesis. Therefore, this thesis can be consider as guidance for the planning stage of the proposed interconnection.

# Contents

Declaration of the candidate & Supervisor	i
Dedication	ii
Acknowledgements	iii
Abstract	iv
Table of content	v
List of Figures	vii
List of Tables	xi
List of abbreviations	xii
1. Introduction	
1.1. Background	1
1.2. Thesis objectives	5
1.3. Thesis outline	6
2. Literature Survey	
2.1. Introduction	7
2.2. Worldwide interconnections	8
2.3. Technological Overview of Power Interconnection	11
2.4. Configuration and Layout of HVDC system	20
2.5. Control of HVDC converter and systems	25
3. System Modeling	
3.1. Introduction	36
3.2. System condition selection for modeling	37
3.3. Steady State mathematical modeling	
3.3.1. Assumptions	40
3.3.2. Converter transformers parameter calculation	41
3.3.3. Rectifier AC network	44
3.3.4. Sri Lankan model	48
3.3.5. Filter circuit design	50
3.3.6. DC line design	54

3.3.7. DC smoothing reactor	54
3.3.8. HVDC control system	56
4. AC-DC interaction	59
5. Simulation results, Stability analysis & Discussion	
5.1. Introduction	67
5.2. Steady State Simulation Results	68
5.3. System verification	71
5.4. AC System Impedance Increment Condition	79
5.5. QMPC Vs DMPC of the system	81
5.6. Perturbed scenario results analysis	82
6. Discussion	91
7. Conclusions and Recommendations	
7.1. Main contribution of the thesis	94
7.2. Conclusions	95
7.3. Future work	97
Reference List	98

# List of Figures

Figure		Page
Figure 2.1	HVDC systems worldwide	08
Figure 2.2	ABB HVDC projects till 2011	09
Figure 2.3	India-Sri Lanka Transmission alternatives	10
Figure 2.4	Current Source Converters	11
Figure 2.5	Voltage Source Converters	11
Figure 2.6	Conventional HVDC (CSC HVDC) with current source Converters	12
Figure 2.7	Reactive power compensation for conventional HVDC (CSC HVDC) converter station	13
Figure 2.8	CCC configuration	14
Figure 2.9	HVDC with voltage source converters	14
Figure 2.10	HVDC converter development	15
Figure 2.11	HVDC light extended range	15
Figure 2.12	Operating range for voltage source converter HVDC transmission	17
Figure 2.13	HVDC Configurations	20
Figure 2.14	bipolar HVDC system configurations	21
Figure 2.15	Bipolar Transmission line	21
Figure 2.16	Bipole, Metallic Return configuration	21
Figure 2.17	Monopolar HVDC system with 12-pulse converters	22
Figure 2.18	Monopolar HVDC Transmission line	22
Figure 2.19	Monopole, Metallic Return configuration	22
Figure 2.20	Monopole, Midpoint grounded configuration	23
Figure 2.21	Monopole, Midpoint grounded Transmission line	23
Figure 2.22	back to back configurations	24
Figure 2.23	Multi terminal configurations	24
Figure 2.24	Typical HVDC linking two AC systems	26
Figure 2.25	Identification of Pole and valve group	26
Figure 2.26	Block diagram of HVDC control in one terminal	26



Figure 2.27	Two terminal DC link	28
Figure 2.28	Equivalent circuit of DC link with inverter	29
Figure 2.29	Control characteristic curves	30
Figure 2.30	VDCL characteristic	32
Figure 2.31	Rectifier current control block diagram	34
Figure 2.32	Inverter gamma control block diagram	34
Figure 2.33	Inverter gamma control and current control selection	34
Figure 2.34	overall controls	35
Figure 3.1	Modeled HVDC network	40
Figure 3.2	rectifier side schematic diagram	44
Figure 3.3	Equivalent network of above Indian network	45
Figure 3.4	Thevenin's equivalent impedance of Indian network	45
Figure 3.5	Algebraic diagram of Indian network	45
Figure 3.6	Modeled Sri Lankan networks	49
Figure 3.7	Low pass filter & High pass Filter diagrams	50
Figure 3.8	Low pass filter components	50
Figure 3.9	High pass Filter components	52
Figure 3.10	DC transmission line with smoothing reactors	54
Figure 3.11	Rectifier Current controller optimizing block diagram	56
Figure 3.11	Characteristic curve of the modeled system	57
Figure 4.1	Defining SCR and ESCR	61
Figure 4.2	Simplified representation of a dc link feeding an AC system	63
Figure 4.3	DC power - dc current curve for $\gamma$ minimum	64
Figure 5.1	Steady state DC powers	67
Figure 5.2	Steady state DC voltages	68
Figure 5.3	steady state rectifiers firing	68
Figure 5.4	steady state inverter extinction angles	68
Figure 5.5	Steady state MPC and AC voltage profiles	69
Figure 5.6	Comparison of steady state MPC curve with reference graph	70
Figure 5.7	DC power at 1- phase one cycle fault	71
Figure 5.8	DC voltage at 1- phase one cycle fault	72
Figure 5.9	rectifier firing angle at 1- phase one cycle fault	72

Figure 5.10	inverter firing angle at 1- phase one cycle fault	72
Figure 5.11	Comparison of DC power at 1- phase one cycle fault	72
Figure 5.12	Comparison of DC voltage at 1- phase one cycle fault	73
Figure 5.13	Comparison of rectifier firing angle at 1- phase one cycle fault	73
Figure 5.14	Comparison of inverter firing angle at 1- phase one cycle fault	73
Figure 5.15	DC power at 1- phase five cycle fault	74
Figure 5.16	DC voltages at 1- phase five cycle fault	74
Figure 5.17	rectifier firing angle- 1-phase five cycle faults	74
Figure 5.18	inverter firing angle at 1- phase one cycle fault	74
Figure 5.19	Comparison of DC power at 1- phase five cycle fault	75
Figure 5.20	Comparison of DC voltage at 1- phase five cycle fault	75
Figure 5.21	Comparison of rectifier firing angle- 1-phase five cycle fault	75
Figure 5.22	Comparison of inverter firing angle at 1- phase one cycle fault	75
Figure 5.23	DC power at 3- phase fault	76
Figure 5.24	DC voltages at 3- phase fault	76
Figure 5.25	rectifier firing angle at 3- phase fault	76
Figure 5.26	inverter firing angle at 3- phase fault	77
Figure 5.27	Comparison of DC power at 3- phase fault	77
Figure 5.28	Comparison of DC voltage at 3- phase fault	77
Figure 5.29	Comparison of rectifier firing angle at 3- phase fault	77
Figure 5.30	Comparison of inverter firing angle at 3- phase fault	78
Figure 5.31	MPC for normal state and high impedance state conditions	78
Figure 5.32	Reference graphs for normal state and high impedance state conditions	79
Figure 5.33	MPC for 3 coal units unavailable	80
Figure 5.34	MPC comparisons with high SCR/ESCR –graph 1	80
Figure 5.35	MPA comparisons with high SCR/ESCR –graph 2	80
Figure 5.36	QMPC and Slow DMPC graphs plot	81
Figure 5.37	QMPC and Slow DMPC reference graphs	81
Figure 5.38	Clarification for power order increment by characteristic curve	82
Figure 5.39	DC power curve for power order increment	83
Figure 5.40	DC voltage curve for power order increment	83

Figure 5.41	DC power curve for power order increment	83
Figure 5.42	Reference plot for power order increment at 0.04s-0.1s	84
Figure 5.43	DC power curve for 300 MW unit tripped condition	85
Figure 5.44	DC voltage curve for 300 MW unit tripped condition	85
Figure 5.45	AC voltage curve for 300 MW unit tripped condition	85
Figure 5.46	DC power curve for sudden AC load rejection	86
Figure 5.47	DC voltage curve for sudden AC load rejection	86
Figure 5.48	AC voltage curve for sudden AC load rejection	86
Figure 5.49	DC power curve for a transmission line tripped condition	87
Figure 5.50	DC voltage curve for a transmission line tripped condition	87
Figure 5.51	AC voltage curve for a transmission line tripped condition	87
Figure 5.52	DC power curve for sudden DC load rejection	88
Figure 5.53	DC voltage curve for sudden DC load rejection	88
Figure 5.54	AC voltage curve for sudden DC load rejection	88
Figure 5.55	Effect of exciter on MPC	89

## List of Tables

Table		Page
Table 2.1	Comparison between CSC-HVDC and VSC-HVDC	18
Table 2.2	Hierarchical levels of HVDC control in order of authority	27
Table 3.1	Comparison of Two Technologies for optimum modeling	38
Table 3.2	Investment costs for proposed HVDC configurations	39
Table 3.3	Selection of AC system strength based on SCR	44
Table 3.4	Rectifier thevenin network parameters	34
Table 3.5	Rectifier side shunt filter & capacitor parameters	54
Table 3.6	Inverter side shunt filter parameters	54
Table 3.7	DC smoothing reactor parameter	55
Table 4.1	Categories of AC systems based on SCR	62

## List of Abbreviations

Abbreviation	Description
AC	Alternative current
CC	constant current
CSC	Current source converter
CEA	Constant extinction angle
CEC	Current error control
CIA	Constant ignition angle
DC	Direct current
DMPC	Dynamic maximum power curve
ESCR	Effective short circuit ratio
HVDC	High voltage direct current
MPA	Maximum power availability
MPC	Maximum power curve
QMPC	Quasi-static maximum power curve
SCR	Short circuit ratio
VDCL	Voltage dependent current order limit
VSC	Voltage source converter

# Chapter 1

---

## Introduction

### 1.1. Background

Industrial development in Sri Lanka pressurizes electric power production in the country to grow up rapidly with respect to the time line. This ever growing electric energy demand keens electric power industry to build more power generation plants in the island or borrow power through the interconnections from a neighboring country which has excess of power. As per the latter option mentioned, it is proposed to import power from the Sri Lanka's neighboring country India. This proposal has got apparent advantages despite in electric energy sector, in economic, social, environmental and political sectors relative to the other available options [1]. According to the prefeasibility study, the primitive objectives of this proposed interconnection are [1],

- 1) The interconnection would enhance the reliability and system security of both the countries.
- 2) The interconnection could facilitate the development of power exchange between the two countries

Sri Lanka produces her own electric power requirement by diverse energy sources such as large hydro, coal, natural gas, oil and renewable energy resources such as small hydro, wind, solar and bio mass. For the moment, almost all the hydro power plants are constructed already and meeting the electric power demand only through the hydro power plants is unrealistic and unreliable due to the limited hydro resources possessed in this small island and hydro plants dependency heavily upon the unpredictable weather condition. Meeting the requirement of ever growing electric energy demand through imported fuel is unrealistic due to the higher cost of generation. That leads the country development to be standstill due to lack of further investments and returning back established investments by unbearable electricity cost for the utilizers.

Therefore Sri Lanka turns in the next option that exporting power from neighboring country, India. In other terms, a transnational Interconnection could achieve economic and social benefits for the overall system such as supply stability, lower production cost, and environmental benefits [2].

The above mentioned three benefits are the driving factors which motivates countries for the transnational interconnection [2]. As mention again,

- security of supply

Security and reliability of electricity supply is one of the potential benefits to encourage power interconnection. Interconnection would be able to provide a pool of operational support and additional reserve capacity, which would otherwise demand additional investment for each of the systems involved.

- economic efficiency

The potential economic benefits are expected from the expansion of the power system to a certain extent. The nature of power supply industry encourages the combination of individual power system to achieve economies of scale.

Once interconnection is established the power system is expanded by the combination, therefore achieving economies of scale. In this case, interconnection offers the following opportunities:

- Sharing reserve margin is regarded as an additional source of power in addition to the existing generation capacity in those interconnected economies. Large power systems resulting from interconnection can reduce the need for reserve capacity.
  - Larger generating units can be introduced for better power quality and lower costs.
  - Optimizing the investment in the power supply systems.
- 
- Environmental satisfaction.

The increasing concern on air pollution, especially CO<sub>2</sub> emission, forces the power sector to seek alternative clean and environment friendly supply. In this regard, environmental protection could become an important factor in the decision making for cross border power interconnection.

HVDC technology is technically feasible with respect to HVAC technology to link as an interconnection between two independent countries [2]. HVDC interconnections tend towards larger capacity to make interconnection economically feasible. These links could be sized at hundreds of MWs, which is competitive with conventional power plants. Consequently, grid integration of such size HVDC links seriously impact the operation and dynamic stability of the interconnected power system. HVDC link is characterized by independent active and reactive power control and hence is able to provide reactive power / voltage support during grid voltage disturbances. These characteristics are highly depending on the grid characteristics and HVDC control systems. In order to achieve the full advantages of the HVDC interconnection, the grid with HVDC should perform appropriately for different kinds of disturbances and system conditions. Thus, it is essential to study



the grid and HVDC link performance under different disturbance scenarios. As the Sri Lankan power system is weak and very small, proper analysis of dynamic behavior of the link is very critical.

There are particularly applications of HVDC transmission systems which possess distinct superiorities over EHV-AC transmission systems. The three major HVDC applications which are not practical to be substituted by HVAC are [3],

- Long distance bulk power transmission,
- Cable transmission
- System interconnection.

It is not going to detail about the HVDC applications despite the HVDC system interconnection application.

As it needs to keep the two countries power network independent from each other it is necessary to interconnect two islands via an asynchronous transmission system. Therefore it always tends to interconnect two independent power systems at least by one DC transmission line. Integration of AC and DC power makes the simple power transmission network more complex. Therefore it is necessary to predict the performance of the transmission network during the planning stage.

This thesis describes the modeling and simulation details of the proposed Indu-Sri Lanka HVDC interconnection for transient and dynamic stability and a systematic way to ensure that there are no risks of adverse interactions due to the links. The simulation results obtained for different disturbances to compare the system performances with the proposed link are also presented. It is essential to ensure that the system is asymptotically stabilized at the disturbances with this proposed link and when it is not stabilized, it is necessary to provide supplementary actions to ensure the stability of the HVDC-HVAC network.

## 1.2. Thesis Objectives

The purpose of this research study in this thesis is to analyze the performance of the AC-DC interaction on the inverter side of the interconnection. There are several ways to study about the AC-DC interaction as, power, voltage and frequency instabilities; harmonic resonance- related instabilities; sub synchronous torsional interactions; temporary overvoltage and recoveries from AC and DC faults [4]. This research work selected to study about the power and voltage stability of the AC-DC interaction at inverter terminal of the model; which means that study about the power/voltage stability at the Sri Lankan AC-DC interaction point.

The goal of this thesis is to understand the AC-DC interaction between inverter side Sri Lankan AC network and the proposed HVDC link during transient periods of the selected perturbed conditions. For this purpose, the complete work comprises of two parts.

1. Model HVDC link interconnected in between detailed Sri Lankan network and thevenin's equivalent of Indian network on PSCAD software.

The system was modeled in this study as India feeds power to Sri Lanka rated 500 MW under 400 kV rated DC voltage. Power transmits in monopolar transmission mode. The power requirement is regulated by inverter master control. The control system of the complete model is the basic control system without additional supplementary control loops so as to check for the asymptotic stability of the AC-DC interaction.

2. Study the AC-DC interaction between inverter side Sri Lankan AC terminal and HVDC terminal.

As mentioned above the main objective of this thesis is to study about the power and voltage stability of the HVDC-HVAC interaction for different perturbed scenarios.

This thesis primarily considers the transient stability of the HVDC-HVAC interaction. For analysis, three main qualitative and quantitative tools were used in this thesis; Maximum power curve, Short circuit ratio and transient period of time domain analysis.

### **1.3. Thesis outline**

The organization of the thesis is as follows.

Chapter 1 (this chapter) provides introduction to the thesis. It is included here the literature review done on the basic factors of the HVDC industry. This literature survey is used to select the system conditions for modeling HVDC link for the study.

Chapter 2 comprises of modeling analysis of the HVDC-HVAC network on PSCAD/EMTDC software. Steady state mathematical modeling and each parameter selection is comprehensively analyzed in this chapter.

Chapter 3 is to introduce the AC-DC interaction with the tools which are using to evaluate the stability of the interaction in this thesis. AC-DC interaction primarily depends upon the AC system impedance and the AC system inertia. In this research work, it is only consider the system impedance influence on the AC-DC interaction as it consider only the transient stability period of the post-fault behavior.

Chapter 4 is analyzing the results obtained from the analytical tools described in chapter 3.

Chapter 5 discusses about the modeling and simulation results in the Discussion section.

Chapter 6 gives the conclusion of the work done in this research study.

# Chapter 2

---

## Literature Survey

### 2.1. Introduction

HVDC interconnection is not a brand new technology to the world. It has been in the power transmission industry since 1945. However, the first commercial transnational interconnection was 20-MW, 100-kV undersea cable between the Swedish mainland and the island of Gotland commissioned in year 1954 [5]. When it becomes year 2010, the total HVDC transmission capacity in the world was 145 projects with 140,000 MW which were in operation or under construction [6].

However, HVDC interconnection is a new concept to Sri Lankan power system although it's not new to India. India has four electrical regions named as North, South, East and West. All those four regions are connected asynchronously by HVDC interconnections.

HVDC integration in to Sri Lankan pure AC transmission network needs to be studied thoroughly. The study can be done in two aspects. They are performance analysis of the AC-DC interaction and impact on AC network electrical and mechanical parameters by the newly integrated DC link.

There are three publications that had been done upon the India- Sri Lanka HVDC interconnection so far. Rodrigo WDAS et al [7] had done modeling and transient analysis of HVDC bipolar link. They have studied about the dynamic behavior of the DC link and the AC systems in time domain. They have modeled the India and Sri Lanka power sources in thevenin's equivalent models. Jowsick, A.J.M.I. et al had implemented this interconnection in VSC technology [8].

They have studied about impact from the transients due to frequency fluctuation and country blackout on the HVDC transmission line's operations. The third publication which is related with this thesis is the modeling of HVDC interconnection on CSC technology with detailed inverter side AC network and it studied about the impact on AC-DC interaction inverter side [9].

## 2.2. Worldwide interconnections

### 2.2.1. HVDC Classic and Light projects

In total almost 140,000 MW HVDC transmission capacities in operation or under construction in some 145 projects around the world. ABB has been entrusted with orders for more than 70 of these projects with an installed transmission capacity of about 60,000 MW [6]. Figure 2.1 illustrates complete HVDC power production capacity from 1950 till 2010.

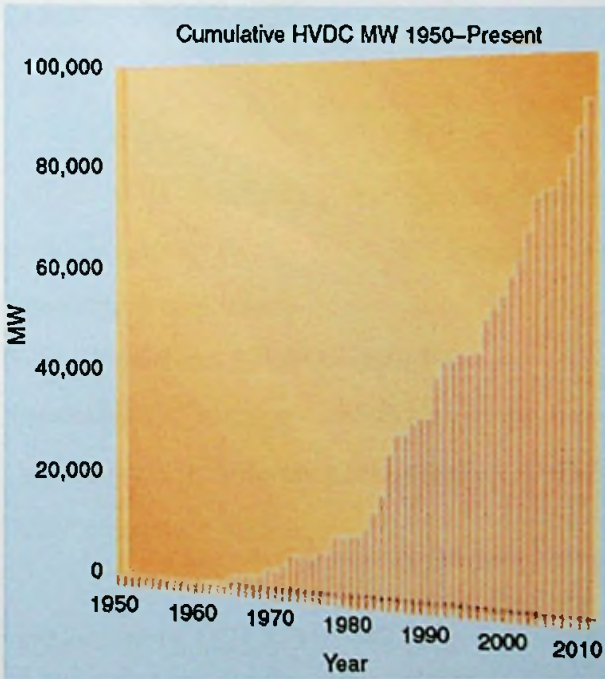


Fig 2.1: HVDC systems worldwide: Cumulative megawatts versus year of commissioning [9]

The complete projects list with the main data are available in “HVDC Projects listing” report, Prepared by IEEE DC and Flexible AC Transmission Subcommittee, D. Melvold. [10]

The figure 2.2 world map illustrates the worldwide distribution of the HVDC projects starting from the first commercial HVDC project in 1954 until projects commissioned in 2011, which administered by ABB [6].

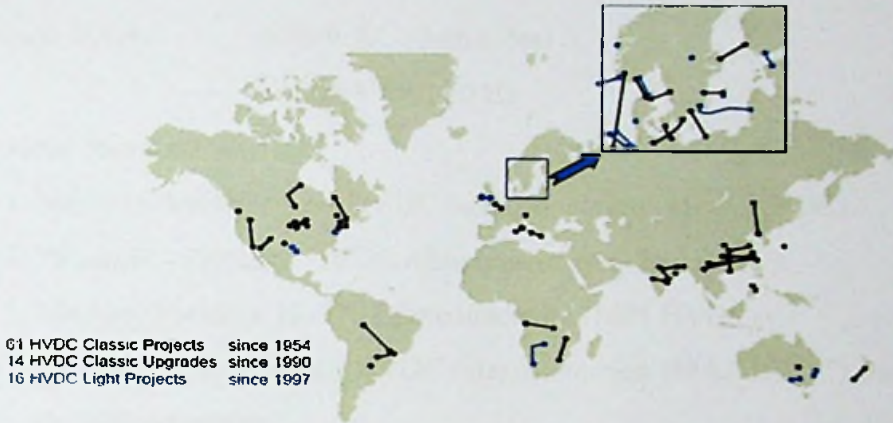


Fig 2.2: ABB HVDC projects till 2011

In this report it is mentioning the special featured HVDC projects. The features selected with respect to the India- Sri Lanka HVDC interconnection main attributes. The specified features are,

- Power transfer – 500 MW-600MW
- Operating DC voltage –  $\pm 400$  kV
- Asynchronous Interconnection(only HVDC link without parallel HVAC interconnection)

HVDC Classic projects [11], [12], [13], [14], [15]:

- Italy- Greece 500 MW
- Kontek 600 MW
- Basslink 600 MW
- StoreBaelt 600 MW
- Fenno-Skan 500 MW

### 2.2.2. India – Sri Lanka HVDC Interconnection:

The main data of the proposed India- Sri Lanka HVDC interconnection are as below.

- objectives –
  1. The interconnection would enhance the reliability and system security of both the countries.
  2. The interconnection could facilitate the development of power exchange between the two countries.
- Power Rating – 500 MW
- Voltage Levels – 400kV AC (both sides)  
± 400 kV DC, 50 Hz
- Proposed locations –
  1. Madurai-Anuradhapura HVDC interconnection (MAI- HVDC)
  2. Tuticorin - Puttalam HVDC interconnection (TPI-HVDC)
  3. Madurai-Puttalam HVDC interconnection (MPI HVDC)
  4. Madurai-Anuradhapura HVDC interconnection (MAI\_BBDC) Back-to-back interconnection
- Proposed configurations – Bipolar, Monopolar, Back- to-Back

The above locations were proposed in year 2002 prefeasibility study. The map with above proposed locations are shown in figure 2.3.

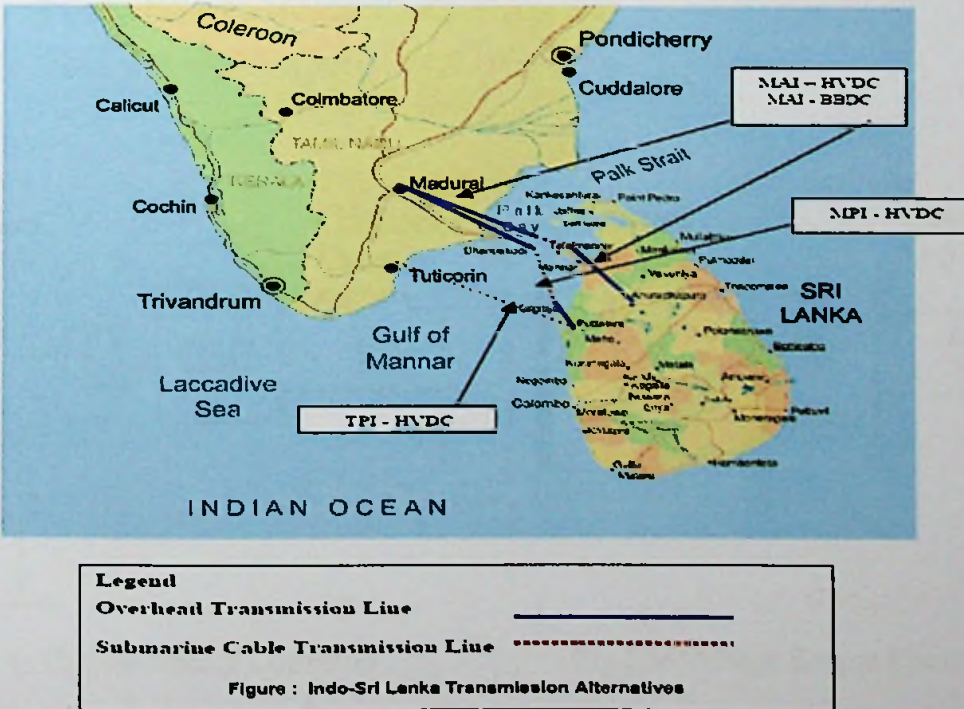


Fig 2.3: India-Sri Lanka Transmission alternatives

▪ Prefeasibility Study background

This transnational interconnection was under consideration since mid-1970. The pre-feasibility study was conducted with the assistance of USAID in 2002 by Nexant Inc. In 2006 the review of the prefeasibility study was conducted by Nexant/power Grid Corporation of India with the assistance of USAID.

There were the bilateral discussions by Secretary, Ministry of Power and Energy Sri Lanka and Secretary Ministry of Power, India in Dec 2006. Cabinet of Ministers, Sri Lanka approved in principle in Dec 2006, to study the feasibility of power interconnection and to appoint a Steering Committee Co-Chaired by Secretaries of Power Ministries and to appoint a Task Force for technical, commercial, regulatory and legal aspects.

### 2.3. Technological Overview of Power Interconnection

#### 2.3.1. Core HVDC technologies

Two basic converter technologies are used in modern HVDC transmission systems. These two divisions are based upon the configurations of the three phase converter that use in the conversion process [16],

1. Current Source converter (CSC)- Figure 2.4
2. Voltage Source Converter (VSC)- Figure 2.5

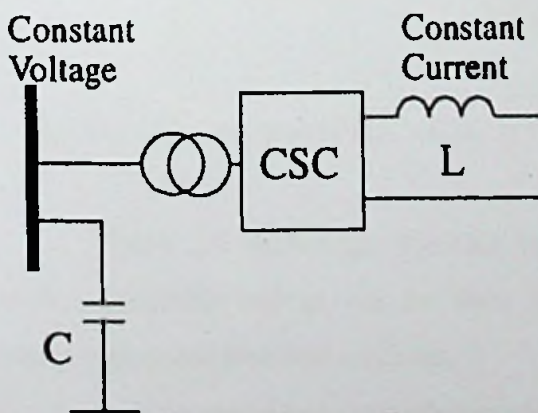


Fig 2.4: Current Source Converter

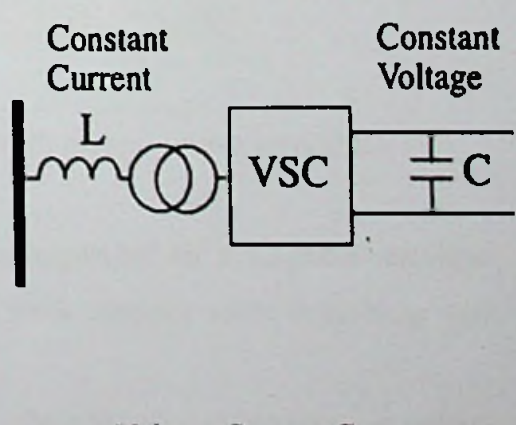


Fig 2.5: Voltage Source Converter





### 2.2.1.1. CSC technology

All the details were cited from reference [17].

This is the conventional and matured technology that has been using since the first HVDC project. This modern HVDC transmission technology employs line commutated CSCs with thyristor valves. Such converters require a synchronous voltage source in order to operate. This technology is well established for high power, typically around 1000 MW.

According to the reference, Thyristor valves operate as switches which turn on and conduct current when fired on receiving a gate pulse and are forward biased. A thyristor valve will conduct current in one direction and once it conducts, will only turn off when it is reverse biased and the current falls to zero. This process is known as line commutation.

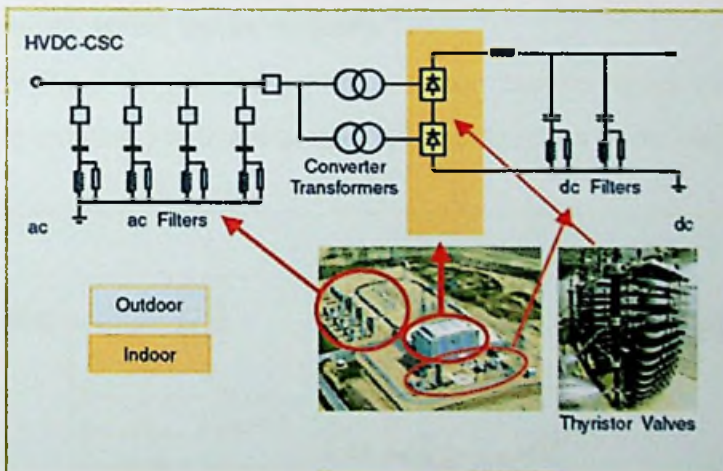


Fig 2.6: Conventional HVDC (CSC HVDC) with current source converters.

figure 2.6 shows the thyristor valve arrangement for a 12-pulse converter with 3 quadruple valves, one for each phase. Each thyristor valve is built up with series connected thyristor modules.

Line-commutated converters require a relatively strong synchronous voltage source in order to commutate. The three-phase symmetrical short circuit capacity

available from the network at the converter connection point should be at least twice the converter rating for converter operation.

Line commutated CSCs can only operate with the ac current lagging the voltage, so the conversion process demands reactive power. Reactive power is supplied from the ac filters, which look capacitive at the fundamental frequency, shunt banks, or series capacitors that are an integral part of the converter station. Any surplus or deficit in reactive power from these local sources must be accommodated by the ac system. This difference in reactive power needs to be kept within a given band to keep the ac voltage within the desired tolerance. The weaker the ac system or the further the converter is away from generation, the tighter the reactive power exchange must be to stay within the desired voltage tolerance.

As the active power transfer varies, the corresponding changes in the reactive power produce AC system voltage fluctuations. The AC voltage drops cause additional reactive power consumption and further voltage reduction, which may lead to voltage instability. To prevent this instability, a minimum short-circuit ratio (SCR), defined as the ratio between the short-circuit power and converter power ratings, is required, which can be typically 2.

Figure 2.7 illustrates the reactive power demand, reactive power compensation, and reactive power exchange with the ac network as a function of dc load current.

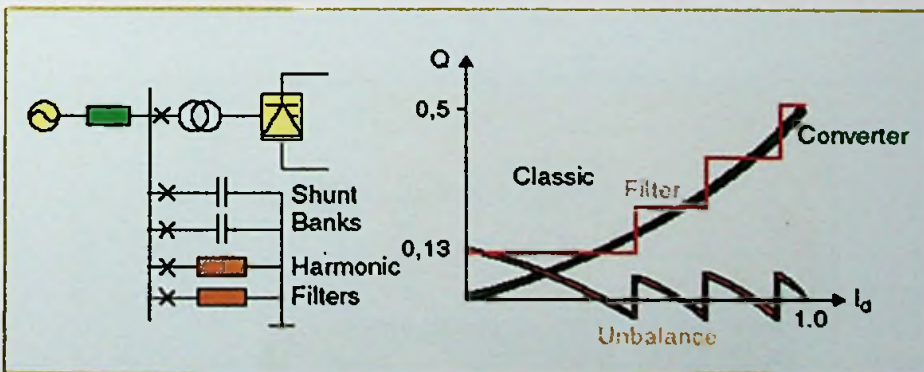


Fig 2.7: Reactive power compensation for conventional HVDC (CSC HVDC) converter station

Converters with series capacitors connected between the valves and the transformers were introduced in the late 1990s for weak-system, back-to-back applications. These converters are referred to as capacitor-commutated converters (CCCs). The series

capacitor provides some of the converter reactive power compensation requirements automatically with load current and provides part of the commutation voltage, improving voltage stability. The overvoltage protection of the series capacitors is simple since the capacitor is not exposed to line faults, and the fault current for internal converter faults is limited by the impedance of the converter transformers.

The CCC configuration figure 2.8 allows higher power ratings in areas where the ac network is close to its voltage stability limit.

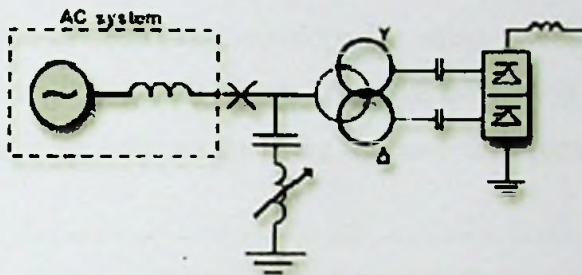


Fig 2.8: CCC configuration

### 2.2.1.2. VSC technology:

DC power transmission by self-commutated semiconductor devices based on voltage sourced converters is known as VSC transmission technology in figure 2.9.

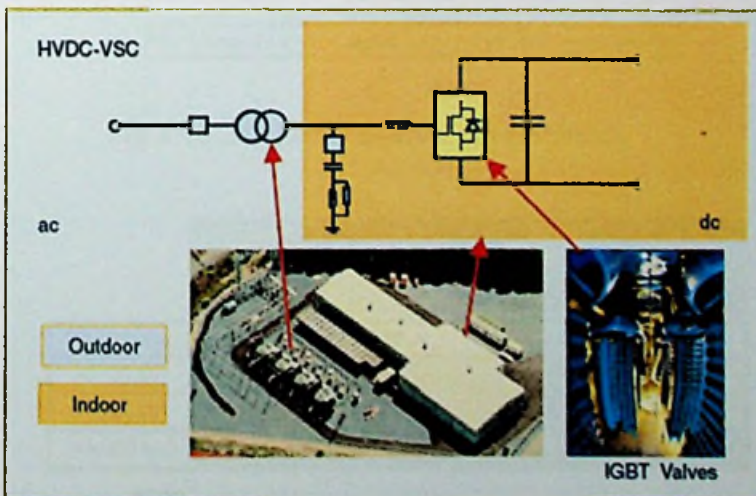


Fig 2.9: HVDC with voltage source converters.

According to the reference [17] citations, HVDC transmission using VSCs with pulse-width modulation (PWM) was introduced in the late 1990s. Since then the progression to higher voltage and power ratings for these converters has roughly paralleled that for thyristor valve converters in the 1970s. These VSC-based systems are self-commutated with insulated-gate bipolar transistor (IGBT) valves or Gate turn off thyristors (GTO) valves and solid-dielectric extruded HVDC cables. The first HVDC VSC transmission commercial availability started from GTO and then secondly, IGBT changed the scene. Figure 2.10 illustrates solid-state converter development for the two different types of converter technologies using thyristor valves and IGBT valves. The latest development which is HVDC light expanding ranges development is illustrated in figure 2.11. The use of VSC has taken off in the past 10 years, and new applications are being announced frequently [16].

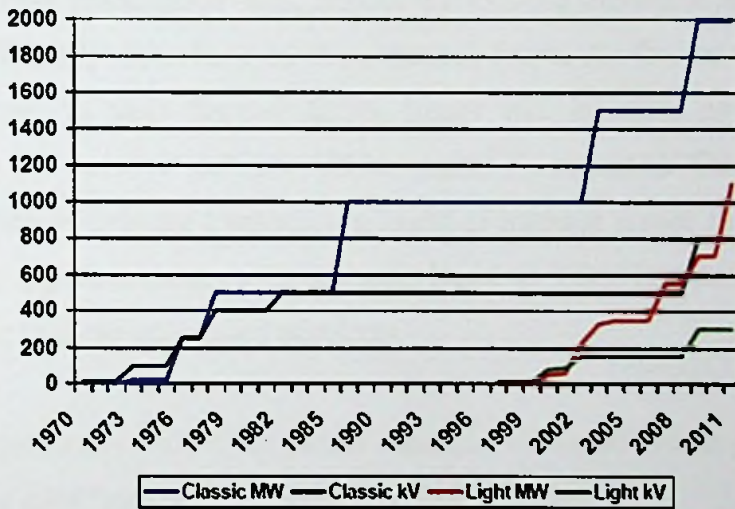


Fig 2.10: HVDC converter development.

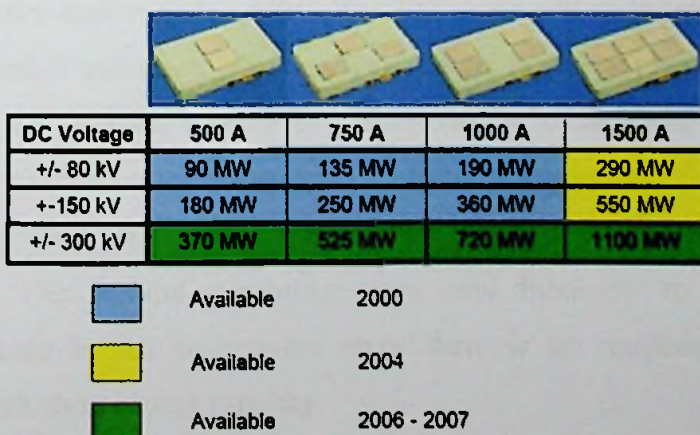


Fig 2.11: HVDC light extended range

However, due to the higher cost of a VSC compared to a CSC on a per kW basis, the VSC applications are reserved for niche applications which could not be served by CSCs. As the cost of VSCs comes down, the number and variety of applications will increase due to the increased benefits offered by such converters. [16]

Two prominent manufacturers refer to the new technology of dc transmission using VSCs by commercial trade names such as HVDC Light (by ABB) and HVDCPLUS (the “plus” stands for Power Link Universal Systems) (by Siemens). [16]

The recent interest in this HVDC light technology has grown due to a number of factors. According to the cited details from reference [16], deregulation in the electric power industry, coupled with continued load growth and the difficulty of obtaining ROWs for new transmission lines, implies that existing transmission system assets be utilized efficiently and closer to their thermal limits. As the existing ac lines are loaded nearer to their thermal limits, losses will increase, power quality will deteriorate and network stability will be negatively impacted. This will necessitate modifications of existing transmission assets to increase power density on existing ROWs. An approach using dc transmission based on VSCs has the potential to aid in the solution to these anticipated problems.

HVDC transmission with VSCs can be beneficial to overall system performance. The points were cited from references [16] and [18].

- The figure 2.12 shows the active and reactive power operating range for a converter station with a VSC. The VSCs provide an independent control of both active and reactive power. This feature is very attractive in a city centre (with a significant number of underground ac cables) where reactive power control is both complicated and expensive to implement. Reactive power can also be controlled at each terminal independent of the dc transmission voltage level. This control capability gives total flexibility to place converters anywhere in the ac network since there is no restrictions on minimum network short-circuit capacity.

- Operating point can be selected anywhere inside the area.
- Unlike conventional HVDC transmission, the converters themselves have no reactive power demand and can actually control their reactive power to regulate ac system voltage just like a generator.

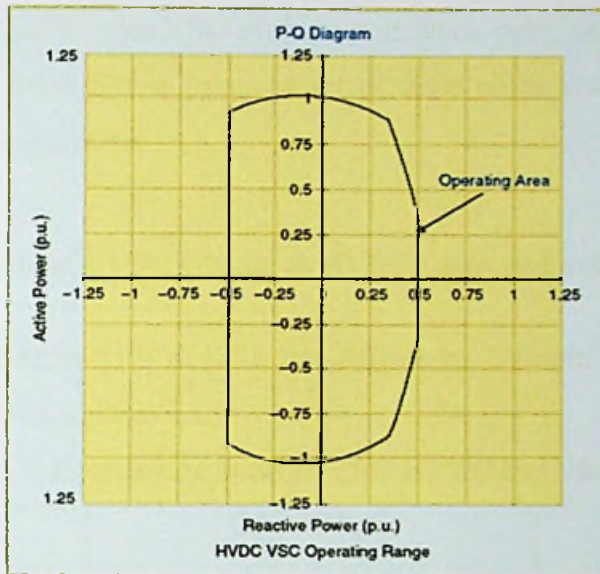


Fig 2.12: Operating range for voltage source converter HVDC transmission.

- Compact, modular, standardized construction of the convertor permits a factory-tested station which can be rapidly installed/ commissioned on site. Furthermore, the station size can be expanded in a staggered manner to suit the system growth.
- The new XLPE (Cross Linked Poly-Ethylene) extruded polymer dc cables can fit into existing ac cable ducts or ROWs and can provide almost a 50% power transfer capacity increase at the same time.
- Avoidance of commutation failures due to disturbances in the AC network.
- No need of transformers for the conversion process.



- Possibility to connect the VSC-HVDC system to a “weak” AC network or even to one where no generation source is available and naturally the short circuit level is very low.
- Self-commutation with VSC even permits black start; i.e., the converter can be used to synthesize a balanced set of three phase voltages like a virtual synchronous generator.

### 2.2.1.3. Comparison of HVDC Classic & HVDC Light technologies

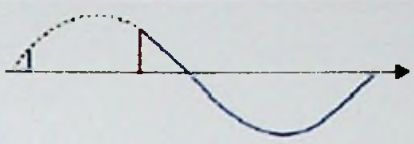
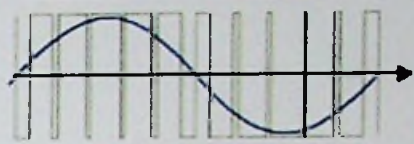
As cited from references [19] & [20], the differences between HVDC classic and HVDC light are shown in table 2.1.

Table 2.1: Comparison between CSC-HVDC and VSC-HVDC

Attribute	CSC-HVDC	VSC-HVDC
Alternative names	Line Commutated Thyristor technology “HVDC Classic <sup>3</sup> ”	Self-commutated IGBT technology “HVDC Light <sup>4</sup> ” “HVDC PLUS <sup>5</sup> ”
Converter Technology	Thyristor valves, grid commutation	IGBT, self-commutation
Max converter rating at present	6400 MW, ± 800 kV (OH)	1200 MW, ± 320 kV(cable) 2400 MW, ± 320 kV(overhead)
Technology Cable	Oil paper Field joints (5 days) Sea cable installation from special ship (3 available)	Extruded Prefabricated land joints (1 day) Sea cable installation from barge (> 200 available)
Typical delivery time	30-36 months	20-24 months
Active power flow control	Continuous ±0.1 Pr to ± Pr (Due to the change of polarity)	No reactive power demand
Reactive power compensation & control	Discontinuous control (Switched shunt banks)	Continuous control (PWM built in converter control)
Scheduled maintenance	Typically < 1%	Typically < 0.5%
Typical system losses	2.5-4.5%	4-6%
Multi terminal configuration	Complex, limited to 3 terminals	Simple, no limitations
Robustness at AC voltage drop	Total loss of power transfer if voltage drop is bigger than 10%.	Continued power transfer and dynamic voltage support during fault

AC network requirement	Maximum power transfer limited to about 50% of short circuit capacity in AC network	Maximum power transfer can be 100% of short circuit capacity in AC network. Power can be supplied to blacked out network
Telecommunication	Needed for start and operation	Not needed (multi terminal operation may require communication depending on configuration)
Operation at low power	Blocked below minimum power	Never blocked, operation through 0 MW possible
Power reversal	Can be done in about one second by blocking the converter and start up again with the opposite polarity (the current direction does not change)	Can be done instantaneously. No special sequence is needed. The sequence is needed. The polarity is unchanged and the current direction is altered continuously
Multi terminal operation	Complex to build and operate in reality limited to 3 terminals. Reliability issue as commutation failure in one inverter will affect all inverters. Change of power direction requires switching.	Can be built easily. High reliability since faults on the AC side are not sensed on the DC side and other stations are not affected. Seamless change in power flow without switching in any direction and without change of the polarity
Emergency power	Can be used as emergency power if one station is energized	Can be used as emergency power if one station is energized. If batteries are connected to the DC bus, full power can be fed into the AC system from both converters at a sudden power loss or shortage
Dimensions	Relatively high valve hall and normally relatively big outdoor AC yard    Above footprint (600 MW ): 200x120x22 m	Very compact valve arrangement. Low profile and indoor AC and DC yard.    Above footprint (500 MW): 120 x50x11 m
Control	Phase angle control	Pulse width control both active and reactive power:



	 <p>Thyristor cannot be switched off with a control signal. It automatically ceases to conduct when the voltage reverses. Line commutated 50/60 Hz</p>	 <p>The IGBT can be switched off with a control signal. Forced commutation up to 2000 Hz.</p>
Operation experience	>20 years	<5 years

## 2.4. Configuration and Layout of HVDC system

### 2.4.1.1. DC system Configurations

HVDC transmission systems can be configured in many ways to take into account cost, flexibility and operational requirements. There are 4 basic configurations as shown in figure 2.13.

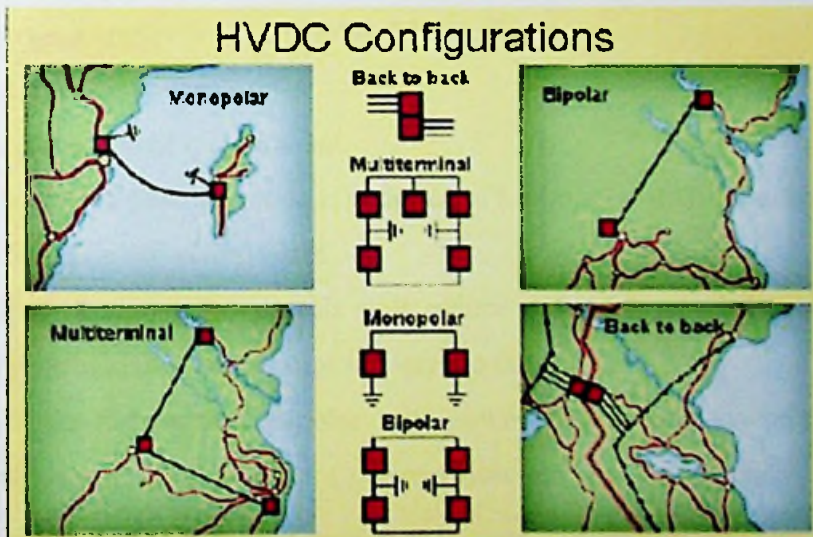


Fig 2.13: HVDC Configurations

1. Bipolar Configuration
2. Monopolar Configuration
3. Back to back Configuration
4. Multi terminal Configuration

1. Bipolar lines –

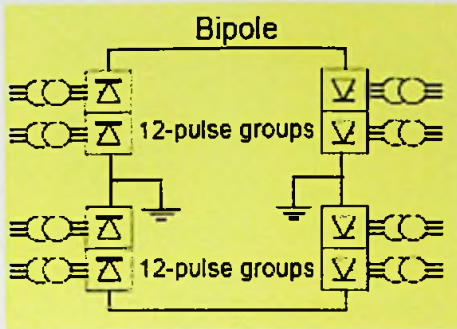


Fig 2.14: Bipolar HVDC system configuration

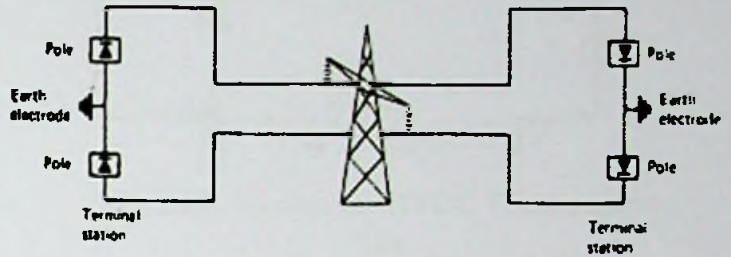


Fig 2.15: Bipolar Transmission line

- 2 poles and one positive with respect to earth and other negative.
- Pole includes substation pole and transmission line pole.
- The midpoint of bi-poles in each terminal is earthed an electrode line and an earth electrode.
- Earth electrodes located about 5-25 km away from terminals.
- Capacity up to approximately 3000 – 7000 MW

Remarks:

- Most commonly used arrangement.
- During fault on a pole the mode is changed to Monopolar with reduced power flow through one pole and return earth

For a fault on one pole controls will reduce direct current and voltage of the affected pole to zero in an attempt to clear the fault.

- Normal mode of operation: Bipolar, with power flow through line conductors and negligible current through earth. ( Current flow out from the positive pole returns via the negative line)

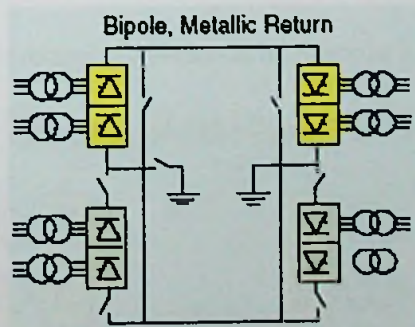


Fig 2.16: Bipole, Metallic Return configuration

## 2. Monopolar –

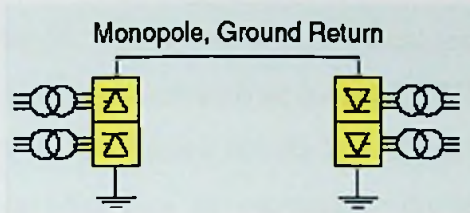


Fig 2.17: Monopolar HVDC system with 12-pulse converters.

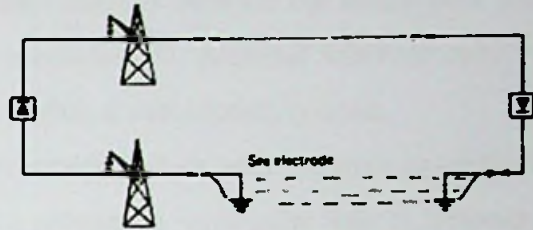


Fig 2.18: Monopolar HVDC Transmission line

- One pole and return earth
- Earthing of poles via electrode line and earth electrode.
- Earth electrode located away from terminal substation.
- The pole is normally negative with respect to earth
- Capacity up to approximately 1500 MW.

Remarks:

- Power rating almost  $\frac{1}{2}$  of the rating of bipolar system
- Used for HVDC submarine cables.
- Recent HVDC projects are all bipolar and earlier monopolar systems are being extended to bipolar
- Simplest and least expensive systems for modern power transfers since only two converters and one high-voltage insulated cable or line conductor are required.
- Sea electrodes have been used successfully in Figure 2.18 on several schemes for continuous monopolar operation, low resistivity sea water providing a permanent return path. The resistivity of sea water is in the order of 0.2 m compared with 10 m for earth at an ideal land site or 100 m for fresh water.
- Other arrangements of monopolar system is Monopole Metallic Return

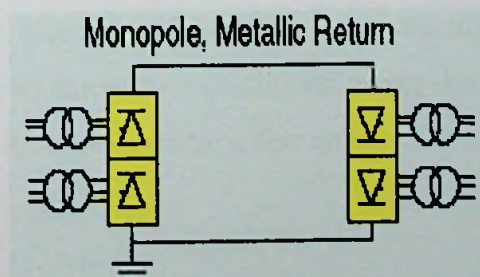


Fig 2.19: Monopole, Metallic Return configuration

- For the area conditions such as, in heavily congested areas, fresh water cable crossings, or areas with high earth resistivity conditions, it is using the Monopolar Metallic Return configuration or low voltage cable is used for the return path and the DC circuit uses a simple local ground connection for potential reference only.
- In applications with dc cables (i.e. HVDC Light), a cable return is used.
- Since the corona effects in a dc line are substantially less with negative polarity of the conductor as compared to the positive polarity, a monopolar link is normally operated with negative polarity.
- In some research papers it says that metallic return can also be used where concerns for harmonic interference and/or corrosion exist.

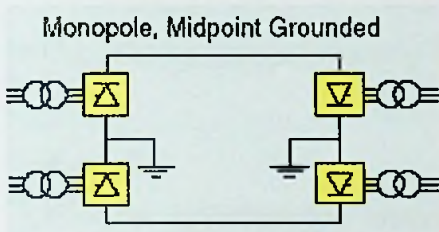


Fig 2.20: Monopole, Midpoint grounded configuration

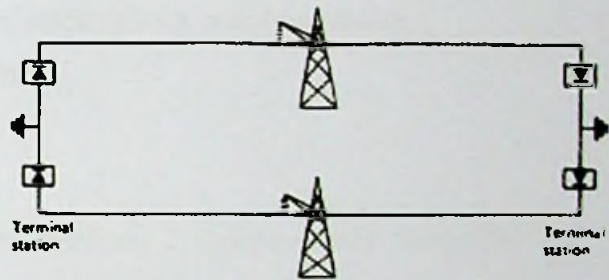


Fig 2.21: Monopole, Midpoint grounded Transmission line

- As an economic alternative to a monopolar system with metallic return, the midpoint of a 12-pulse converter can be connected to earth directly or through an impedance and two half-voltage cables or line conductors can be used. The converter is only operated in 12-pulse mode so there is never any stray earth current.
- There are circumstances where the probability of line failure arising from environmental conditions is high, 2 monopolar towers have been used on separate rights-of-way although the system operates as a bipole.
- A monopolar line can be operated using earth return with the connection to earth made via a ground electrode. However, ground electrodes have so far only been constructed for use in emergency conditions, being designed to operate only for a matter of hours, or in some cases for a few months.

### 3. Back – Back Configuration –

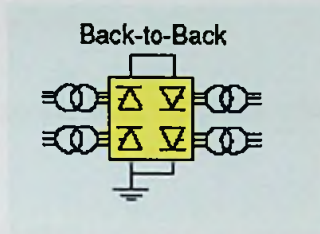


Fig 2.22: Back to Back configuration

- Usually bipolar without return earth
- Reference earth provided for protection, controls, and measurements.
- Converter and inverter located in the same substation.
- No HVDC transmission line
- 2 AC systems linked by a single HVDC Back to back coupling station.
- Capacity up to approximately 1000 MW.

#### Remarks:

- Provides asynchronous interconnection between 2 independently controlled AC networks and use AC lines to connect on either side.
- Improves system stability
- Power transfer can be in either direction depending upon control characteristics
- Power exchange can be rapidly varied.
- Very popular method of interconnection between adjacent AC networks.
- Power transfer is limited by the relative capacities of the adjacent ac systems at the point of connection.
- If there is a need to connect two nearby systems by HVDC, economies can be achieved by combining two converter stations in a back-to-back arrangement

### 4. Multi terminal Configuration

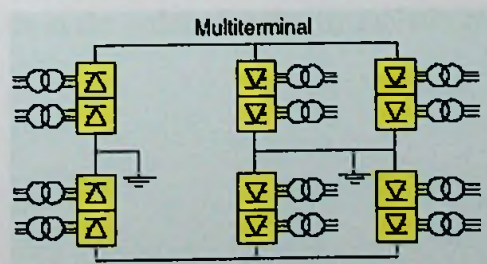


Fig 2.23: Multi terminal configuration

- 3 or more terminal substations.
- Bipolar
- Some terminals feed power in HVDC bus, some receive power from HVDC bus

Remarks:

- Recently introduced (1986)
- Provides interconnection between the 3 or more AC networks.
- Exchange between AC networks can be controlled accurately, rapidly.
- System stability of AC networks can be improved.

The details above are cited from references [1], [8], [9], [10] and [20].

## **2.5. Control of HVDC converter and systems**

### **2.5.1. Functions of HVDC controls**

In a typical two terminal DC link connecting two AC systems the primary functions of the DC controls are to [16]:

- Control power flow between the terminals,
- Protect the equipment against the current/voltage stresses caused by faults
- Stabilize the attached AC systems against any operational mode of the DC link

Hierarchy of controls [16], [21]–

There is a hierarchical levels arranged in order of rank or decision making authority. The control functions are arranged in different hierarchical levels as illustrated in figures 2.24 and 2.26. Figure 2.25 illustrates the definition of the pole.

The hierarchical levels in the order of authority include in table 2.2.

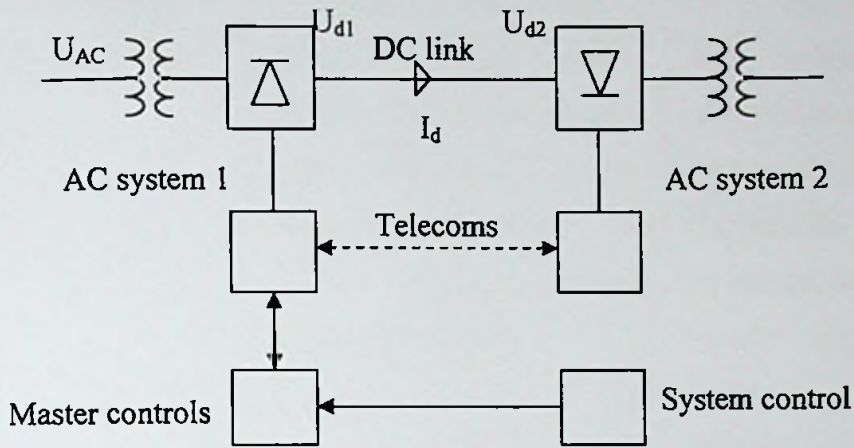


Fig 2.24: Typical HVDC linking two AC systems

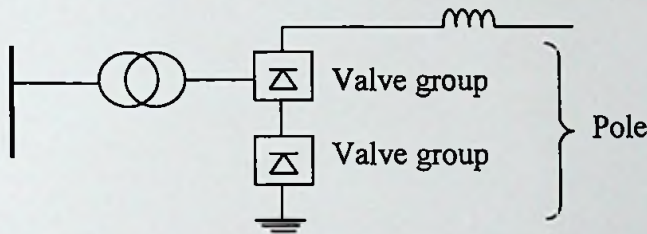


Fig 2.25: Identification of Pole and valve group

Following block diagram is for the monopolar HVDC control in one terminal [21].

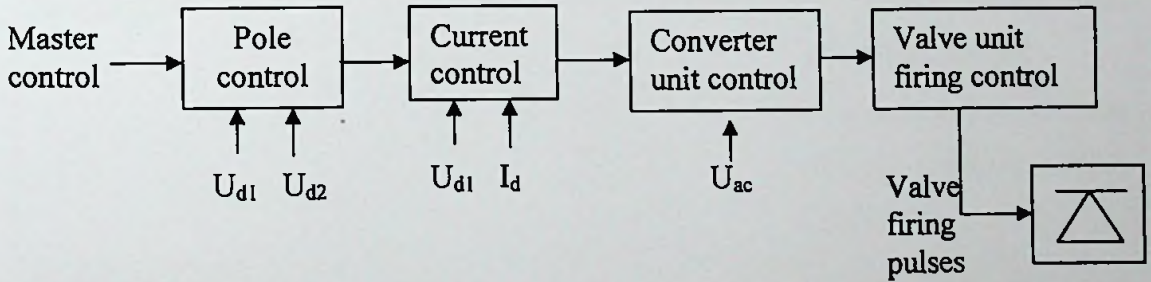


Fig 2.26: Block diagram of HVDC control in one terminal

Table 2.2- Hierarchical levels of HVDC control in order of authority

Hierarchical level	Location and coverage	Function
HVDC system control	-Terminal of overall control -Entire HVDC transmission system comprising 2 or more terminal substation and HVDC lines. Includes telecommunication	-Has authority over master control located at each terminal station -To provide orders for current orders to various terminal substations to achieve required functions.
Master control	Terminal of overall control and remote terminal. Master control is located at leading terminal and trailing terminal	-Receives orders from HVDC system control
HVDC substation control	Substation control room Entire substation	-under master control -commands pole controls -To receive orders from substation control
Pole control	-Each terminal substations -one for each pole	-To receive orders from substation control - To give orders to each of its converter unit control
Converter unit control	-Control room of each terminal substation -respective convertor unit and its valves	-To control all the valves in the convertor -various protective, control and monitoring functions in the respective control unit
Valve unit control	-Control room of each terminal substation	-To control and monitor respective valve



	-respective valve	-Under the converter control -One unit for each valve
--	-------------------	--

### 2.5.2. Control basics for a two terminal DC link [16]

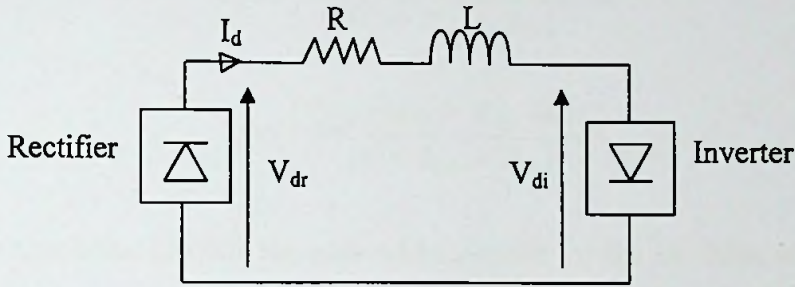


Fig 2.27: Two terminal DC link

A two terminal DC link is shown in figure 2.27 with a rectifier and an inverter. The DC system is represented by an inductance L and a line resistance R; the value of the inductance L comprises the smoothing reactors, DC line inductance whereas the value of R includes the resistances of the smoothing reactors and the resistance of the DC line etc.

Using ohm's law, the DC current  $I_d$  in the DC link depicted in the figure is given as,

$$I_d = \frac{(V_{dr} - V_{di})}{R}$$

The power flow transmission of the DC link is therefore given by,

$$P_d = V_d \times I_d$$

From converter theory, in the case of a CSC the  $V_d$ - $I_d$  relationship for a rectifier is given by,

$$V_{dr} = V_{dor} \cos \alpha - R_{cr} I_d$$

From converter theory, in the case of a CSC the  $V_d$ - $I_d$  relationship for an inverter is given by,

$$V_{di} = V_{dor} \cos \beta - R_{ir} I_d$$

Or, depending on choice of control variable

$$V_{di} = V_{dor} \cos \gamma - R_{ir} I_d$$

Using equations describing  $V_{dr}$  and  $V_{di}$  for the case of a CSC, the DC line current is given by either one of two options depending upon the choice of the control mode at the inverter;

$$I_d = \frac{(V_{dor} \cos \alpha - V_{doi} \cos \beta)}{(R + R_{cr} + R_{ci})}$$

or

$$I_d = \frac{(V_{dor} \cos \alpha - V_{doi} \cos \gamma)}{(R + R_{cr} - R_{ci})}$$

These equations provide the equivalent circuits for the DC link, as shown in figure 2.28.

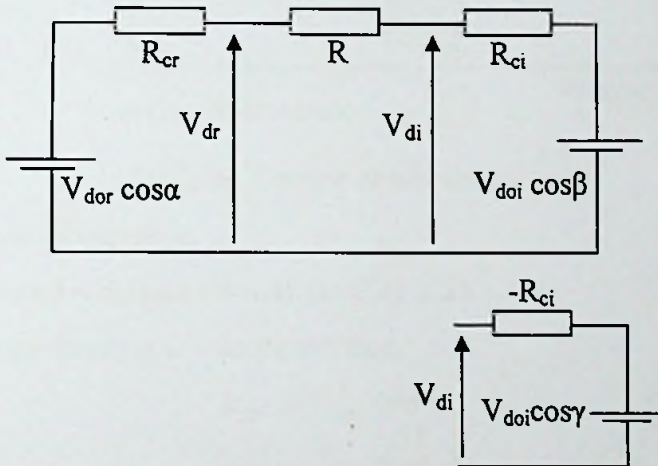


Fig 2.28: Equivalent circuit of DC link with inverter

$R_{cj}$  = equivalent commutation reactance (j denotes i or r for inverter or rectifier respectively)

The choice of control strategy is selected to enable a fast and stable operation of the DC link whilst minimizing the generation of harmonics, reactive power consumption and power transmission losses [16]

Based on the above equations the characteristic control graph is implemented. Following is the complete characteristic control graph illustrated in figure 2.29.

The intercepting point of rectifier characteristic curve and inverter characteristic curve is the operating point of the HVDC system. Below shown is the characteristic

graph that used for this thesis and the explanation is based upon the graph used for this thesis. As per the requirement, each characteristic curve part can be added to the particular rectifier and inverter characteristic curves as per the theory in HVDC theory references.

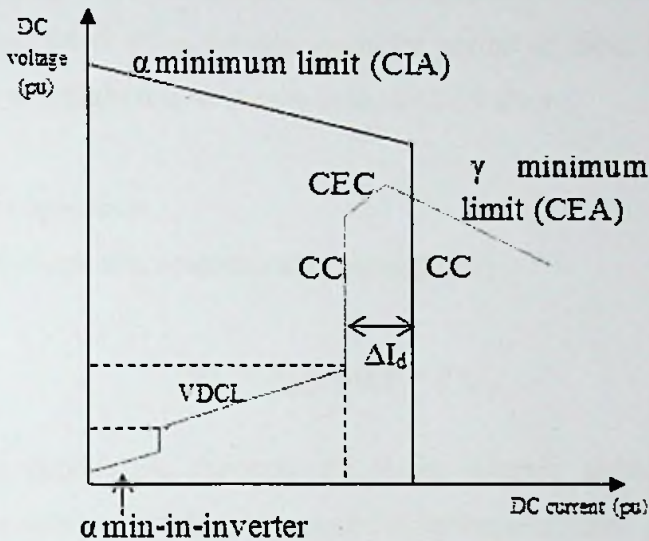


Fig 2.29: Control characteristic curve

### Rectifier mode of operation

#### 1. α minimum characteristic at rectifier (CIA)

From converter theory it can be shown that,

$$V_{dr} = V_{dor} \cos \alpha - R_{cr} I_d$$

$$R_{cr} = \frac{3}{\pi} X$$

X = per phase leakage reactance of each of the converter transformer

The line is shown in the above figure 2.29 by a straight line. The slope of this characteristic is the value  $-R_{cr}$  which is defined as the equivalent commutation resistance; a low value of  $R_{cr}$  would imply a strong AC system, and the characteristic would be almost horizontal. The intercept of this characteristic on DC voltage axis is  $V_{dor} \cos \alpha$ . The maximum limit of the voltage  $V_d$  will be defined by the value of  $\alpha = 0^\circ$ . i.e. when the rectifier is a theoretical diode converter with firing angle equal to zero. In reality, a minimum value of about  $\alpha = 2-5$  degs, is normally required to ensure that the converter valves have a minimum positive voltage for tuning on.

Once  $\alpha_{\min}$  is reached, no further voltage increase is possible and the rectifier will operate at that mode. This mode is known as Constant ignition angle (CIA) [22].

## 2. Constant current (CC) characteristic –

The converter valves have limited thermal inertia, and therefore cannot carry a large current over their rated value for any extended period of time.  $I_d$  constant current characteristic is a straight line as shown in figure 2.29 above.

### Inverter mode of operation

#### 1. $\gamma$ minimum characteristic at inverter (CEA) –

$$V_{di} = V_{d0r} \cos \gamma - R_{ir} I_d$$

Above equation defines the characteristic at the inverter; although there are two possibilities, the minimum extinction angle ( $\gamma$ ) option is utilized generally. The line shown in figure 2.29 above defines this mode of operation. The slope of this line is usually more pronounced than the corresponding one for the rectifier due to the relative strength of the inverter-end AC system. This characteristic curve is referred to as Constant Extinction angle control mode (CEA).

#### 2. Constant current characteristic (CC)

In order to maintain a unique operating point of the DC link, defined by the cross over point of the characteristics of the rectifier and inverter, a current margin of  $\Delta I_d$  is normal for the current orders given to the rectifier ( $I_{dor}$ ) and inverter ( $I_{doi}$ ) i.e.  $I_{dor} - I_{doi} = \Delta I_d$ .

However, the current demanded by the inverter  $I_{di}$  usually less than the current demanded by the rectifier  $I_{dr}$  by the current margin  $\Delta I$  which is typically about 0.1 pu; its, magnitude is selected to be large so that the rectifier and inverter constant current modes do not interact due to any current harmonics which may be superimposed on the DC current. This control strategy is termed the current margin method [22].

If the AC side rectifier voltage decreases significantly, the DC current starts to decrease. Eventually, this causes the output of the CC controller of the inverter to decrease. The firing angle order given by the CC controller of the inverter becomes less than the firing angle order given by CEA controller of the inverter. Thus, the inverter will operate in CC control mode. The CEC (Current Error Control) give a smoother transition between the CC and CEA control modes. A small decrease in the rectifier AC side voltage will cause quite a large change in the operating point. By using the CEC a more gradual change in the operating point is possible [23].

### 3. Voltage dependent current order limit (VDCL) –

This modification is made to limit the DC current as a function of either the DC voltage or in some cases, the AC voltage. This modification assists the DC link to recover from the faults. This limit is associated to low voltage conditions. Under these circumstances, it is desirable to reduce the maximum DC current available in order to reduce the reactive power demand and prevent commutation failures [16]. The characteristic is illustrated in figure 2.30.

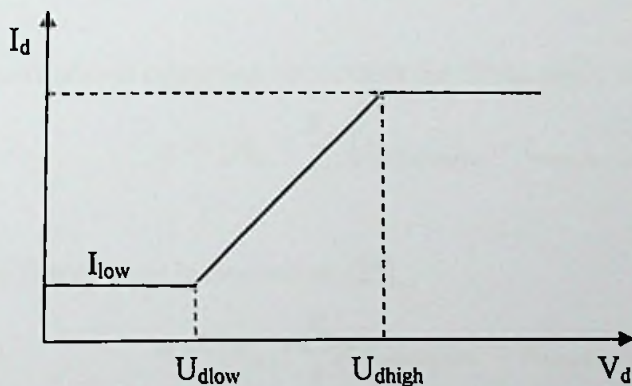


Fig 2.30: VDCL characteristic

If there is a fault in the inverter end voltage would decrease greatly, if the VDCL is not activated, power control mode will increase the current to keep the power constant. Increased current will increase the reactive power consumption of converter; it will increase the risk of subsequent commutation failures if the AC system is relatively weak.

If the DC voltage reaches the threshold value, current order is decreased down rapidly to pre-defined lower value to prevent the consecutive commutation failure during inverter side AC fault [23].

#### 4. $\alpha_{\min}$ limit at inverter [16]

The inverter is usually not permitted to operate inadvertently in the rectifier region, i.e. a power reversal occurring due to say an inadvertent current margin sign change.

### 2.5.3. Control block diagrams

Following are the open loop control systems shown for each control characteristic of rectifier and inverter. Following are the transfer functions which were used in the control block diagrams.

#### 1. Controller circuit

The controller is usually the PI controller [24]. When the measured current is larger than the ordered value, the PI controller acts to increase the firing angle  $\alpha$ , thus decreasing the current to the ordered value and vice versa. The transfer function is,

$$K_p + \frac{K_i}{s}$$

If the converter is operating as rectifier the firing angle order is expressed as,

$$\alpha = \left(K_p + \frac{K_i}{s}\right)(I_{reference} - I_{measured})$$

Inverter firing angle is derived as [25],

$$\alpha = \left(K_p + \frac{K_i}{s}\right)(Y_{minimum} - Y_{measured})$$

#### 2. Measured circuit [24]–

The current is measured through a measuring circuit which can be represented by a first order circuit. The transfer function is,

$$\frac{G}{1 + Ts}$$

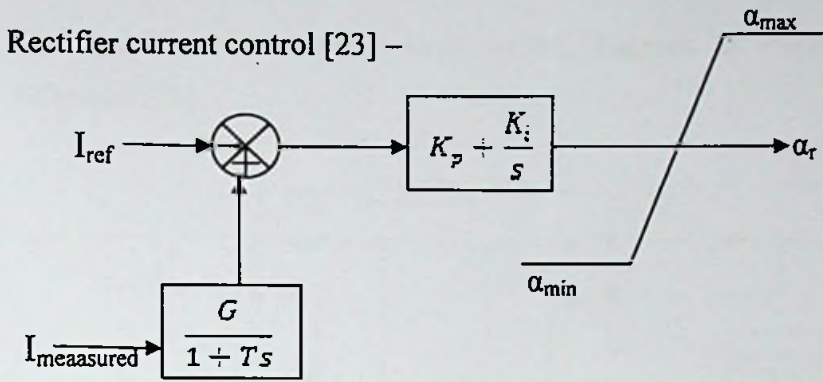


Fig 2.31: Rectifier current control block diagram

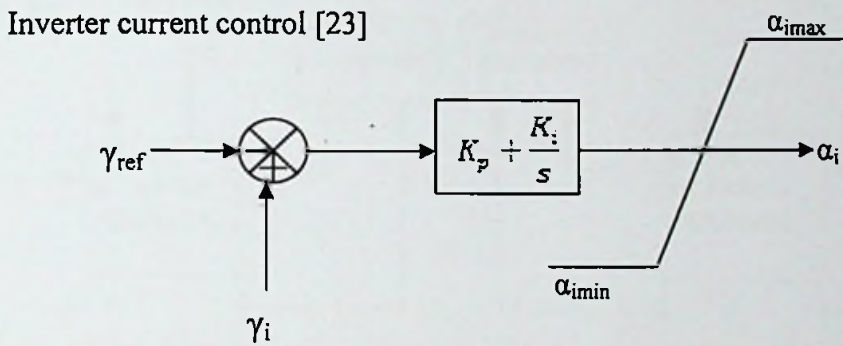


Fig 2.32: Inverter gamma control block diagram

Selection between CC and CEA control modes for the inverter [23]

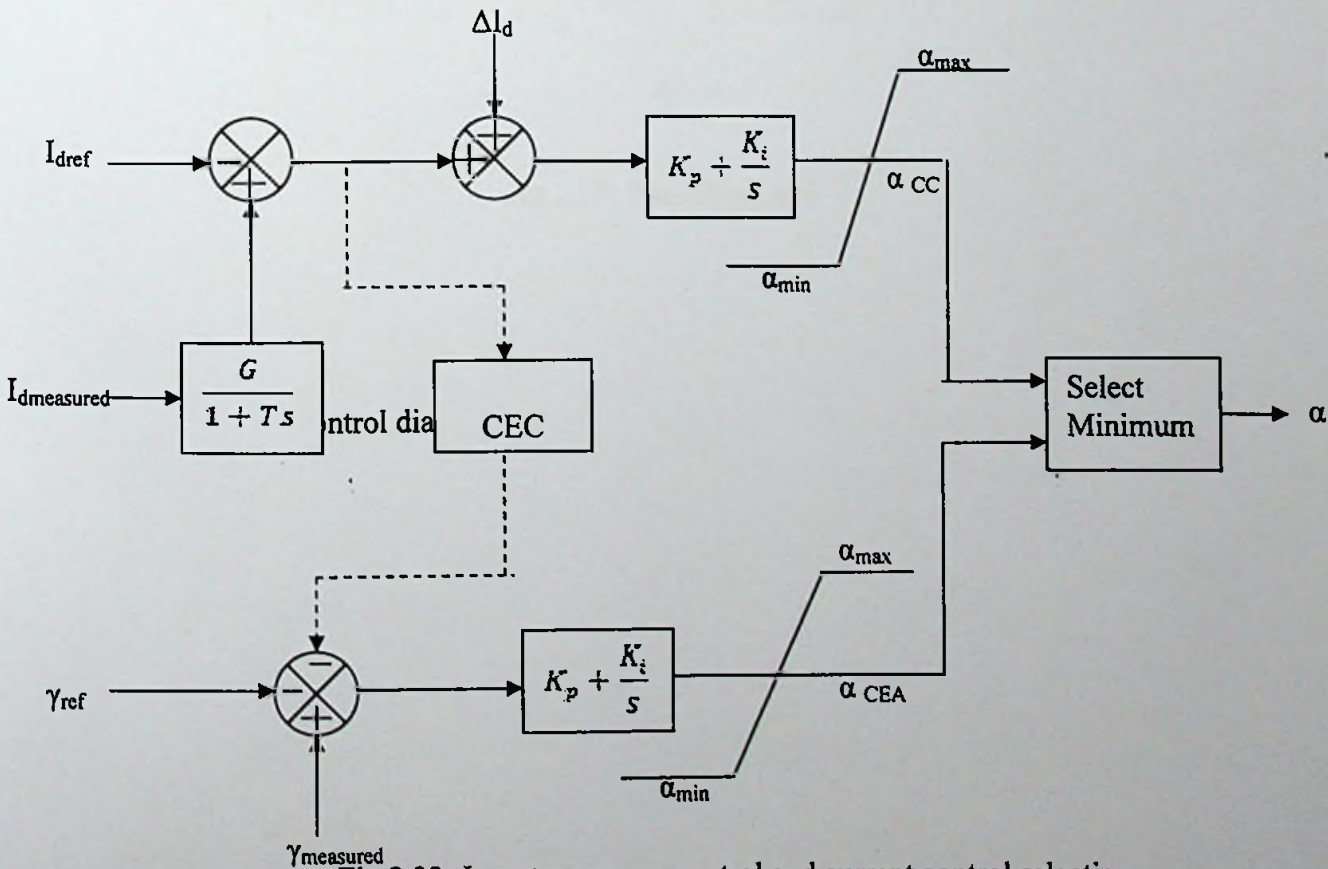


Fig 2.33: Inverter gamma control and current control selection

Figure 2.34 comprehensive total control diagram is extracted from the reference [23].

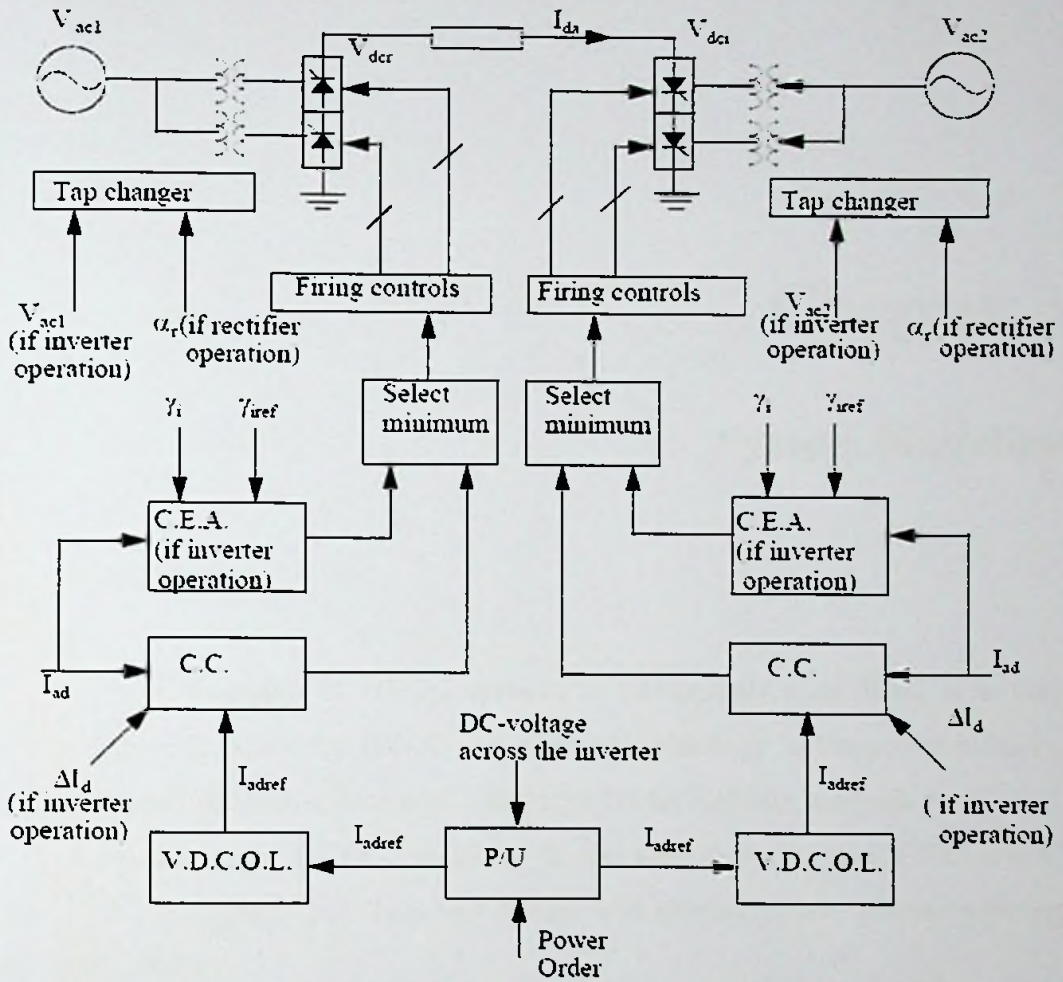


Fig 2.34: Overall control



# Chapter 3

---

## System Modeling

### 3.1 Introduction

The analytical modeling of HVDC systems is traditionally considered as a very difficult task [25]. Since the HVDC is a matured technology in the power industry, different analytical models have been developed for the stability analysis.

An important step in HVDC modeling is the development of CIGRE HVDC benchmark test system [26]. This test system was primarily used as the modeling basis in this thesis.

Other than that, there are similar models that have been developed for particular stability studies same like this thesis study. Reference [27] modeled AC network with generators in thevenin sources behind its transient impedances. Reference [25] provides HVDC-HVAC analytical models built for small signal stability analysis and verified the results with the CIGRE HVDC benchmark test system on PSCAD/EMTDC responses. Reference [25] also taken as a guidance for the modeling HVDC-HVAC network in this thesis.

In reference [28] it has categorized the HVDC models. According to the level of modeling of DC line and DC controls HVDC models are usually categorized in to three.

1. Simple model
2. Response model
3. Detailed model

The simple model is using where do not have significant impact on the results of the stability analysis. The DC link is represented as constant active and reactive power injections at the converter buses or represented by the static converter equations and the interface between AC and DC systems is treated in a manner similar to power flow analysis.

Response model has more detail than simple model and less detail than detailed model. The DC line represents only by resistance and omits the effects by capacitance and the inductance of the transmission line. The pole control action is assumed to be instantaneous. This model provides a compromise between simulation accuracy and modeling efficiency.

Detailed model provides the detailed descriptions of the DC line and controls. The DC line represents by its resistive and capacitive effects and pole controls represents different control options such as constant current control, constant extinction angle control, constant direct current control etc.

This thesis modeled HVDC-HVAC detailed model for more accurate stability analysis on PSCAD/EMTDC software with the steady state response model features.

### **3.2 System condition selection for modeling**

In the section 2.0 literature survey, there were several options available to implement this proposed HVDC interconnection in between India and Sri Lanka. For this thesis it is necessary to select the optimum choices of the main system conditions so as to make feasible the implementation. This section discusses the options selected under the following main system conditions.

1. Power transfer technology
2. HVDC configuration

### 3. Selection of terminus points of two AC systems power network

#### 1. Power transfer technology

There are two basic converter technologies in modern HVDC transmission systems namely (1) Current Source converter (CSC) and (2) Voltage Source Converter (VSC). Both technologies were compared and analyzed in section 2.3 comprehensively. Both technologies have pros and cons. However, based upon that analysis, CSC technology was selected as converter technology for HVDC link implementation in this thesis. The selection Comparisons of two technologies are given in Table 3.1 [19], [29].

Table 3.1-Comparison of Two Conversion Technologies for optimum modeling purpose

Attribute	CSC technology classic	VSC technology Light/Plus
Max converter rating at present (range for converter selection)	6400 MW, ± 800 kV (Overhead lines)  (wide range)	350 MW, ± 150 kV(cable)  (Narrow range)
Typical converter losses	2.5-4.5%	4-6%
Reliability indexes	Reliability/Availability proven	No formal records available present
Per MW cost	40-60 kEUR/MVA	50-70 kEUR/MVA
Technology maturity	More than 54 projects by 2010	About 11 projects by 2010

Based upon the above table 3.1 comparison, it was decided that CSC technology is the optimum selection for the proposed HVDC interconnection between India and Sri Lanka. CSC technology is the matured, reliable and economical option available compared to the VSC technology.

#### 2. HVDC configuration

There are 3 HVDC configurations available and the each configuration analysis is done in section 2.4. Following are the 3 configuration options available.

##### 1. Monopolar configuration

2. Bipolar configuration
3. Back to back configuration

For the HVDC implementation it was selected monopolar technology to transfer 500 MW power over one transmission line because, according to the reference [30] it is proposed in first phase to implement 500 MW transfer through monopolar HVDC link. Therefore, it is selected the monopolar configuration in this thesis.

### 3. Selection of terminus points of two AC systems power network

According to the section 2.2.2, there are 4 alternatives that have proposed for India-Sri Lanka HVDC interconnection.

1. Madurai-Anuradhapura HVDC interconnection (MAI- HVDC)
2. Tuticorin - Puttalam HVDC interconnection (TPI-HVDC)
3. Madurai-Puttalam HVDC interconnection (MPI HVDC)
4. Madurai-Anuradhapura HVDC interconnection (MAI\_BBDC) Back-to- back interconnection

In reference [30], the cost based analysis has done and following is the table 3.2 extracted from it.

Table 3.2: Investment costs for proposed HVDC configurations

Option	Investment cost (USD-M)
MAI-HVDC	116/153
TPI-HVDC	153/175
MP-HVDC	138/156
MAI-HVDC	140

Based upon the above cost analysis, it was selected MAI- HVDC for the transmission line implementation in the model. According to that, Madurai-Anuradhapura HVDC interconnection (MAI- HVDC) comprises of following sub sections.

- overhead HVDC transmission line from Madurai to Dhanushkodi (200 km)

- An under-sea HVDC (submarine cable) transmission line from Dhanushkodi to Talaimanar (30 km)
- An overhead HVDC transmission line from Talaimanar to Anuradhapura (150km)

### 3.3 Steady State mathematical Modeling

This single- infeed HVDC interconnection is modeled as India is feeding scheduled 500 MW power to Sri Lankan network at New Anuradhapura bus-bar under rated 400 kV DC voltage. The modeled complete system is illustrated in figure 3.1.

#### 3.3.1. Assumptions

For the modeling and analysis purpose, this study made the following assumptions.

- Master control is at the inverter terminal
- 400 kV is inverter terminal DC voltage
- India feeds 500 MW to Sri Lanka
- Transformer reactance ( $X_c$ ) is 0.18 pu.
- Tap changer of transformers is avoided and has constant transformer ratio
- At the steady state operating point, rectifier firing angle is  $20^\circ$  and inverter extinction angle is  $18^\circ$ .
- Governor action is neglected
- Rectifier AC bus is an infinite bus

All the parameters of the modeled system were derived using mathematical differential and algebraic equations extracted from references [21], [22], [27], [29], [31], [32], [33]. Each equation is mentioned at the relevant modeled sub system.

In the equations labels r and i denote rectifier and inverter quantities respectively.

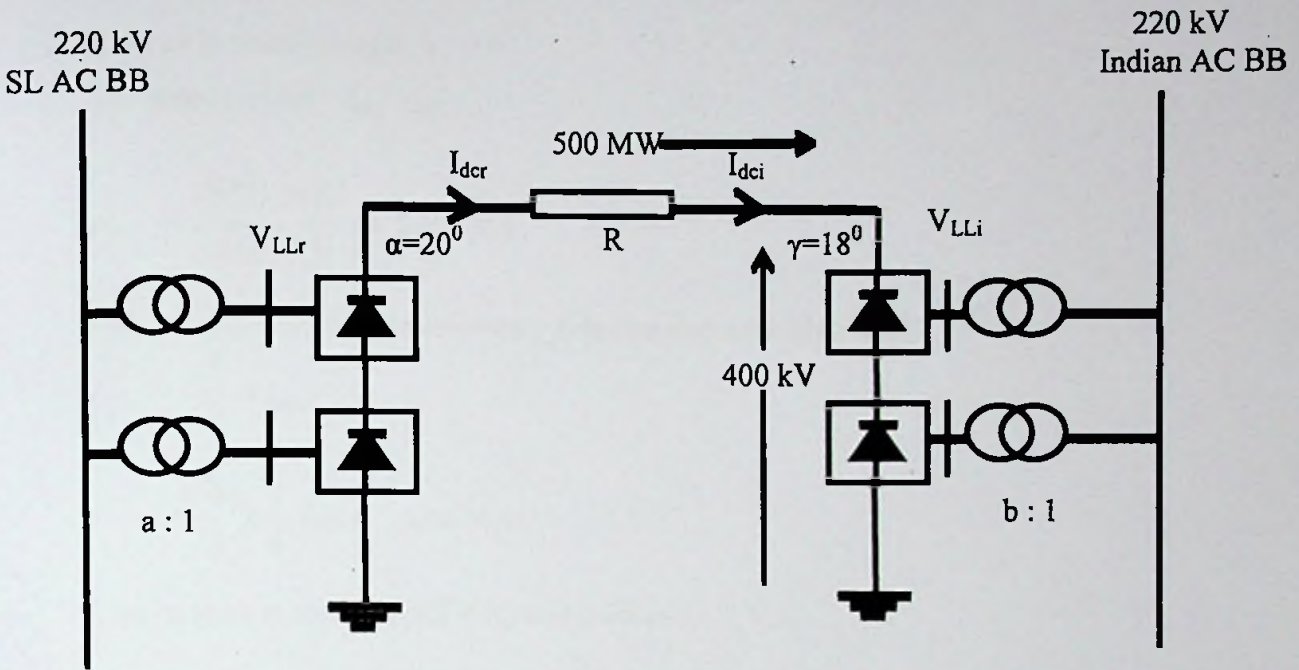


Figure 3.1: Modeled HVDC network

### 3.3.2. Converter transformer parameter calculation

A 12-pulse converter has 2 six-pulse converter bridges connected in series; one supplied by a star-star transformer and the other by a star-delta transformer, in order to provide  $30^\circ$  phase shift for 12 – pulse operation. The reactance is taken as 0.18 p.u. To limit the fault surge current in the thyristor valves to an acceptable level, a transformer reactance is specified as 15% in reference [34]. However, in the first benchmark model for HVDC control studies has used transformer reactance 18% [26]. Hence, for this study, it is used, 18% as the transformer impedance. HVDC converters are usually built as 12- pulse circuits. This is a serial connection of two fully controlled 6-pulse converter bridges and requires two 3-phase systems which are spaced apart from each other by 30 electrical degrees. The phase difference effected to cancel out the 6-pulse harmonics on the AC and DC side.

#### 3.3.2.1. Inverter Transformer steady state parameters calculation

DC power to be delivered = 500 MW

DC voltage level at inverter busbar = 400 kV

Rectifier firing angle ,  $\alpha = 20^\circ$

Inverter extinction angle,  $\gamma = 18^\circ$

DC rated current  $I_{dci} = I_{dcr}$

$$I_{dci} = \frac{500 \text{ MW}}{400 \text{ kV}} = 1.25 \text{ kA}$$

rms value of transformer secondary side line current (valve side)

$$I_{LLi} = \frac{\sqrt{2}}{\sqrt{3}} \times I_{dci}$$

$$= \frac{\sqrt{2}}{\sqrt{3}} \times \frac{5}{4} \text{ kA} = 1.0206 \text{ kA}$$

Line voltage (valve side) of inverter transformer =  $V_{LLi}$

MVA of each transformer =  $S_{Ti} = \sqrt{3} \times V_{LLi} \times I_{LLi} = \text{Base MVA}$

$$S_{Ti} = \sqrt{3} \times V_{LLi} \times I_{LLi} = 1.768 V_{LLi}$$

$$\text{Base impednace } Z_{base i} = \frac{V_{LLi}^2}{S_{Ti}} = \frac{V_{LLi}}{1.768} = 0.5657 V_{LLi}$$

Transformer leakage reactance ( $X_L$ ) =  $0.18 \text{ pu} = 0.18 \times Z_{base i}$

$$= 0.18 \times 0.5657 V_{LLi} = 0.1018 V_{LLi}$$

$$\text{Voltage across 6-pulse bridge} = \frac{400 \text{ kV}}{2} = 200 \text{ kV}$$

$$U_{dr} = U_{dTo} \cos(\alpha) - I_{dr} R_{cj}$$

$$200 = 1.35 V_{LLi} \cos(\gamma) - \frac{3 \times I_{dci} \times X_{Li}}{\pi}$$

$$= 1.35 V_{LLi} \cos(18^\circ) - \frac{3 \times 1.25 \times 0.1018 V_{LLi}}{\pi}$$

$$= 1.28393 V_{LLi} - 0.12152 V_{LLi}$$

$$= 1.16242 V_{LLi}$$

$$V_{LLi} = 172.06 \text{ kV}$$

Rating of the inverter transformer,  $S_{Ti} = 304.2 \text{ MVA}$

Turns Ratio

$$Y/\Delta \text{ transformer} = b = \frac{220}{\sqrt{3}} / 172.06$$

$$Y/Y \text{ transformer} = b = \frac{220}{\sqrt{3}} / 172.06$$

### 3.3.2.2. Rectifier Transformer steady state parameters calculation

Cable resistance =  $5 \Omega$

$$\text{Voltage drop} = I_{dci} \times R = 1.25 \times 5 = 6.25 \text{ kV}$$

$$\text{Cable loss (} P_{\text{cable}} \text{)} = I_{dci}^2 \times R = 7.8125 \text{ MW}$$

DC power to be delivered ( $P_{dcr}$ )

$$\begin{aligned} P_{dcr} &= P_{dci} + P_{\text{cable}} \\ &= 500 + 7.8125 = 507.8125 \text{ MW} \end{aligned}$$

DC voltage level ( $V_{dcr}$ )

$$\begin{aligned} V_{dcr} &= V_{dci} + V_{\text{drop}} \\ &= 400 + 6.25 = 406.25 \text{ kV} \end{aligned}$$

DC rated current ( $I_{dcr}$ )

$$I_{dcr} = \frac{P_{dcr}}{V_{dcr}} = 1.25 \text{ kA}$$

rms value of the secondary line current (valve side) ( $I_{LLr}$ )

$$I_{LLr} = \frac{\sqrt{2}}{\sqrt{3}} \times I_{dcr} = 1.0206 \text{ kA}$$

Line voltage (valve side) of the rectifier transformer =  $V_{LLr}$

MVA of each transformer ( $S_{Tr}$ )

$$S_{Tr} = \sqrt{3} \times V_{LLr} \times I_{LLr} = \text{Base MVA}$$



$$= \sqrt{3} \times V_{LLr} \times 1.0206 = 1.768V_{LLr}$$

Base impedance =  $Z_{base}$

$$Z_{base} = \frac{V_{LLr}^2}{0.5657 V_{LLr}}$$

Transformer leakage reactance ( $X_L$ )

$$X_L = 0.18 pu$$

$$= 0.18 \times 0.5657V_{LLr}$$

$$\text{Voltage across 6-pulse bridge} = \frac{V_{dcr}}{2} = \frac{406.25}{2} = 203.125 kV$$

$$\frac{V_{dcr}}{2} = 1.35 \times V_{LLr} \times \cos(\alpha) - \frac{3 \times I_{dcr} \times X_{Lr}}{\pi}$$

$$\frac{406.25}{2} = 1.269V_{LLr} - 0.1215V_{LLr}$$

$$203.125 = 1.147V_{LLr}$$

$$V_{LLr} = 177.08 kV$$

Transformer rating ( $S_{Tr}$ )

$$S_{Tr} = 1.768 \times 171.18$$

$$= 313.08 MVA$$

Turns Ratio

$$Y/\Delta \text{ transformer} = a = \left[ \frac{220}{\sqrt{3}} \right] / 177.08$$

$$Y/Y \text{ transformer} = a = \left[ \frac{220}{\sqrt{3}} \right] / 177.08$$

### 3.3.3. Rectifier side AC network

The Indian network is represented by the thevenin's equivalent voltage source. The modeled thevenin system is comprehensively illustrated in figure 3.2. The assumed strength of the Indian network is 5 for steady state modeling purpose. The strength of

the system is given in terms of the Short circuit ratio SCR levels as shown in table 2 [22].

Category AC system	SCR range	ESCR range
Weak	< 3	< 3
Intermediate	3 to 5	2 to 3
Strong	> 5	> 3

Table 3.3: Selection of AC system strength based on SCR

In this research paper it is assumed that Indian network is intermediately a strong network. SCR mentions how strong the AC system is relative to the HVDC link.

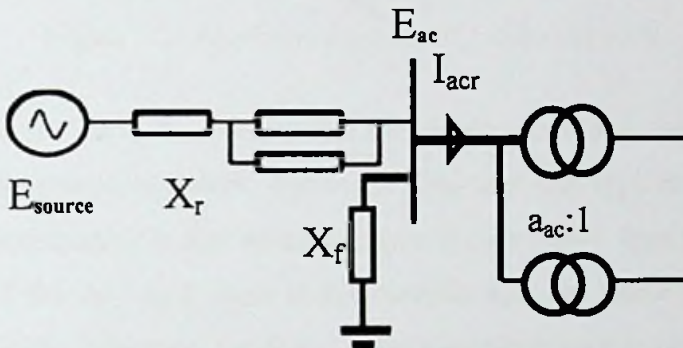


Figure 3.2: rectifier side schematic diagram

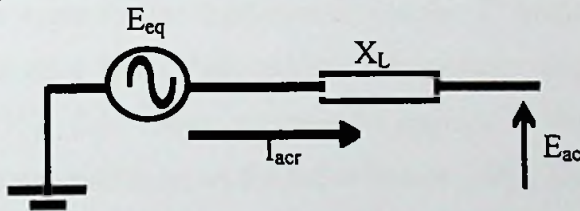


Figure 3.3: Equivalent network of above Indian network

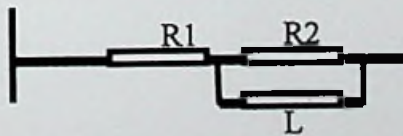


Figure 3.4: Thevenin's equivalent impedance of Indian network

The equivalent Indian voltage source modeled on PSCAD is shown above figure 3.4. The algebraic diagram of the network is represented in figure 3.5.

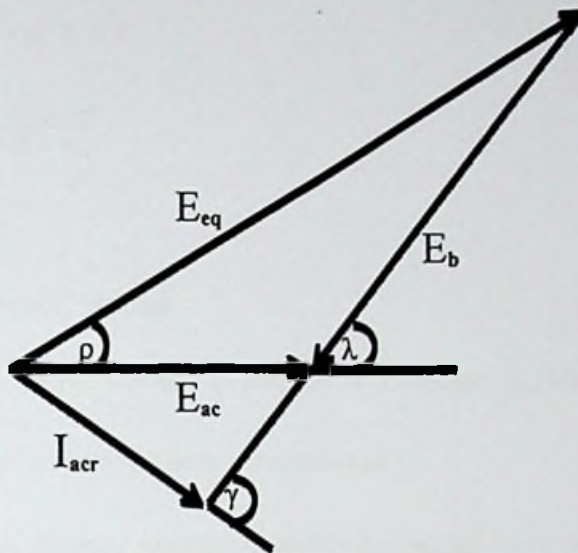


Figure 3.5: Algebraic diagram of Indian network

To represent rectifier side AC network, this paper uses R-R-L impedance type as the equivalent thevenines network. Reference [26] uses that type for the stability study purpose. Accordingly, in this research paper, it uses R-R-L type ( $R1 + R2//L$ ) for the modeling of the AC equivalent at the rectifier side for stability analysis purpose. According to the reference, the R-R-L type sometimes uses to obtain more easily the same impedance angle for the fundamental and the 3<sup>rd</sup> harmonic (in this thesis 84<sup>o</sup> same as for reference [26]). The maximum impedance angle should be in 75-85 degrees range [35]. This thesis, assumes 84 degrees as the maximum impedance angle at the rectifier side same as for the reference [26]. The calculation is derived from reference [25]. The requirement is to find  $E_{source}$  voltage.

$$SCR = \frac{MVA}{P_{dc}}$$

$$\begin{aligned} MVA &= SCR \times P_{dc} \\ &= 5 \times 500 \\ &= 2500 \end{aligned}$$

$$MVA = \frac{V_{ac}^2}{x_L}$$

$$2500 = \frac{220^2}{x_L}$$

$$I_{acr} = I_{dc} \times \frac{\sqrt{6}}{\pi} \times a_{ac} \times \sqrt{2}$$

$$\cos \rho_{ac} = \cos \alpha - \frac{R_c \times I_{dc} \times \pi}{6\sqrt{3} \times E_{ac}}$$

$$6\sqrt{3} E_{ac} = 3\sqrt{2} E_{LL}$$

$E_{LL}$  = Line to line rms AC voltage

$\rho_{ac}$  = angle between the AC current  $I_{ac}$  and the AC voltage  $E_{ac}$  for rectifier

$R_c = \frac{3x_c}{\pi}$  = equivalent commutation resistance

$x_c$  = equivalent transformer reactance at fundamental frequency

$E_b = |I_1| \times |X_L|$  = voltage drop across the AC system equivalent

$X_L$  = thevenin impedance

$$X_L = |X_L| \angle \zeta = \frac{X_r \times X_f}{(X_r + X_f)}$$

$$\lambda = \zeta - \rho$$

$\zeta$  = constant

$\lambda$  =  $E_b$  voltage phase angle

$$|E_{sq}|^2 = |E_{ac}|^2 + 2|E_{ac}||E_b| \cos \lambda + |E_b|^2$$

$$E_{eq} = E_{source} \times \frac{X_f}{(X_r + X_f)}$$

$E_{eq}$  = thevenin voltage

$E_{source}$  = constant voltage source of rectifier side

Table 3.4: Rectifier thevenin network parameters

System data used for the calculation	Final Parameters calculated
SCR = 5	R1 = 1.758 $\Omega$
V <sub>ac</sub> = 220 kV	L = 0.07602 H
I <sub>dc</sub> = 1.25 kA	E <sub>source</sub> = 244.76 kV
a <sub>ac</sub> = 177.08 / 220/ $\sqrt{3}$	
$\alpha = 20^{\circ}$	
E <sub>ac</sub> = 220/ $\sqrt{6}$ kV	
Xc = 0.18 pu	
$\tau = 84^{\circ}$	
R2 = 2160.633 $\Omega$	

### 3.3.4. Sri Lankan model

Proposed transmission network for 2017 AC power system for HMNP (Hydro Maximum Night Peak) [36] as a case study for the model. Modeled AC network is shown in figure 3.6 below. It was modeled only with the 132 kV and 220 kV transmission network. Transmission lines were modeled as Bergeron model [37]. The loads were modeled as constant impedance loads for the stability studies [38]. It was modeled as transformers are not saturated. The synchronous generators modeled with the simplified exciter characteristics since the generator excitation systems respond is important in maintaining transient stability [39]. As the actual power system, it used the relevant DC exciter or AC exciter or the static exciter for the relevant power plant generator modeled. It was taken that synchronous generators has one field coil on d- axis and one damper coil on q- axis. The governors did not added to synchronous generators since governor effect on transient stability of the AC network is negligible [40]. Therefore, the power output of the generators is constant under all conditions of change of load angle and speed. This research study primarily focused on the transient stability of the AC-DC interaction on inverter side.



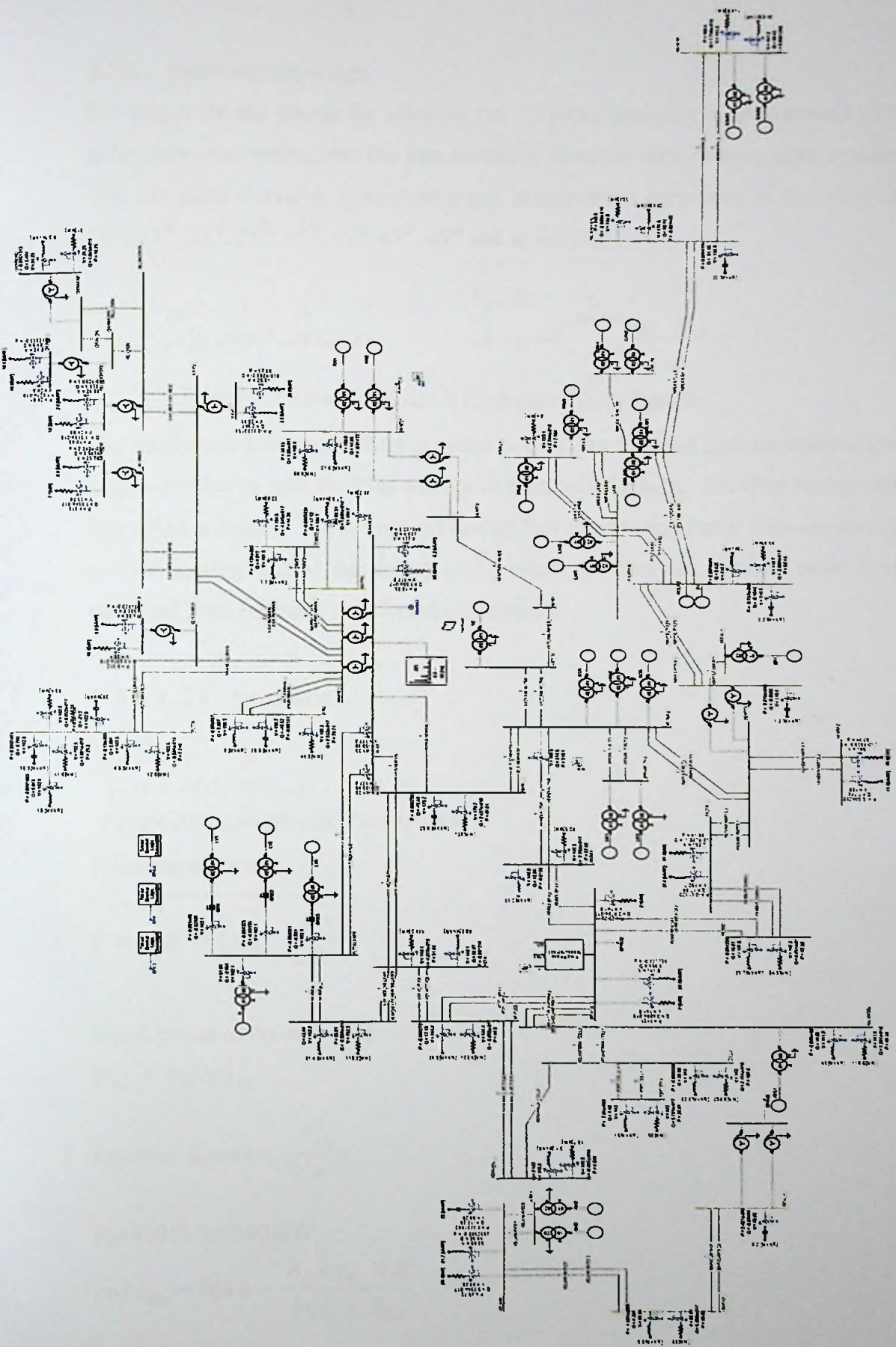


Figure 3.6: Modeled Sri Lankan network

### 3.3.5. Filter circuit design

For this study the reason for selecting the 12 pulse converter system instead of 6 pulse converter system was the less harmonic filtration with cheaper filter system. The 12- pulse converter system generates characteristic harmonics of the order of 11<sup>th</sup>, 13<sup>th</sup>, 23<sup>rd</sup>, 25<sup>th</sup>, 35<sup>th</sup>, 37<sup>th</sup>, 47<sup>th</sup>, 49<sup>th</sup> and so on. [33]

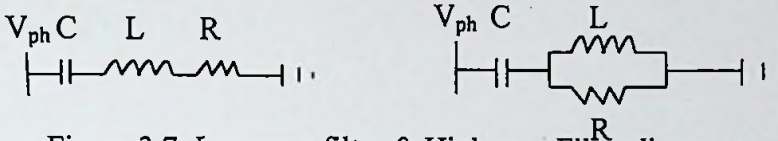


Figure 3.7: Low pass filter & High pass Filter diagrams

The single tuned low pass filters are used to filter out 11<sup>th</sup> and 13<sup>th</sup> harmonics. The high pass filter is used for 23<sup>rd</sup> and above harmonic filtration. The filter circuits are illustrated in figure 3.7. The required quality factor and tuning factor were selected as per the requirement of the design [41]. Capacitor cost and inductor costs were extracted from reference [42] for the calculations.

#### 3.3.5.1. 11<sup>th</sup> harmonic

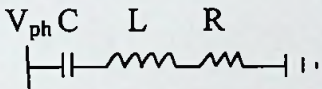


Figure 3.8: Low pass filter components

Filter impedance

$$Z = \sqrt{R^2 + \left(\omega L - \frac{1}{\omega C}\right)^2}$$

Rated power of the converter

$$P_{dn} = V_{dn} \times I_{dn}$$

$$\text{reactive power} = \frac{V_{ph}^2}{Z^2 \omega C}$$

$$P_n = 400 \times 1.25 = 500 \text{ MW}$$

$$\cos \rho_{ac} = \cos \alpha - \frac{R_c \times I_{dc} \times \pi}{6\sqrt{3} \times E_{ac}}$$

$$\cos(\rho_{ac}) = 0.867$$

$\rho_{ac}$  = angle between the AC current  $I_{ac}$  and the transformer primary side AC voltage

$E_{ac}$  for rectifier

Full load fundamental AC line current =  $I_L$

$$I_L = \frac{P_{d1}}{3V \cos \rho_{ac}} = \frac{500}{3 \times 0.867 \times \frac{220}{\sqrt{3}}} = 1.513 \text{ kA}$$

11<sup>th</sup> harmonic current from one bridge of the converter

$$= \frac{1513}{11 \times 2} = 68.77 \text{ A}$$

$$k = A.S + \frac{B}{S}$$

k = cost (k\$)

S = size (Mvar)

A, B constants (k\$/Mvar and k\$.Mvar respectively)

$U_C, U_L$  = unit cost of capacitor and inductor respectively

h = harmonic number

$$A = U_C + \frac{U_L}{h^2} = 20^c + \frac{45}{11^2} = 20.37 \times 10^5 \text{ Rs/MVar}$$

$$B = V_1^2 \times I_{hf}^2 \times (U_C + U_L) \\ = \left(\frac{220}{\sqrt{3}}\right)^2 \times \frac{68.77^2 \times 65}{11} \times 10^{-6} \times 10^5$$

$$= 45.086 \times 10^6 \text{ RsMVar}$$

$$S_{min} = \sqrt{\frac{45.086 \times 10^6}{20.37 \times 10^5}} = 4.705 \text{ MVar/ph is the size for minimum cost.}$$

Capacitance C

$$C = \frac{S_{min}}{\omega_1 \times V_1^2} = \frac{4.705 \times 10^6}{314.16 \times \left(\frac{220}{\sqrt{3}}\right)^2 \times 10^6} = 0.928 \mu\text{F}$$

$$L = \frac{1}{C(h\omega_1)^2} = \frac{10^6}{0.928 \times (11 \times 314.16)^2} = 0.0902 \text{ H}$$

$$\omega_1 = 2\pi f$$

V1 = fundamental voltage

Q = quality factor of inductor or sharpness of tuning of filter

Finding Optimum Q for impedance angle ( $\phi_m$ ) of the rectifier AC network

$$\phi_m = 84^\circ$$



$\delta$  = deviation of frequency from tuned frequency

$\delta_m$  = maximum value of  $\delta$

For each tuned filter branch, there is an optimum value of  $Q$ , depending on the assumed values of maximum frequency deviation  $\delta_m$  and maximum network impedance angle  $\phi_m$ . [42]

Optimum  $Q$  for impedance angle  $85^\circ$  is,  $\frac{0.55}{\delta_m}$  as derived from the reference [42],

$\delta_m$  is taken as 0.02

$$Q = \frac{0.55}{0.02} = 27.5$$

Resistance of the filter

$$R = \frac{1}{Q_0} \sqrt{\frac{L}{C}} = \frac{1}{27.5} \times \sqrt{\frac{0.0502}{0.928 \times 10^{-8}}} = 11.337 \Omega$$

13<sup>th</sup> harmonic filter also calculate in the same manner.

### 3.3.5.2. Second order HP filter

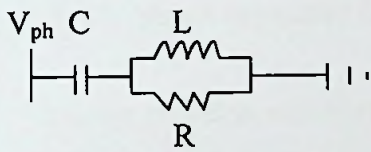


Figure 3.9: High pass Filter components

Filter impedance

$$Z = \frac{1}{j\omega C} + \left( \frac{1}{R} + \frac{1}{j\omega L} \right)^{-1}$$

Defining following quantities

Resonant frequency

$$\omega_r = \frac{1}{\sqrt{LC}}$$

Per unit frequency

$$f = \frac{\omega}{\omega_r}$$

$$\text{Characteristic impedance } X_C = \sqrt{\frac{L}{C}}$$

$$\text{Quality factor } Q = \frac{R}{X_C}$$

HP filter for 23<sup>rd</sup> and above harmonics filtration.

$$\therefore \omega_r = 23 \times 50$$

For 2<sup>nd</sup> order HP filter, the quality factor is in the range of  $Q = 0.7-1.4$ , and have capacitive reactance at fundamental frequency and low predominantly resistive, impedance over a wide band of higher frequencies [42].

Selected Reactive power requirement for HP filter = 100 MVar

$$C = \frac{100/3}{\left(\frac{220}{\sqrt{3}}\right)^2 \times 2\pi \times 50} = 6.577 \mu\text{F}$$

$$L = \frac{1}{C \omega_r^2} = \frac{10^6}{(2\pi \times 50 \times 23)^2 \times 6.577} = 2.912 \text{ mH}$$

$$R = Q \times X_C = Q \times \sqrt{\frac{L}{C}} = 1 \times \sqrt{\frac{2.912 \times 10^{-3}}{6.577}} = 21.04 \Omega$$

### 3.3.5.3. Shunt capacitor design

$$\begin{aligned} \text{Reactive power at rectifier side converters} &= 540 \times 0.6 \\ &= 324 \text{ MVar} \end{aligned}$$

Total reactive power supply by all shunt filters and capacitors

$$Q_{11\text{th}} + Q_{13\text{th}} + Q_{\text{HP}} + Q_C = 324 \text{ MVar}$$

$$4.705\sqrt{3} + 3.67\sqrt{3} + 100 + Q_C = 324 \text{ MVar}$$

$$C = \frac{\frac{209.5}{3}}{\left(\frac{220}{\sqrt{3}}\right)^2 \times 2\pi \times 50} = 13.778 \mu\text{F}$$

Table 3.5: Rectifier side shunt filter & capacitor parameters

	Rectifier side calculated parameters		
	R	L	C
11 <sup>th</sup> harmonic filter	11.337 $\Omega$	0.0902H	0.928 $\mu$ F
13 <sup>th</sup> harmonic filter	12.3 $\Omega$	0.0828 H	0.724 $\mu$ F
HP filter	21.04 $\Omega$	2.912mH	6.577 $\mu$ F
Shunt capacitor			13.778 $\mu$ F

Table 3.6: inverter side shunt filter parameters

	Inverter side calculated parameters		
	R	L	C
11 <sup>th</sup> harmonic filter	11.91 $\Omega$	0.0948 H	0.8836 $\mu$ F
13 <sup>th</sup> harmonic filter	12.92 $\Omega$	0.087 H	0.689 $\mu$ F
HP filter	21.04 $\Omega$	2.912 mH	6.577 $\mu$ F

### 3.3.6. DC line design

The DC line comprises with 150 km and 200 km long two overhead lines and 50 km long submarine cable. However, due to some limitations the existing blocks for overhead lines and cables couldn't model altogether. Therefore, the overhead lines were modeled as two resistors and submarine cable modeled with the cable block in PSCAD library. Modeled DC system is illustrated in figure 3.10. The overhead line parameters were derived from ACSR Moose conductor [43]. The submarine cable parameters were derived from mass impregnated cable with 1500 mm<sup>2</sup> where used the same cable for the similar interconnection built between Tasmania and Australia [44].

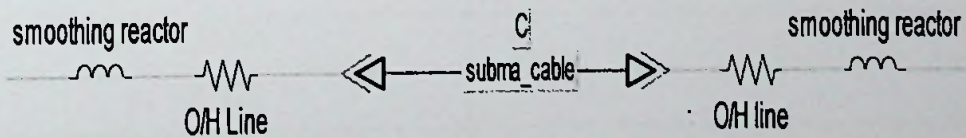


Figure 3.10: DC transmission line with smoothing reactors

### 3.3.7. DC smoothing reactor

The smoothing reactor is an essential part of the DC transmission network. It is always connects in series with each pole of each converter station. These reactors

ensure that overcurrent transient occurring during an inverter commutation failure or a DC line fault is kept within limits acceptable to the valves [34]. The calculation is derived from the reference [41].

$$\cos \beta_n = \cos \gamma_n - \frac{I_d}{I_{s2}}$$

$$\Delta I_d = 2I_{s2}(\cos \gamma_m - \cos(\beta - 1)) - 2I_d$$

$$\Delta t = \frac{\beta - 1 - \gamma_m}{360f}$$

$$L_d = \frac{\Delta V_d \Delta t}{\Delta I_d}$$

$$I_{s2} = \frac{\sqrt{3}V_m}{2X_{cj}}$$

$\sqrt{3}V_m$  = peak line voltage on secondary (valve) side of the converter transformer

$\Delta V$  = rated voltage per bridge

$\gamma_n$  = operating extinction angle

$\gamma_m$  = the minimum extinction angle to be permitted as a result of DC voltage

$\beta_n$  = normal ignition advance angle

$L_d$  = DC reactor

Table 3.7: DC smoothing reactor parameter

System data used for the calculation	Calculated parameter
$\gamma_n = 18^\circ$	$L_d = 0.705 \text{ H}$
$I_d = 1.25 \text{ kA}$	
$\gamma_m = 8^\circ [2]$	
$f = 50 \text{ Hz}$	
$\Delta V = 200 \text{ kV}$	

### 3.3.8. HVDC control system

#### 3.3.8.1. Master control

This system is modeled as manually set the power order. It is assumed in this study that the master control is at inverter terminal. So the manually operated power order values at inverter master control are notified to rectifier side slave control system to change the firing angle as required.

#### 3.3.8.2. HVDC characteristic curve

The figure 3.12 illustrates the HVDC control characteristic curve modeled for this study. The complete description of the HVDC characteristic curve modeled in this thesis is presented in section 2. 5. 2. The measuring circuit transfer function (used in each control block diagram) parameters were derived from the reference [45]. Rectifier characteristic curve comprises with constant ignition angle (CIA) curve and Constant current control (CC) curve. For the CIA curve, the rectifier firing angle  $\alpha$  was taken as  $5^\circ$  which is the minimum value of  $\alpha$  ( $\alpha_{min}$ ) for rectifier side converters to ensure that the converter valves have a minimum positive voltage for turning on [42]. The CIA characteristic curve and CC characteristic curve mathematically is shown in below equations 12 respectively.

$$U_{dro} \cos(\alpha_{min}) - I_{dr} R_{cr}$$

$$U_{dro} \cos(\alpha) - I_{dr} R_{cr}$$

Inverter characteristic curve comprises of Constant Extinction Angle (CEA), Constant Current Control (CC), Voltage dependent current control (VDCL) and Maximum alpha control mode. CEA curve and CC characteristic curve mathematical representation is shown in equation 13 respectively.

$$U_{dio} \cos(\gamma_{min}) - I_{dr} R_{ci}$$

$$U_{dio} \cos(\gamma) - (I_d - \Delta I) R_{cr}$$

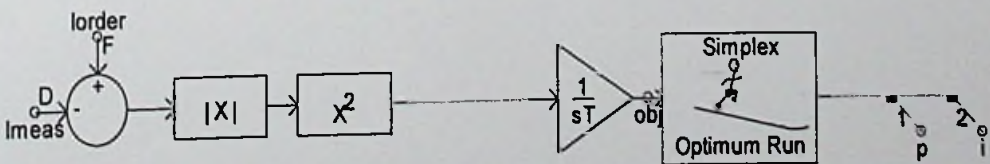


Figure 3.11: Rectifier Current controller optimizing block diagram

At the steady state condition, the rectifier and inverter operate at the interception point in the characteristic curve. At the interception, the rectifier operates at  $20^\circ$  and inverter operates at  $18^\circ$ .

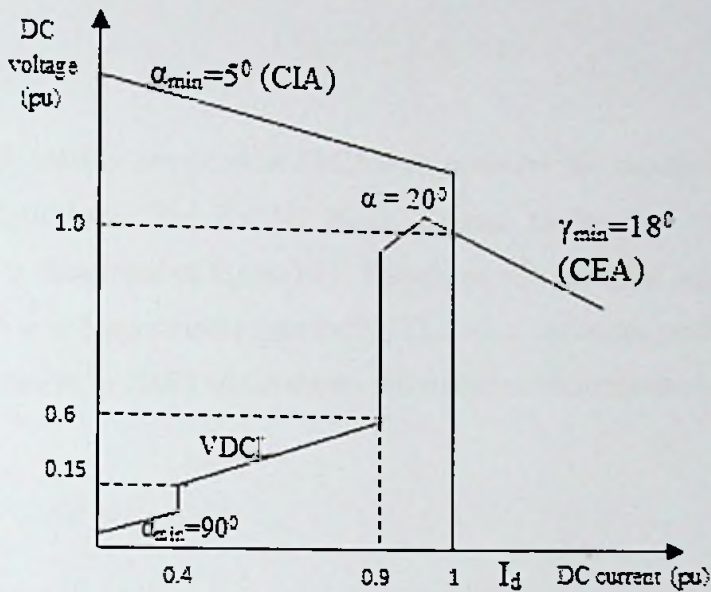


Figure 3.12: Characteristic curve of the modeled system

### 3.3.8.3. Controller optimization

There are three controllers in operation [16] in HVDC system. They are Rectifier current controller, inverter current controller and inverter gamma controller. Before any test of the system, it is recommended to optimize all these three controllers [16]. For that it is necessary to tune up the controller parameters. In HVDC control system, it uses PI controller as its regulator. HVDC control system uses PI controller popularly because it is the simplest and robust controller for complex nonlinear and dynamic systems [24]. The objective of tuning the PI controller is to find the optimum proportional (P) and integral (I) parameters as it gives the correct response as the set value. The relationship between the angle and the P and I parameters are as below.

Rectifier firing angle [12]

$$\left(k_{pr} + \frac{k_{ir}}{s}\right)(I_2 - I_d)$$

Inverter firing angle [12]

$$\left(k_{pi} + \frac{k_{ii}}{s}\right)(\gamma_0 - \gamma)$$

There is the facility provided in PSCAD to optimize the parameters by executing different algorithms. The PSCAD block diagram modeled to tune up the P & I parameters is illustrated in figure 3.11. This paper used simplex algorithm to find the optimum P and I parameters iteratively. The used optimum performance index is integral square error (ISE) which shows the mathematical representation below

$$ISE = \int_0^T e(t)^2 dt$$

T is the simulation time which is longer time than settling time [24]. In the optimizing process, it finds the parameters P and I that minimize the above objective function. The simplex optimum run control block for rectifier side current controller was configured [46] as shown in figure 3. The objective function is the square of the error between current order and the measured current at rectifier side.

# Chapter 4

---

## AC-DC interaction

Integration of DC part in to the AC system makes the interaction more complex. The relationship between HVDC link and the AC system which is connected to, can be considered in two categories. [34]

### A. Dependency of line commutated converter upon the stiffness of the terminal voltage

Out from the two basic technologies of current source converter (CSC) and voltage source converters (VSC) which are using in modern HVDC transmission, this work is selected CSC technology. The type of valve commutation used for the study is the basic natural commutation technique (line commutation technique). [16]. There is an inherent weakness of the selected natural commutation technique. It is that, the commutation is depending upon the stiffness of the terminal AC voltage. [47]

### B. Active power and reactive power delivery between AC system and DC system

If the DC link power transmission is relatively large compared to AC network there is a significant influence on both AC system and DC power transmission.

The AC-DC interaction can be analyzed using the above mentioned two aspects; AC terminal voltage stiffness and active/reactive power delivery in between the interaction. Both of them are depending upon the strength of the AC network.



The strength of the AC system is determined by following two factors [34].

1. AC system impedance
2. AC system inertia

The AC system is defined as weak from two aspects [48].

1. AC system impedance may be high relative to DC power at the point of connection
2. AC system mechanical inertia may be inadequate relative to the DC power infeed.

The interaction between AC and DC systems becomes more pronounced as the impedance of the AC system, as seen from the convertor AC terminals, is increased for a particular DC power. It follows that even a relatively small DC link connected to a point of the AC system having high impedance may have considerable effect on the local AC network, even if the latter may be part of a large AC system [48].

As the commutation of the thyristor valves depend upon the stiffness of the AC voltage, the converters cannot work properly if the connected AC system is weak [47]. If the AC system impedance is high, then the system is considered as weak which leads the AC voltage to be sensitive to power variation of the DC link [47].

If a system receives all or most of its power from a DC link, the inertia of the receiving system may be inadequate, so that upon the interruption of the DC infeed, due to any cause, the system voltage may decrease to unacceptably low values [48].

The aspects related to AC-DC interaction are needed to be carefully analyzed using dedicated analyzing phenomenon. There are several ways to study about the AC-DC interaction as, power, voltage and frequency instabilities; harmonic resonance-related instabilities; sub synchronous torsional interactions; temporary overvoltage and recoveries from AC and DC faults [48]. The phenomenon that is of commonly utilized in planning stage of HVDC-HVAC system interaction is voltage and power stability.

In relation to the AC voltage stiffness and active/reactive power delivery in between the interaction, there are several tools to measure quantitatively and qualitatively the voltage and power stability of AC-DC interaction. Following are the extracted tools which have taken in to consideration in this research study. [43, 50, 51].

1. Short circuit ratio
2. Maximum power availability
3. Time domain behavior

#### 4.1. Short Circuit Ratio (SCR)

SCR is an indication for how strong is the AC system in relation to the HVDC link [21]. The higher the system impedance and the lower the system damping for a given HVDC inverter, it is the greater the effect of the inverter mal-operation on the AC system [34]. In practice, the SCR is used as an indicator to compare relative strength of the AC system with the rated capacity of the HVDC link [21].

In SCR definition, it is the ratio of the AC system short circuit capacity Vs. the DC rated power of the HVDC link [48]. The definition is more comprehensive by figure 4.1.

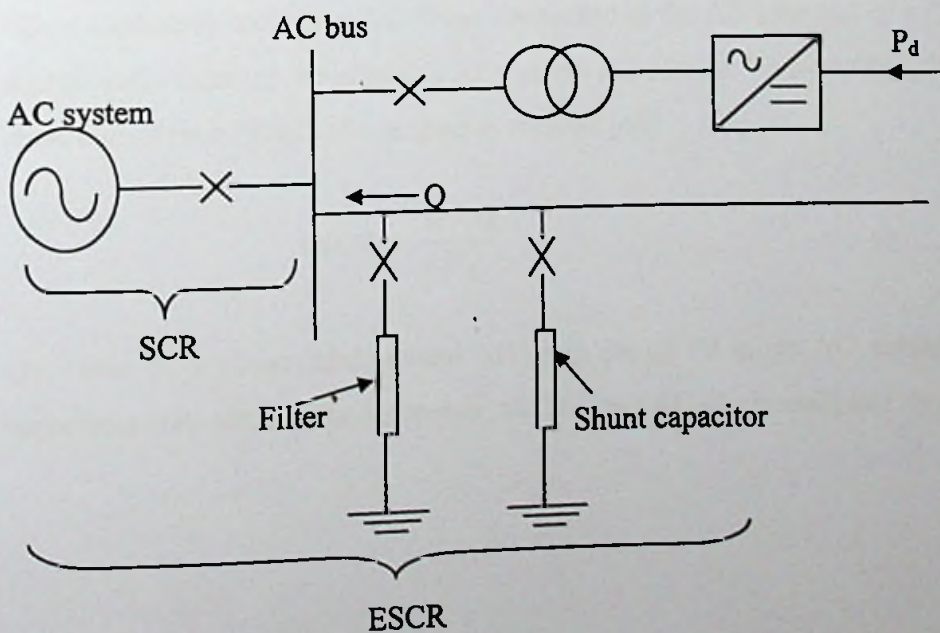


Fig 4.1: Defining SCR and ESCR

$$SCR = \frac{\text{Short circuit level of AC system (MVA)}}{\text{DC power } P_d \text{ (MW)}}$$

$$SCR = \frac{S}{P_d}$$

$S$  = AC system 3 phase symmetrical short circuit level at convertor terminal AC bus bar with 1.0 pu AC terminal voltage

$P_d$  = Rated DC power

The Short circuit level (SCL) of an AC system is

$$SCL = \frac{V_{AC}^2}{Z_{AC}}$$

$V_{AC}$  = AC system voltage

$Z_{AC}$  = short circuit impedance

$$SCR = \frac{V_{AC}^2}{P_d \times Z_{AC}}$$

Shunt capacitors including AC filters connected at the AC terminal of a DC link can significantly increase the effective AC system impedance. To allow this, the effective short circuit ratio (ESCR) is defined as follows [48].

$$ESCR = \frac{S - Q}{P_d}$$

$Q$  = value of 3 phase fundamental MVar in pu of  $P_d$  at pu AC voltage of shunt capacitors connected to the convertor AC bus bar (AC filters and plain shunt banks)

SCR as a guide for planning HVDC link –

AC system should have high fault level at the terminal substation and low equivalent impedance to ensure satisfactory operation of converters and HVDC power flow. From the viewpoint of the HVDC system performance, it is more meaningful to consider the ESCR which includes all the filters and shunt capacitors etc [22,23]. For HVDC link, the AC system is classified as strong, intermediate or weak depending on SCR value [22,23]. Table 4.1 below is the categorizing of the AC system strength with respect to HVDC link. This classification provides a simple assessment of AC/DC interaction problems.

Category AC system	SCR range	ESCR range
Weak	< 3	< 3
Intermediate	3 to 5	2 to 3
Strong	> 5	> 3

Table 4.1: Categories of AC systems based on SCR

#### 4.2. Maximum Power Curve (MPC)

In reference [48], the Maximum power curve is simply defined as, the maximum power that can be obtained by increasing DC current while not controlling the AC voltage.

The general definition, as defined in reference [48] is shortly stated here again.

For a given AC system impedance and other parameters of the AC/DC system shown in figure 1.37, there will be a unique  $P_d/I_d$  characteristic, shown in figure 1.38, provided the starting conditions are defined as in the following paragraph. Additionally, it is assumed that  $I_d$  changes almost instantaneously in response to the change of  $\alpha$  of the rectifier; for example due to a change in current order.

All other quantities AC system emf,  $\gamma$  (minimum) of the inverter, tap changers, AVR, and the value of shunt capacitors and reactors are assumed not to have changed. When considering the inverter power capability, it is also assumed that the rectifier provides no limitation to the supply of DC current at rated DC voltage. Each

subsequent point is calculated by steady state equations. These “quasi- steady state” characteristics give a good indication of dynamic performance.

The Starting conditions are defined to be as follows:

$$P_d = 1.0 \text{ pu}, U_d = 1.0 \text{ pu}, \text{ and } I_d = 1.0 \text{ pu}$$

( $P_d$  =DC power;  $U_L$ = AC terminal voltage-i.e., converter transformer line-side voltage;  $U_d$ =DC voltage of the inverter; and  $I_d$ =DC current)

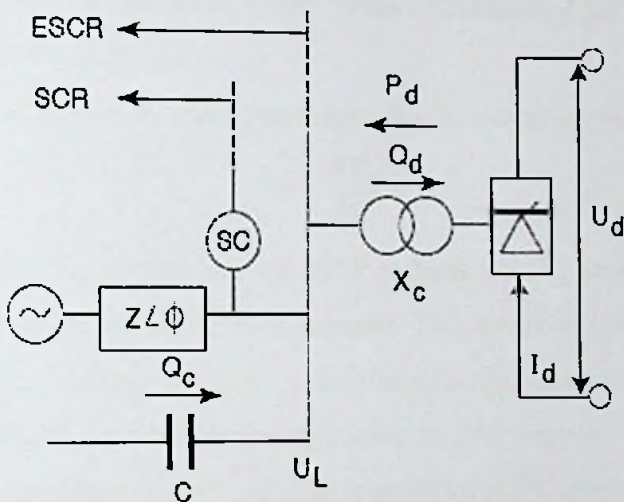


Figure 4.2: Simplified representation of a dc link feeding an AC system with shunt capacitors (Cs) and synchronous compensators (SCs) (if any) at converter station bus-bars

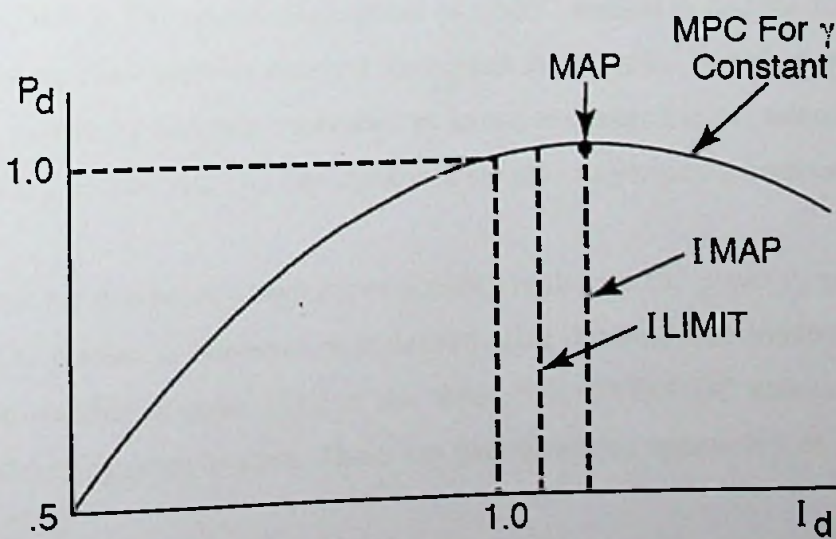


Figure 4.3: DC power - dc current curve for  $\gamma$  minimum

If the inverter is operating at minimum constant extinction angle  $\gamma$ , the resulting curve will represent maximum obtainable power for the system parameters being considered. This curve is termed the Maximum Power Curve (MPC). Any power can be obtained below MPC by increasing  $\alpha$  and  $\gamma$ , but power higher than MPC can be obtained only if one or more system parameters are changed-e.g by reduced system impedance, increased system emf, larger capacitor banks, etc.

A similar MPC curve can be obtained for the rectifier at minimum constant  $\alpha$ .

An MPC exhibits a maximum value, termed Maximum Available Power (MAP) as can be seen in fig. 2.2.

This is defined as the DC power corresponding to a direct current  $I_{MAP}$  where [49],

$$\frac{dP_d}{dI_d} = 0$$

The increase of the current beyond MAP reduces the DC voltage to a greater extent than the corresponding DC current increase. This could be counteracted by changing the AC system conditions-e.g. by controlling the AC terminal voltage. It should be noted that  $dP_d/dI_d$  is positive for operation at DC currents smaller than  $I_{MAP}$ , the current corresponding to MAP;  $dP_d/dI_d$  is negative at DC currents larger than  $I_{MAP}$ .

#### 4.2.1. QMPC Vs DMPC

The above definition of MPC curve is actually for the Quasi static maximum power curve (QMPC). The crucial assumption of QMPC method is that the thevenin AC voltage magnitude remains constant throughout the analysis. Therefore, it represents the AC system by thevenin equivalent so as not to change the AC terminal voltage. The HVDC control and DC line dynamics are also neglected for computing QMPC [49].

The Dynamic maximum power curve (DMPC) is also the DC power  $P_d$  as a function of the DC current  $I_d$ . However, it is derived using dynamic time simulations with a transient stability program [51]; in this thesis, PSCAD/EMTDC software based on the modeled dynamic system. There are two derivation approaches to operate the system [51].

## 1. Nominal-one DMPC

The system is initially in steady state under nominal conditions i.e  $I_d$ ,  $U_L$ ,  $U_d$  are 1.0 pu. The synchronous machine terminal voltage is specified the same as that for the QMPC case with these same nominal conditions, so that comparisons between the QMPC and DMPC would be compatible. The DC current order is then ramped up and down from nominal to the appropriate upper and lower value respectively. The DC power is computed from the corresponding DC current and DC voltage time responses and the DMPC is thus obtained.

## 2. Nominal- zero DMPC

This approach is similar to above but with  $I_d$  initially zero. Then the DC current order is ramped up to the appropriate upper value and the DMPC is similarly obtained.

According to the ramp rate, DMPC is categorized in to two.

1. Fast ramp rate – Automatic DC power order change
2. Slow ramp rate- change the DC power order by the operator manually

In this thesis, only the slow ramp rate is simulated and analyzed the nominal one DMPC.

## 4.3. Time domain analysis

This thesis objective is to analyze the post fault behavior of the HVDC-HVAC interaction. Therefore, the transient period of the disturbance scenarios were simulated and analyzed the time domain results in this thesis. It is said to be transiently stable if the system can regain and maintain synchronism after a large sudden disturbance [39]. The general definition of the transient stability is applicable for DC linked network as well [48].

## 4.4. Usage of the analytical tools

The tools which are using in this research study provide useful guidance for the planning stage of the proposed interconnection.

SCR gives the idea about the strength of the AC network with respect to the proposed DC power delivery. Higher the value of SCR, stronger the AC power system relative to DC power delivery. That ensures the satisfactory operation of converters and DC power flow. SCR is not a constant for a given power system and varies with the system impedance. The classification of the AC system strength based on SCR is provided in table 4.1. Through a comprehensive analysis of different scenarios of the AC-DC interaction model, the required precautions for low SCR valued conditions can be predicted.

MPC determines the power limits for the inverter or rectifier. The MPC (minimum  $\gamma$ ) is the optimum operational power curve. It gives the minimum cost due to the following factors [4]

- Minimum reactive power consumption
- Minimum ratings of valves, transformers and shunt capacitors
- Minimum generation of harmonic currents
- Minimum losses

The operating point of the inverter connected to an AC system having high SCR is will be well below MAP. The operating point is dynamic with respect to the system impedance. As impedance increases, MPC drops down to a new state and operating point is reaching towards the new MAP value. That cause to have a small margin for stable operation of the DC power delivery. The increase of current beyond MAP, DC voltage reduces the to a greater extent than the DC current increase which leads to reduce the DC power required. Through a comprehensive analysis of MPC for such scenarios, unsatisfactory situations can be overcome in the planning stage.

Time domain simulation for transient period gives the AC-DC interaction parameters behavior with respect to time for particular perturbed scenarios. This tool verifies the results obtained by SCR and MPC tools which were using in this research work.



# Chapter 5

---

## Simulation Results, Stability Analysis & Discussion

### 5.1. Introduction

In chapter 4: AC-DC Interaction, it is mentioned about 3 tools which are using for the power and voltage stability analysis of AC-DC interaction in this thesis.

1. Short circuit Ratio
2. Maximum Power Curve
3. Time domain analysis

One tool itself is not giving a comprehensive analysis for the simulation results. Hence all three tools are using in this section to analyze the results obtained for simulations.

The results analysis is categorized in to the following sections as,

1. Steady state simulation results
2. System verification
3. AC system impedance increment
4. QMPC Vs DMPC of the system
5. Perturbed scenario results analysis

The steady state simulation would verify the designed system condition. The accuracy of the modeled DC system is verified by the system verification. Modeled network AC system impedance behavior coherence with the reference models is shown by the third analysis category. Fourth analysis comply the modeled system QMPC and DMPC behaviors with the references. In fifth analysis, different perturbed scenarios were simulated and analyzed the results.

## 5.2. Steady State simulation results

### 5.2.1. Time domain simulation results

The steady state system was designed such that India feeds 500 MW at rated 400 kV DC voltage. At the operating point of the control system, rectifier firing angle is  $20^\circ$  and inverter extinction angle is  $18^\circ$ . These parameters for steady state operation were verified by the time domain results obtained in figure 5.1, 5.2, 5.3 and 5.4. Only the DC voltage has a low value than the assumption due to the tuning problem faced during the system modeling.

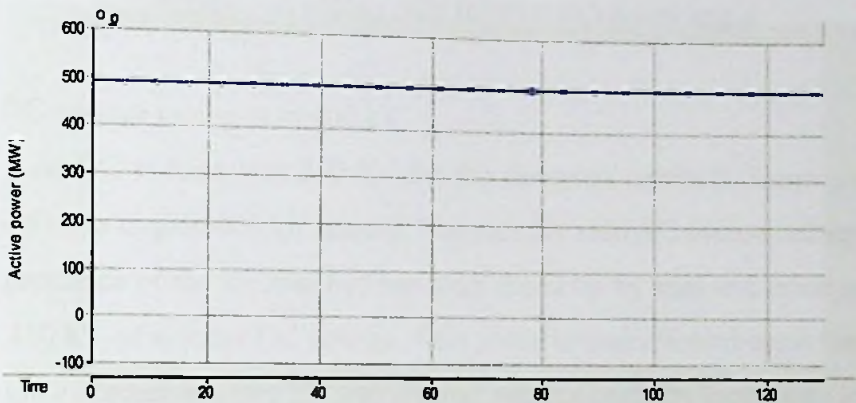


Figure 5.1: Steady state DC power

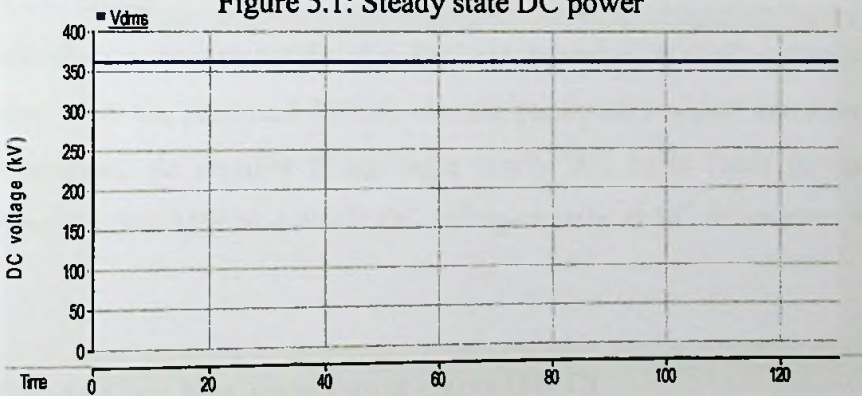


Figure.5.2: Steady state DC voltage

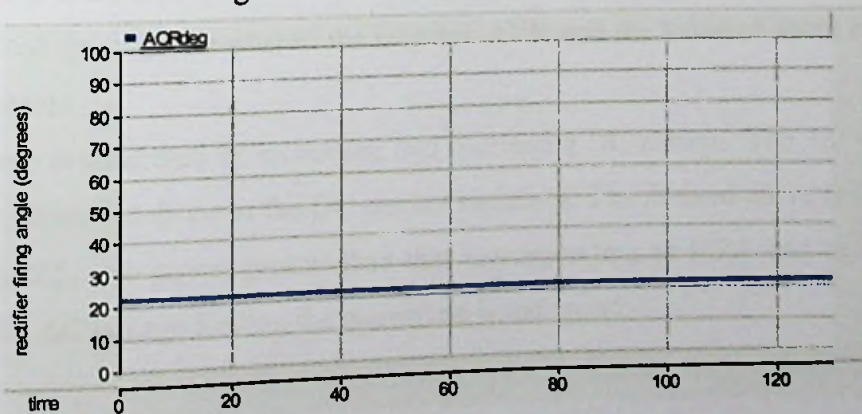


Figure 5.3: Steady state rectifier firing angle

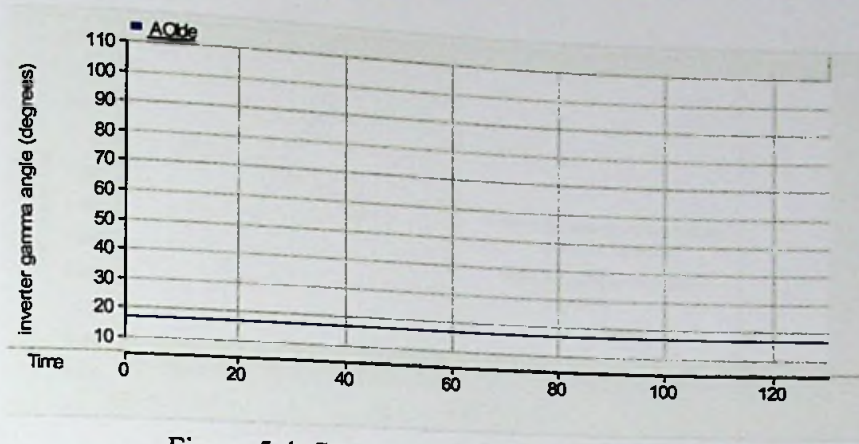


Figure 5.4: Steady state inverter extinction angle

#### 5.2.1.1. DC voltage tuning in to 400 kV

Inverter side DC voltage was 350 kV for the designed network. Some parameters were tuned so as to gain 400 kV instead. The rectifier side AC source voltage and the shunt capacitance of the inverter bus bar were tuned up by trial and error method to gain the 400 kV of inverter DC voltage. This modification affected upon the rectifier firing angle by increasing into  $22^{\circ}$  and inverter gamma angle by increasing in to  $20^{\circ}$ .

#### 5.2.1.2. Conclusion

These simulation results verify the PSCAD modeled HVDC network electric parameters with the proposed HVDC electric parameters which are using for the stability analysis. At rectifier firing angle nearly  $20^{\circ}$ , India feeds power and Sri Lanka receives 500 MW at 400 kV DC voltage nearly at  $18^{\circ}$  of inverter extinction angle.

#### 5.2.2. Steady State Maximum Power Curve (MPC)

As per the definition, the MPC was drawn under the following conditions. The AC system voltage,  $\gamma$  (minimum) of the inverter, AVR and the value of shunt capacitors are constants.

This curve is generated by increasing and decreasing DC current. The AC voltage is not controlled, but drops as the DC current increases. The derived curve is illustrated in figure 5.5. No power greater than that corresponding to MPA can be obtained, unless the AC voltage feeding the converters is increased.



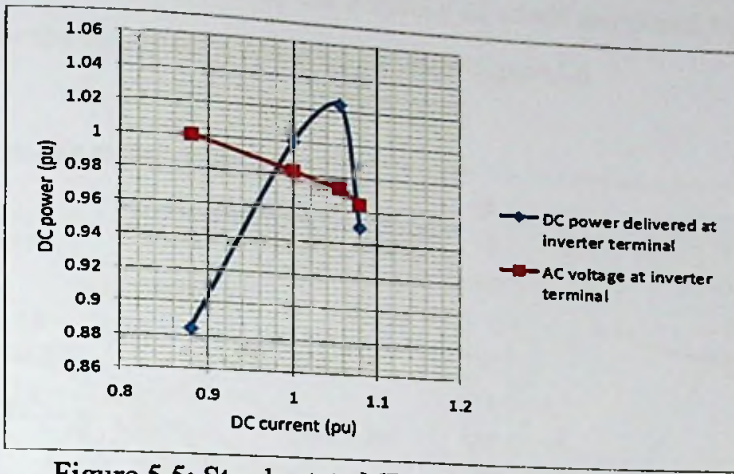


Figure 5.5: Steady state MPC and AC voltage profiles

### 5.2.3. SCR calculation for steady state condition

According to the reference [48] the sub-transient impedance of generators, load impedance, transmission line impedance and transformer reactance were used for the calculation of SCR. For the calculation of ESCR, the admittance of shunt filters and capacitors were included in to the above SCR impedance values. The definition of SCR/ESCR is mentioned in section 4.1. As per the calculation, it can be seen that the inverter terminal AC network; Sri Lankan network is a strong AC network in terms of SCR. The result is verified by the table 4.1.

$$SCR = \frac{V^2}{Z \times P_d}$$

Where;  $V = 220 \text{ kV}$ ,  $Z=16.26\Omega$ ,  $P_d= 500 \text{ MW}$

$$SCR = \frac{220^2}{16.26 \times 500}$$

$$SCR = 5.95$$

$$ESCR = \frac{V^2}{(Z + Z_c) \times P_d}$$

$$ESCR = \frac{220^2}{22.08 \times 500}$$

$$ESCR = 4.38$$

Following graph 5.6 extracted from the reference [21] uses to compare the results obtained by the simulation and calculation. The calculated SCR for the network is 5.95 which can be considered as incline more in to right side according to the

reference graph. It is proved the accuracy of result calculated by the derived MPC curve for the steady state condition in below figure 5.6.

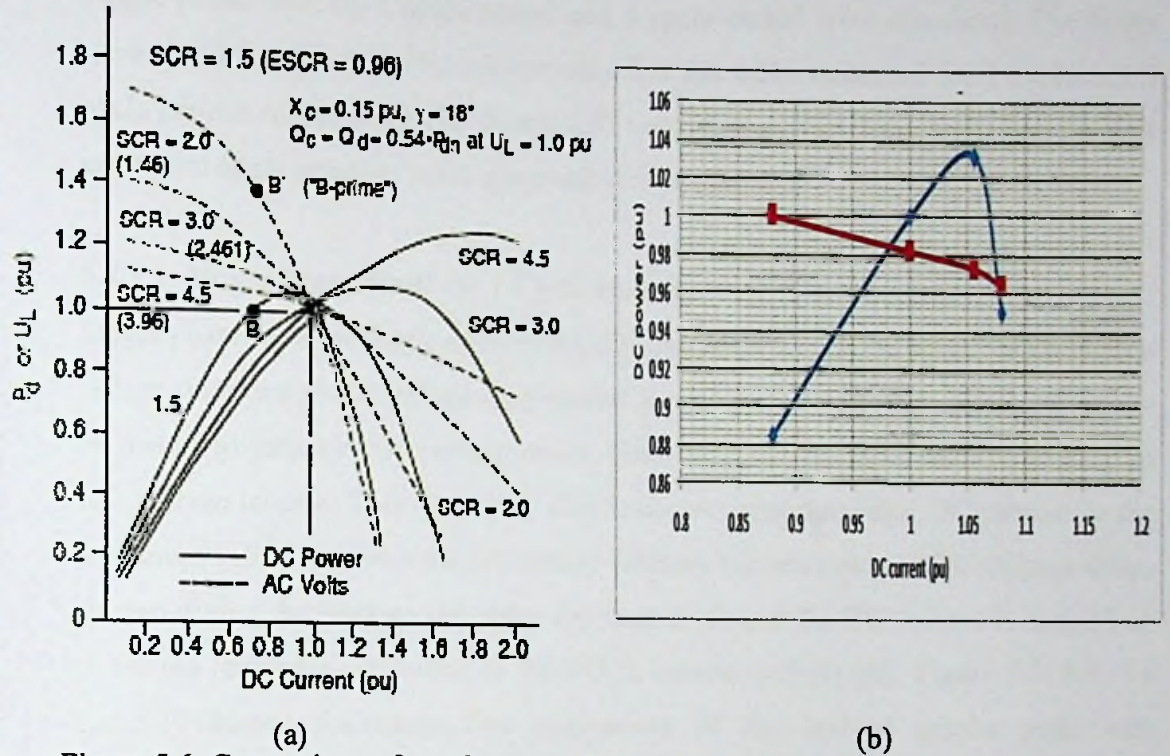


Figure 5.6: Comparison of steady state MPC curve with reference graph, (a) According to reference [22], (b) results obtained through the analysis

### 5.3. System Verification

Despite the steady state normal operation, the system should act stably under perturbed conditions as well. Several scenarios were simulated to verify that the AC-DC interaction performs stably under the system disturbances. Following are the disturbances create to proof the stable operation of the AC-DC interaction at inverter terminal side. The simulated results were compared with the time domain results in reference [16].

- Inverter side single phase fault for 1 cycle period
- Inverter side single phase fault for 5 cycle period
- Inverter side three phase fault for 5 cycle period

### 5.2.1. Inverter side AC faults

Single phase fault for 1 cycle period and 5 cycle period were simulated. The faults were applied at 14s and 15 s respectively. Let the faults sustained for 1 cycle and 5 cycle periods respectively. DC power, DC voltage, Rectifier firing angle and inverter extinction angle behavior were observed in time domain.

#### 5.2.1.1. Single Phase Fault for 1 Cycle Period

Single phase fault for single cycle in AC-DC interaction is called single commutation failure since one phase voltage drop caused for the converter commutation process to be disturbed until the AC voltage resets. This commutation failure results in drop of DC voltage to zero. This causes to VDCL control action to limit DC current to the minimum value. However the DC power delivery becomes zero as DC voltage drops to zero during the fault period. After the fault is cleared the DC current is ramped up to the pre fault level according to the VDCL control action [16]. Figure 5.7, 5.8, 5.9 and 5.10 illustrate the results. The comparison of the derived graphs plots with reference curves are illustrated in 5.11, 5.12, 5.13 and 5.14.

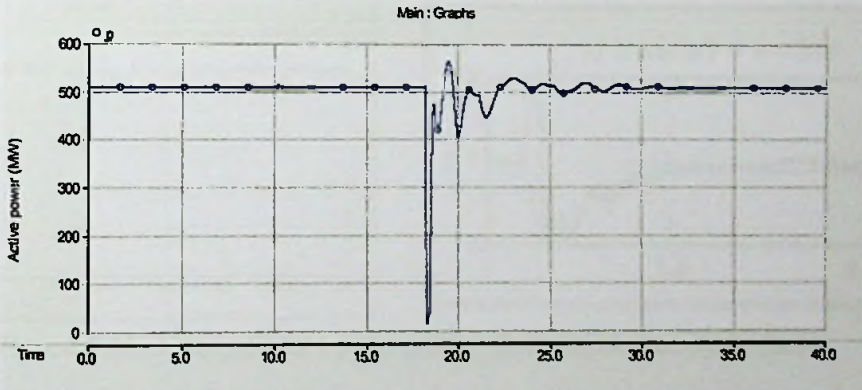


Figure 5.7: DC power at 1- phase one cycle fault

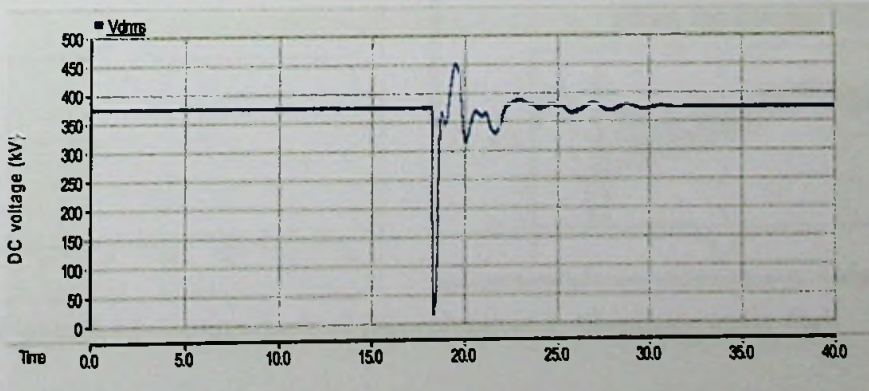


Figure 5.9: rectifier firing angle at 1- phase one cycle fault

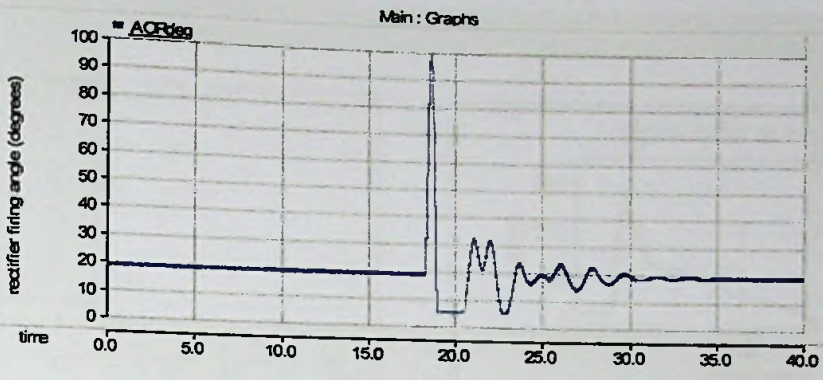


Figure 5.9: rectifier firing angle at 1- phase one cycle fault

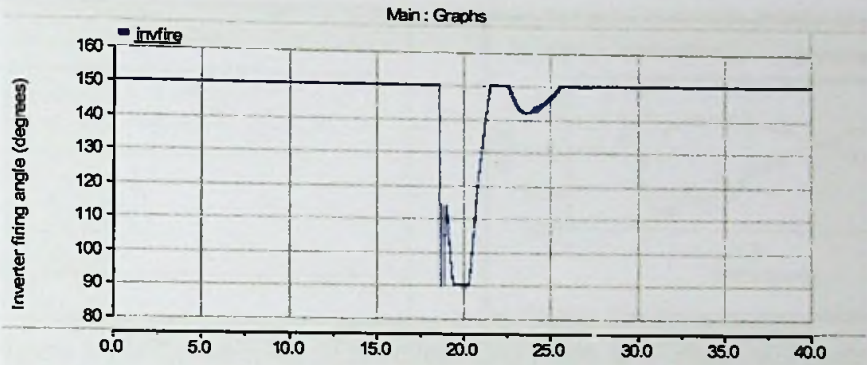


Figure 5.10-inverter firing angle at 1- phase one cycle fault

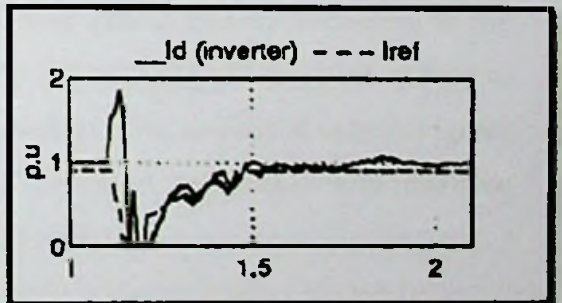
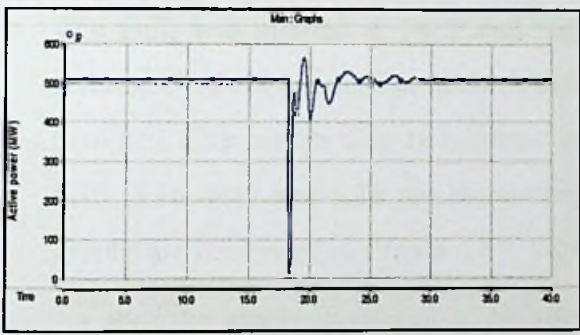


Figure 5.11- Comparison of DC power at 1- phase one cycle fault

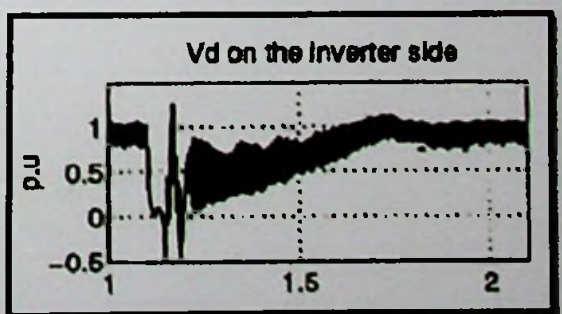


Figure 5.12- Comparison of DC voltage at 1- phase one cycle fault

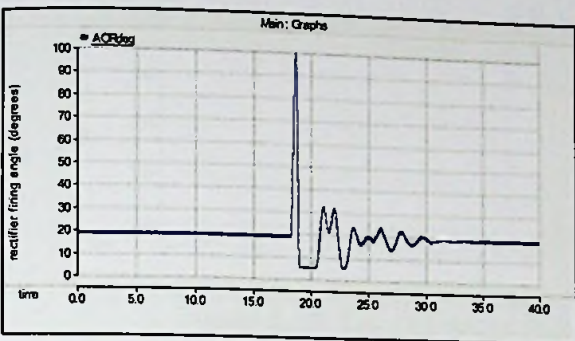


Figure 5.13- Comparison of rectifier firing angle at 1- phase one cycle fault

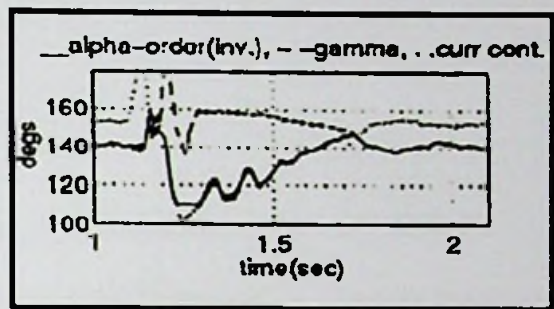
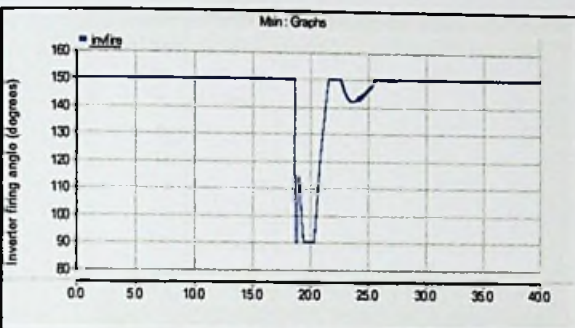
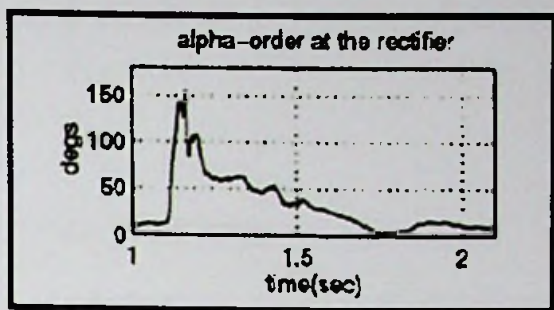


Figure 5.13- Comparison of inverter firing angle at 1- phase one cycle fault

### 5.2.1.2. Single phase fault for 5 cycle period

The single phase fault for 5 cycle period is known as multiple commutation failures. The fault was applied at 14 S and fault cleared after 5 cycles. According to the reference [16] commutation failure caused the DC voltage and DC power to drop to zero and after certain time to increase and stabilize at the scheduled values. Figures 5.15, 5.16, 5.17 and 5.18 are shown below. The results comparison with reference graphs are illustrated in figures 5.19, 5.20, 5.21 and 5.22.

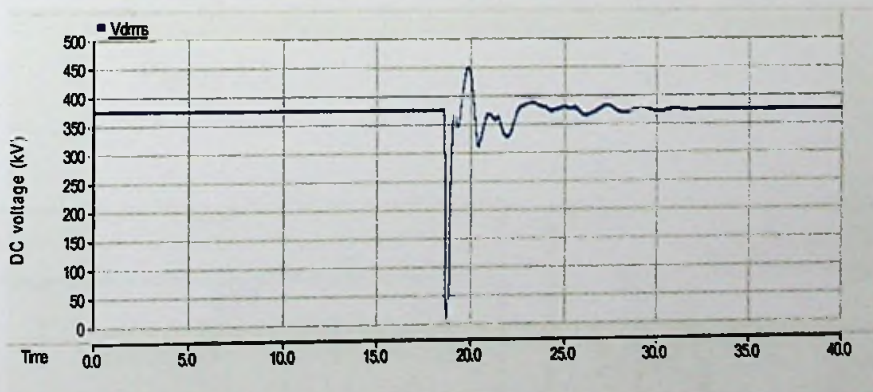


Figure 5.15: DC power at 1- phase five cycle fault



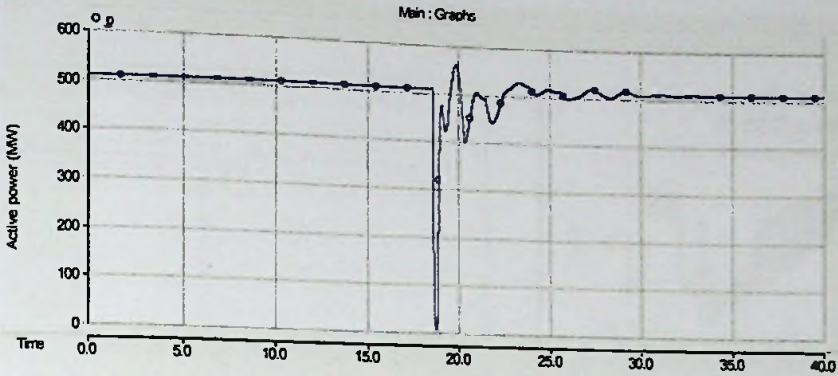


Figure 5.16: DC voltage at 1- phase five cycle fault

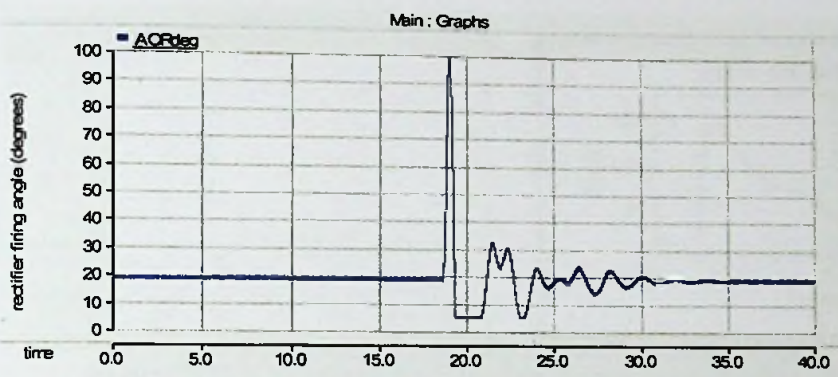


Figure 5.17: rectifier firing angle at 1- phase five cycle fault

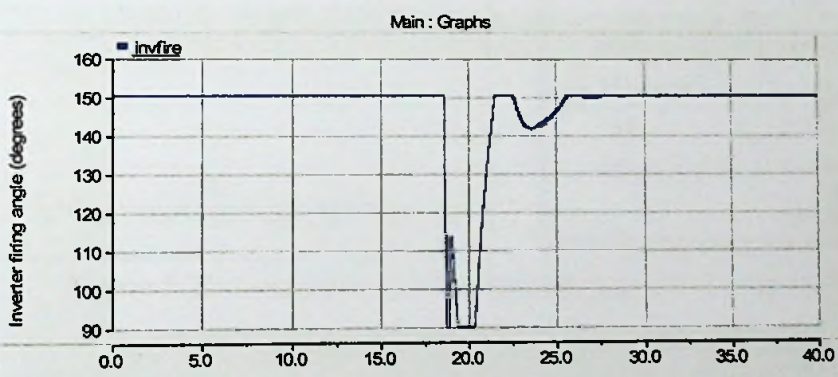


Figure 5.18: inverter firing angle at 1- phase one cycle fault

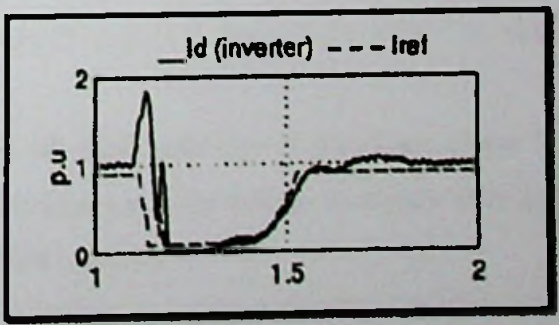
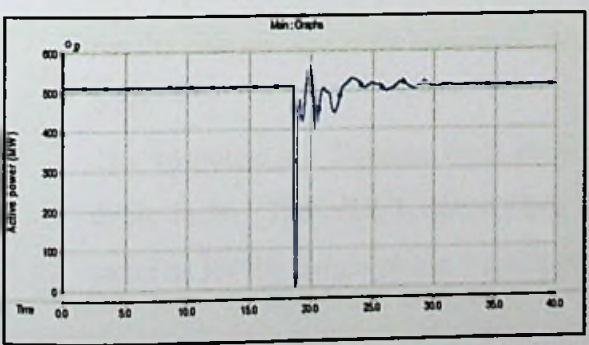


Figure 5.19: Comparison of DC power at 1- phase five cycle fault

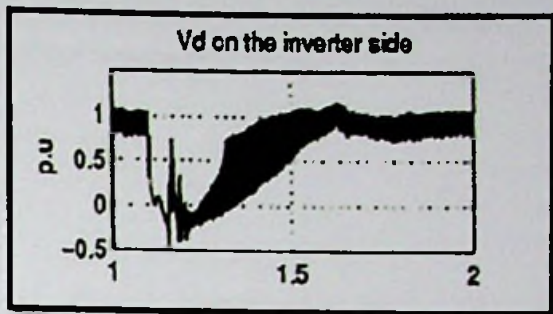
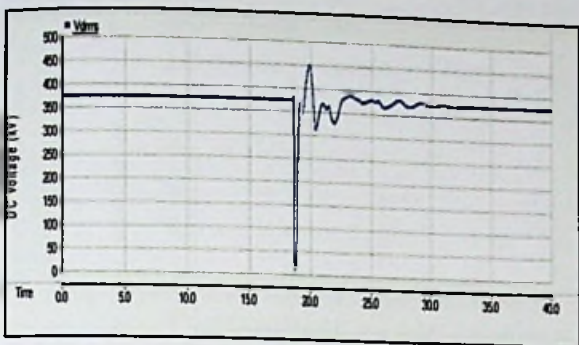


Figure 5.20: Comparison of DC voltage at 1- phase five cycle fault

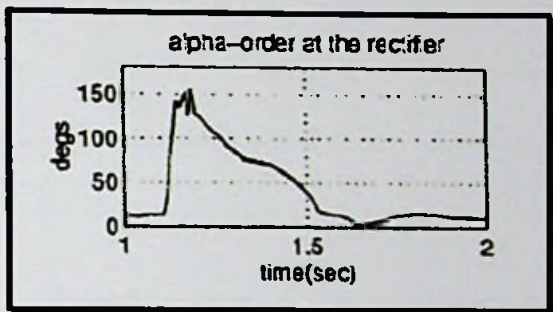
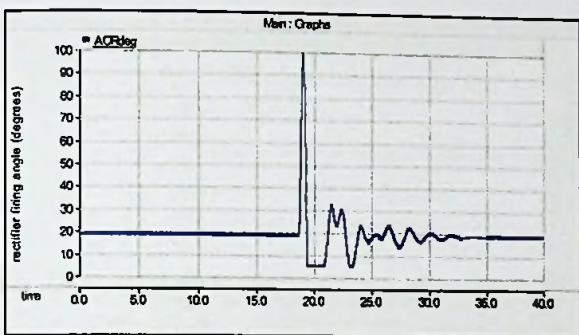


Figure 5.21: Comparison of rectifier firing angle- 1-phase five cycle fault

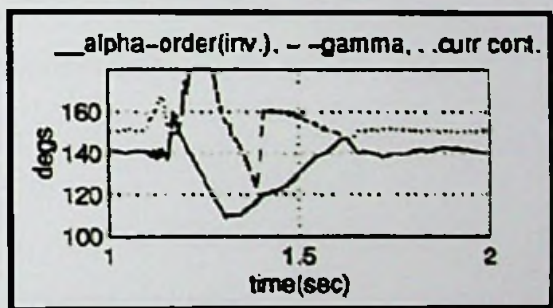


Figure 5.22: Comparison of inverter firing angle at 1- phase one cycle fault

### 5.2.1.3. Inverter side 3- phase fault

At the inverter bus bar, it created a 3- phase 5 cycle fault at 15 S and observed same above parameter behaviors. Figures 5.23, 5.24, 5.25 and 5.26 illustrate them. The results comparison with reference graphs are illustrated in figure 5.27, 5.28, 5.29 and 5.30.

The response for 3-phase fault shows the identical behavior of the single phase 5 cycle fault. The VDCL controlling unit brings back the system to steady state as same as for the single phase 5 cycle post fault behavior.

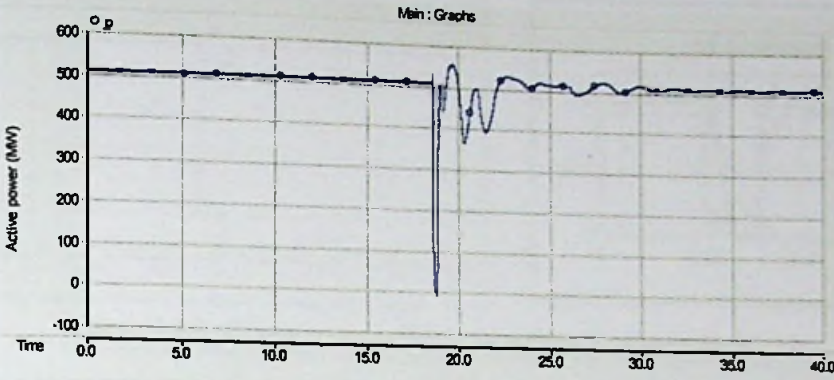


Figure 5.23: DC power at 3- phase fault

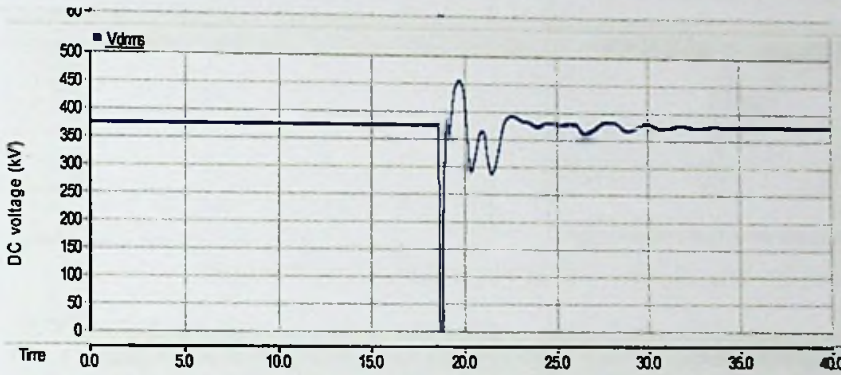


Figure 5.24: DC voltage at 3- phase fault

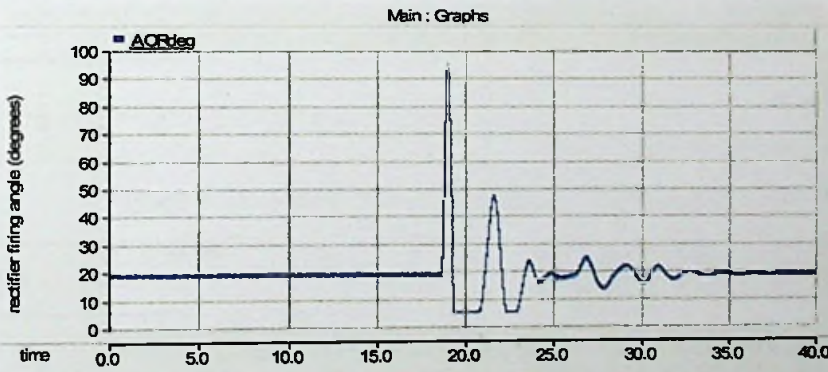


Figure 5.25: rectifier firing angle at 3- phase fault



Fig 5.26: inverter firing angle at 3- phase fault

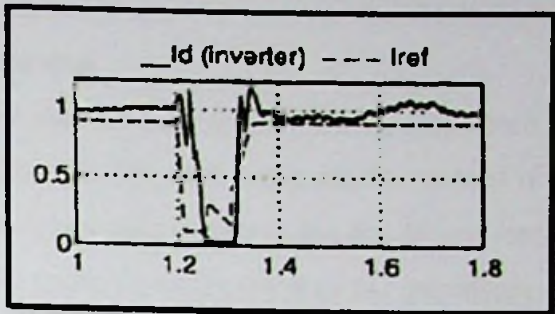
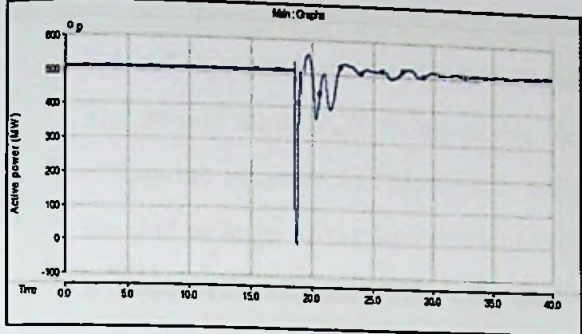


Figure 5.27: Comparison of DC power at 3- phase fault

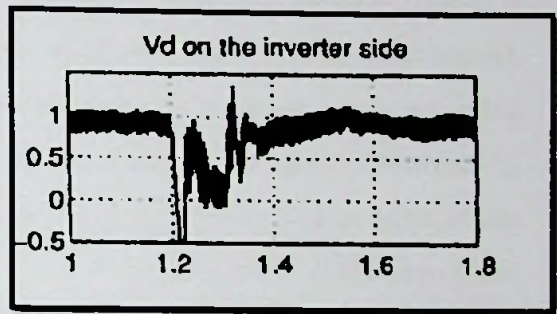
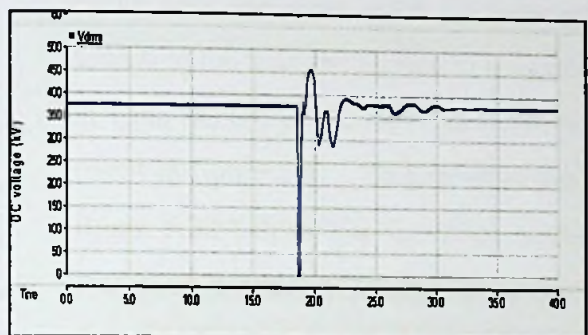


Figure 5.28: Comparison of DC voltage at 3- phase fault

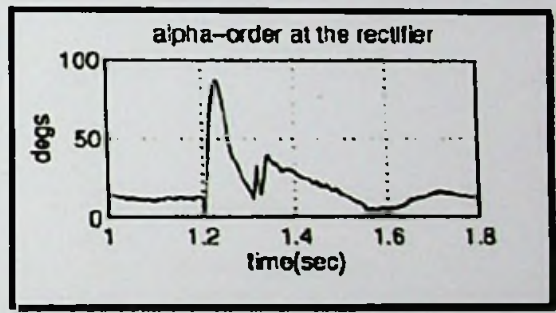
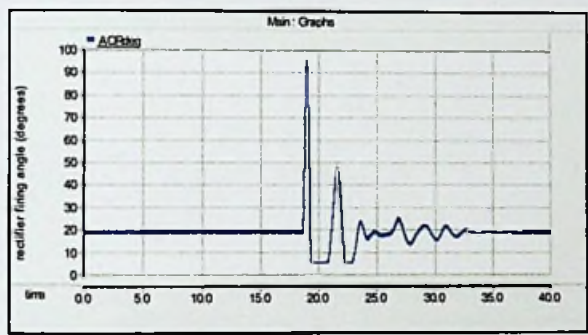


Figure 5.29: Comparison of rectifier firing angle at 3- phase fault

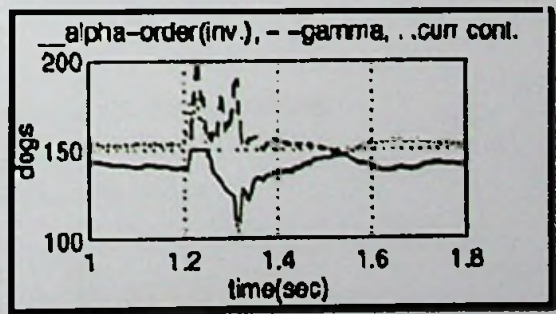


Fig 5.30: Comparison of inverter firing angle at 3- phase fault

#### 5.4. AC system impedance increment condition

The steady state SCR value of the inverter side Sri Lankan network is high which makes the inverter AC network a strong network. The SCR value can be reduced if the AC voltage of the inverter bus-bar is constant only by increasing the AC system impedance increment. Following simulation result shows the result of AC impedance reduction of the strong Sri Lankan network. This resulted in decrement of MPC curve with the new MAP. The operation throughout is at DC currents having a lower- value than the current corresponding to MAP [48]. For the same rated current at 1 pu, the DC power delivers is lower than the rated 1 pu as shown in the simulated result in figure 5.31. This result is verified by the reference [48] graph illustrated in figure 5.32 below. For the same current order, it gives a lower power value at the increased impedance condition. In figure 5.32, the operating point drops from point A in MAP-1 to point B in MAP-2 due to impedance increment [48]. As can be seen the DC power delivery is reduced for the same current order value.

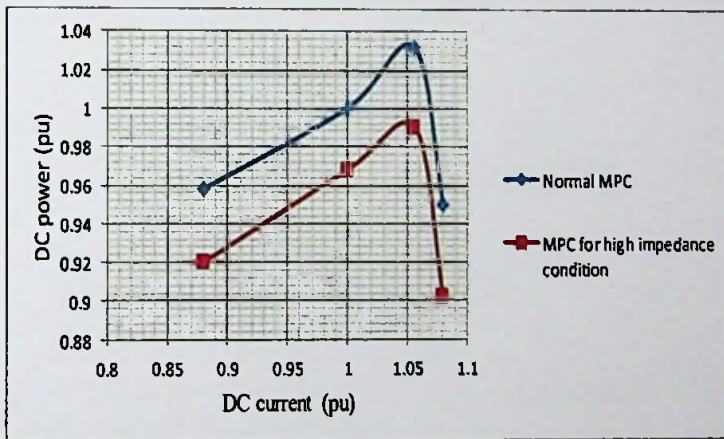


Fig 5.31: MPC for normal state and high impedance state conditions

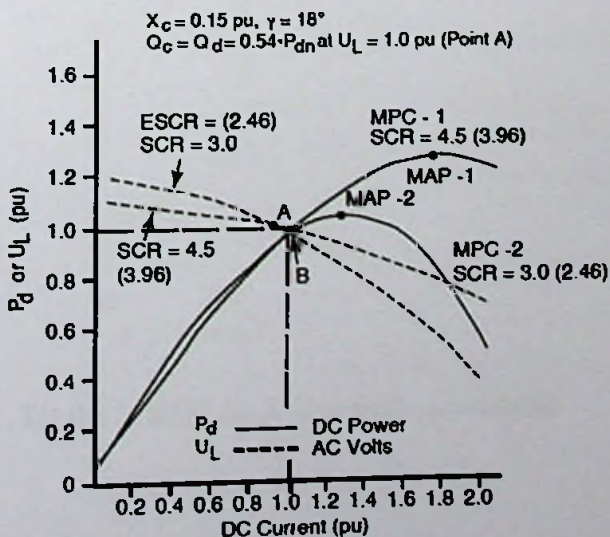


Fig 5.32: Reference graphs for normal state and high impedance state conditions

### 5.3.1. Derived MPC curve accuracy verification

It is necessary to verify the MPC curves accuracy obtained by the results of the simulation on PSCAD. For that, it is used here the 900 MW coal power plants tripping scenario. Under that scenario, the SCR value was calculated and drew the MPC curve using simulation results. Then it was compared with the reference [48] curves for MPC and SCR relationship shown in figure 5.34. The similarity between the curve derived and the reference curve for particular SCR values are more pronounced in the comparison. As the impedance increases, the SCR/ESCR reduces. The effect on MPC curve is shown in figure 5.35 [49] to verify the result. As the SCR/ESCR reduces MPA reduces.

$$SCR = \frac{V^2}{Z \times P_d}$$

$$SCR = \frac{220^2}{30 \times 500}$$

$$SCR = 2.717$$

$$ESCR = \frac{V^2}{(Z + Z_c) \times P_d}$$

$$ESCR = \frac{220^2}{58.38 \times 500}$$

$$ESCR = 1.66$$

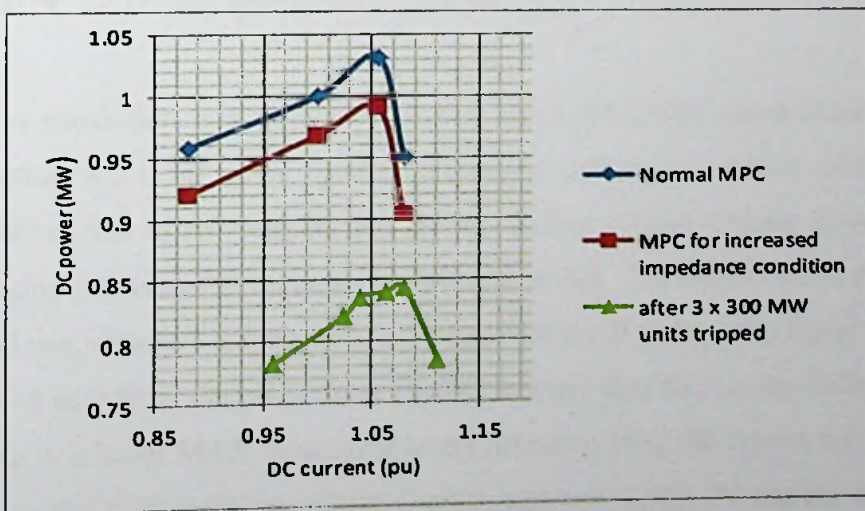


Fig 5.33: MPC for 3 coal units unavailable

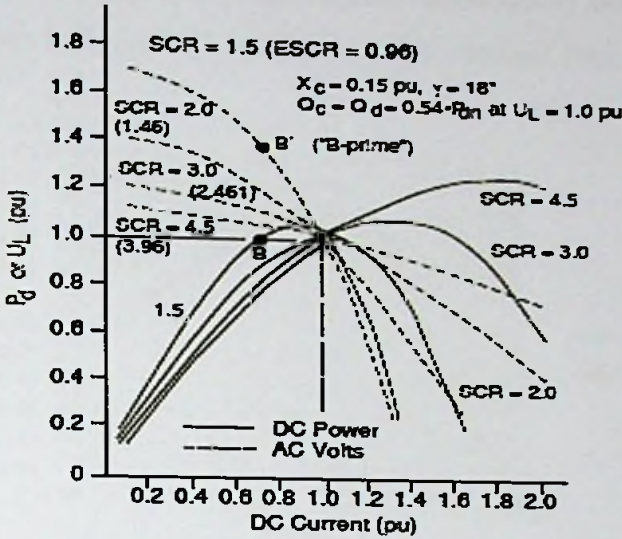


Fig 5.34: MPC comparison with high SCR/ESCR –graph 1

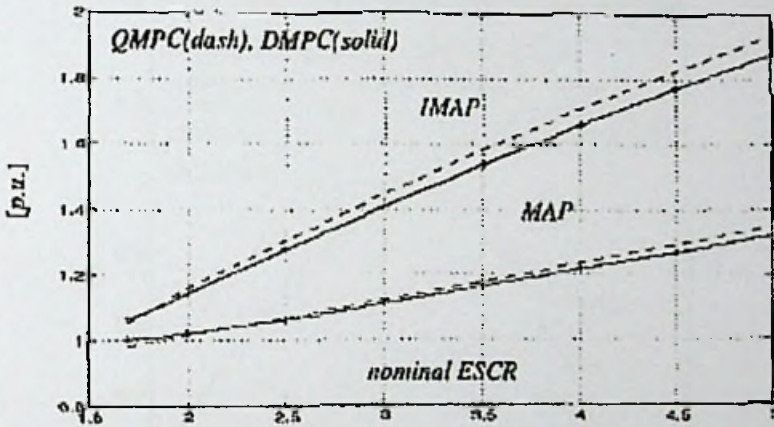


Fig 5.35: MPA comparison with high SCR/ESCR –graph 2

### 5.5. QMPC Vs DMPC for the inverter side

From the simulation, it is derived the QMPC curve and DMPC curve as mentioned in the section 4.2.1 for same system parameter values. To derive QMPC curve generator exciter effect disabled and the AC busbar voltage to keep in constant by rearranging generators in thevenin models in PSCAD. The DMPC curve derived for nominal one, slow DC current order ramping. The result is shown in figure 5.36.

As can be seen from the result, slow DMPC is lower than the corresponding QMPC, resulting in a lower MAP. According to the reference [49], the reason for that is due to the synchronous machine voltage control response to the DC current order ramp

such that the thevenin AC bus voltage is maintained ideally constant. The reference [49] graph shown in figure 5.37 verifies the result obtained from the simulation.

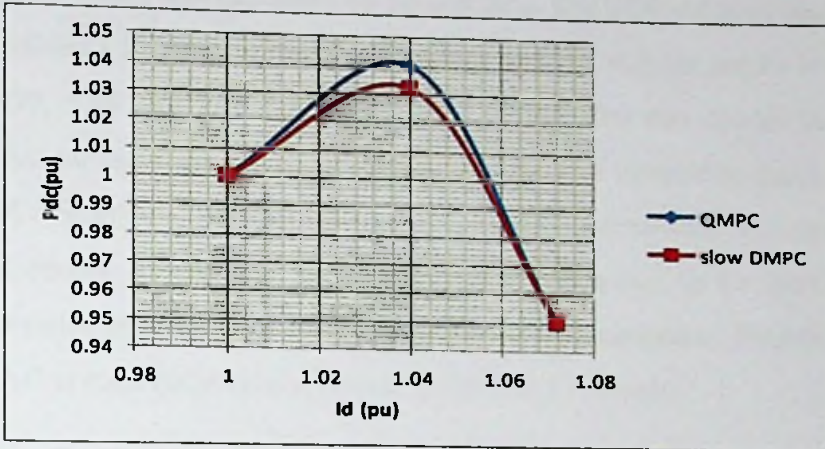


Fig 5.36: QMPC and Slow DMPC graphs plot

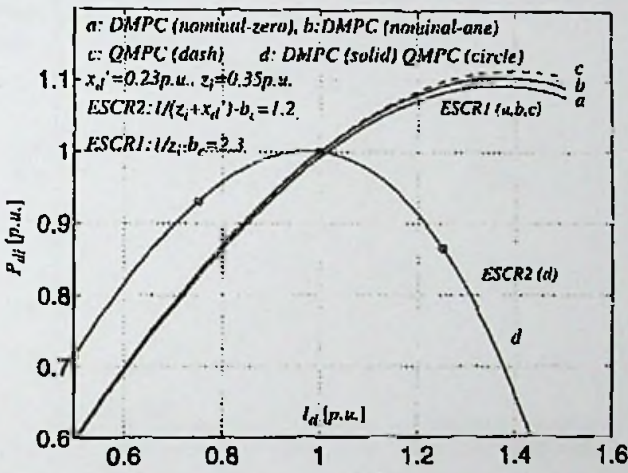


Fig 5.37: QMPC and Slow DMPC reference graphs

### 5.3.2. Perturbed scenario results analysis

Following are the perturbed scenarios which were simulated to examine the AC-DC interaction at inverter side.

1. Power order increment by 10%
2. LVPS 300 MW tripped
3. Sudden load rejection in AC network
4. Sudden DC load rejection
5. Transmission line tripped
6. Exciter effect on the interaction



1. Power order increment by 10%

When DC power delivers 500 MW at 400 kV DC voltage and AC bus bar voltage at 220 kV, power order was increased by 10% at 20 s. The SCR value of the network is 5.1. The resulting DC power curve, DC voltage and AC voltage graphs are shown in figures 5.39, 5.40 and 5.41 for the transient period after the current increment is applied. As can be seen while DC power output was increasing during transient period, DC voltage and inverter terminal AC voltage has reduced. The current order increment causes for inverter reactive power consumption to be increased. This causes for reduction in AC network reactive power consumption. Therefore inverter terminal AC voltage reduces as shown in the simulation result.

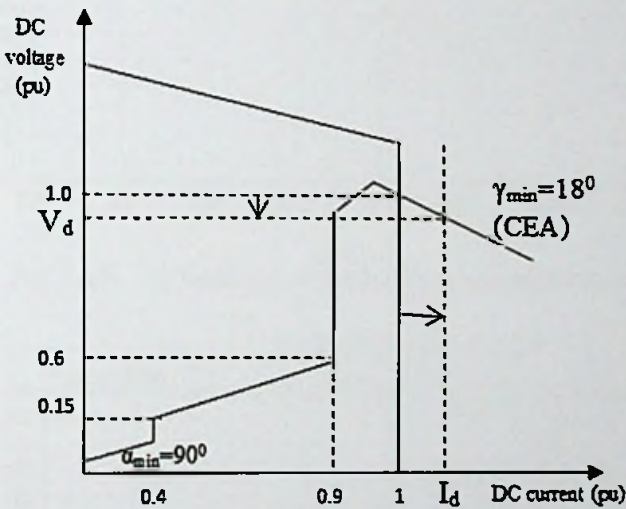


Fig 5.38: Clarification for power order increment by characteristic curve

According to the following DC voltage equation, the DC voltage reduction as the current order increases can be explained. In this equation except current order all other parameters are constant. As current order increases the DC voltage reduces as shown. It is more comprehensive by the figure 5.38 control graph of the network. The reference [48] verifies the result by their own graphs shown in figure 5.42 during the period of 0.04 s – 0.1 s.

$$U_{di} = G_i (U_i \cos \gamma_i - R_{ci} I_d)$$

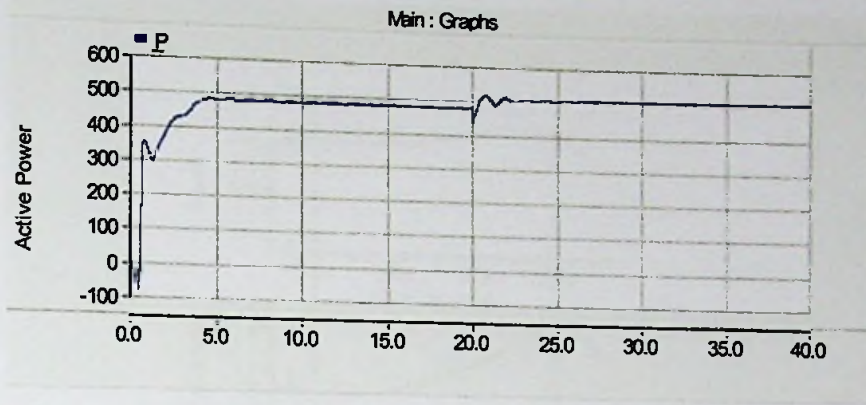


Fig 5.39: DC power curve for power order increment

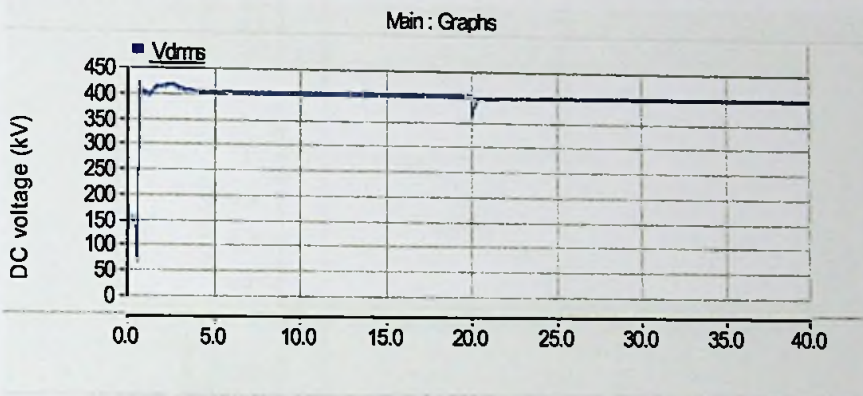


Fig 5.40: DC voltage curve for power order increment

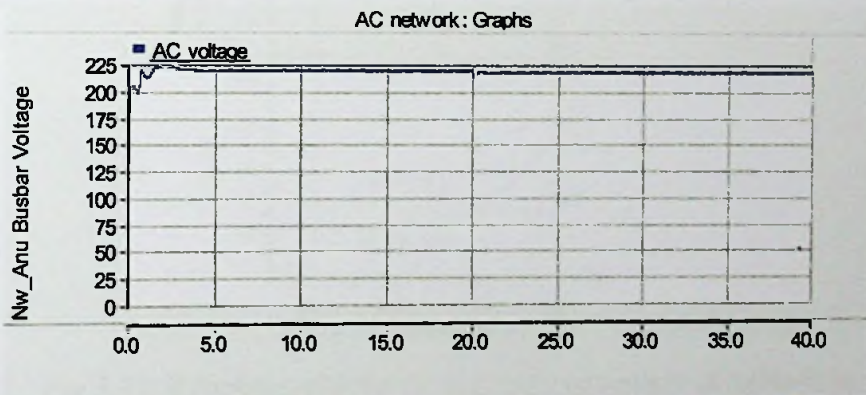


Fig 5.41: DC power curve for power order increment

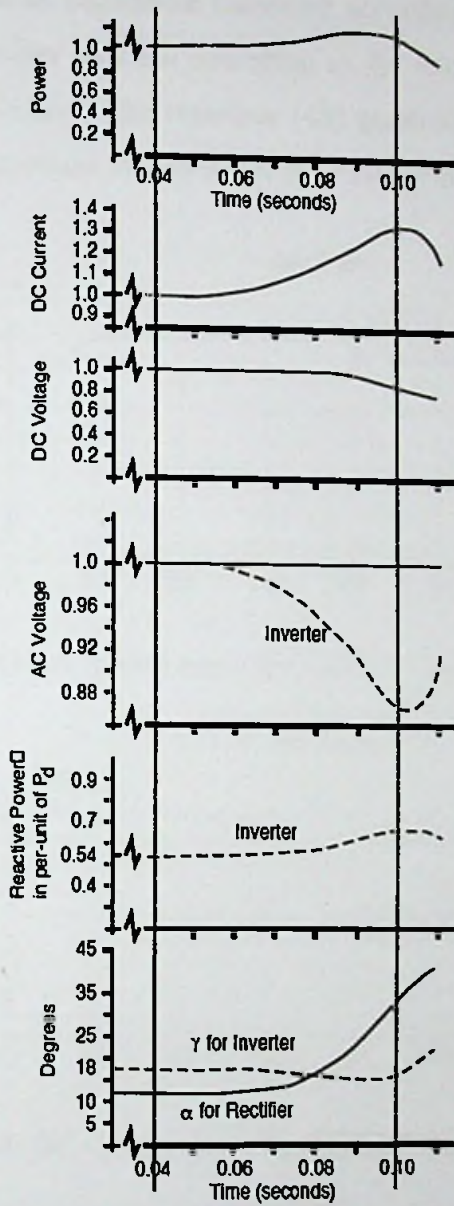


Fig 5.42: Reference plot for power order increment at 0.04s-0.1s

## 2. LVPS 300 MW tripped

At 20 s, tripping of 300 MW unit of coal power plant was applied. The results of interaction for transient period after the fault is applied are shown in the figure 5.43, 5.44 and 5.45. As can be seen, DC power, DC voltage and inverter AC terminal voltage reduced once the unit is tripped. After one generator is tripped, the system

impedance increased. This resulted in AC terminal voltage to be decreased. The SCR value also reduced as impedance increased according to the equation. DC power delivers to the inverter terminal according to the unchanged current order and the new reduced MPC curve. The reference [48] graph in figure 5.32 would verify the result of sudden increment of impedance for a steady state high SCR system.

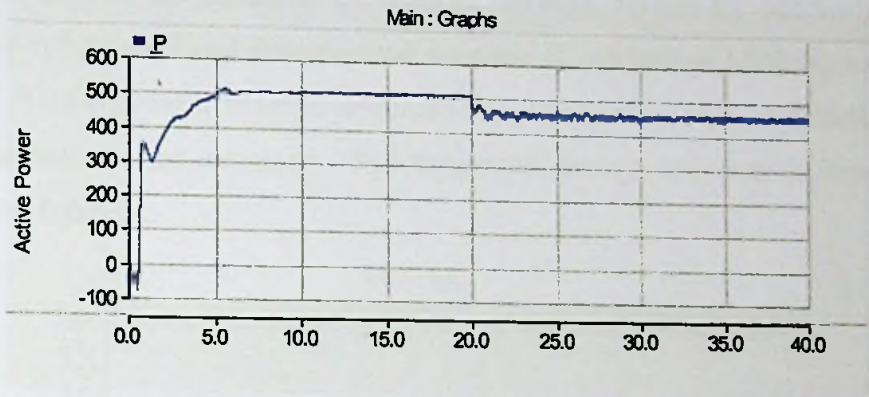


Fig 5.43: DC power curve for 300 MW unit tripped condition

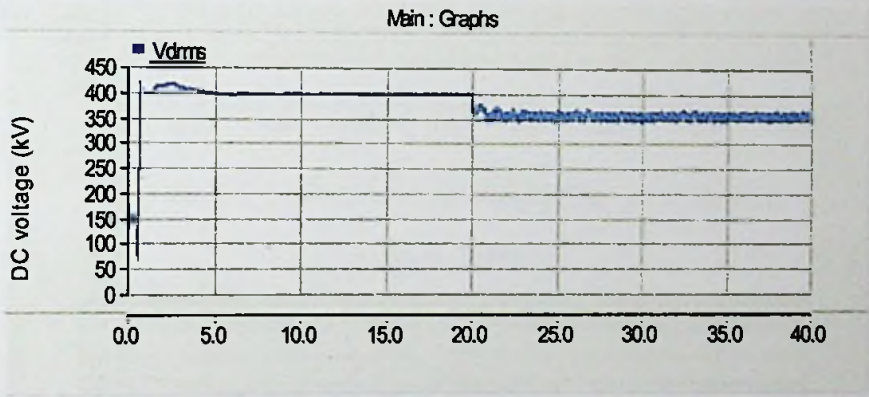


Fig 5.44: DC voltage curve for 300 MW unit tripped condition

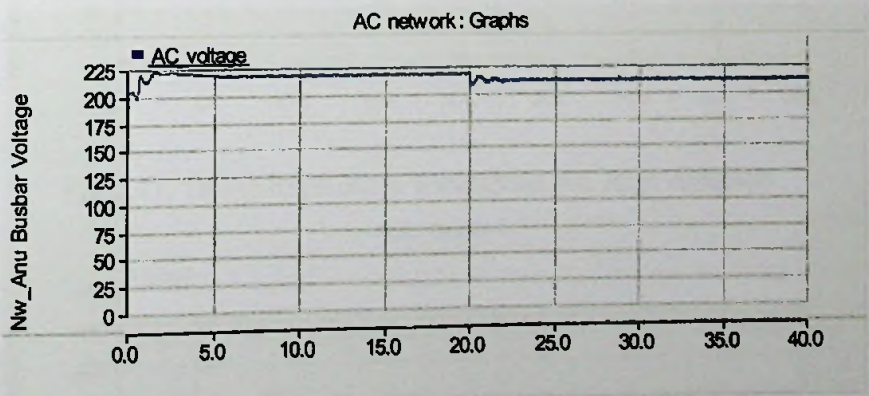


Fig 5.45: AC voltage curve for 300 MW unit tripped condition

#### 4. Sudden load rejection in AC network

At Veyangoda grid 115.2 MW load tripping was applied at 20 s. simulation results are shown in figure 5.46, 5.47 and 5.48. According to the simulation results, DC voltage, DC power and AC voltage has increased. Sudden load rejection at Veyangoda grid in the modeled Sri Lankan network results for sudden system impedance reduction. Load disconnected scenario is resulted in MPC curve to be increased. This effected in inverter terminal voltage to be increased considerably and DC power output to be increased. This behaves in the opposite way to impedance incremental behavior.

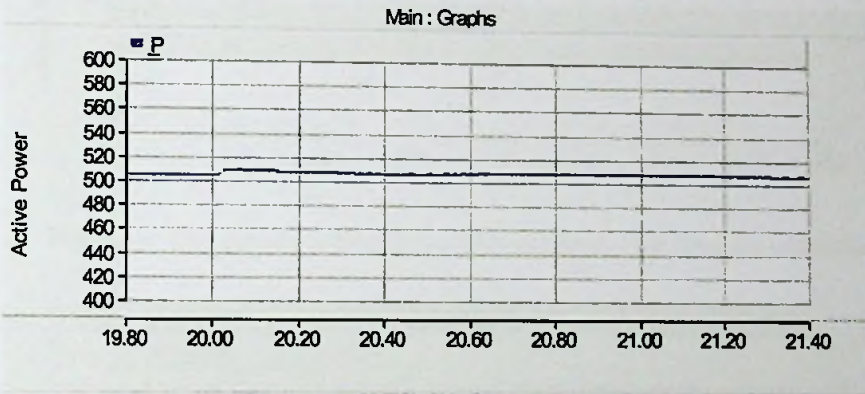


Fig 5.46: DC power curve for sudden AC load rejection

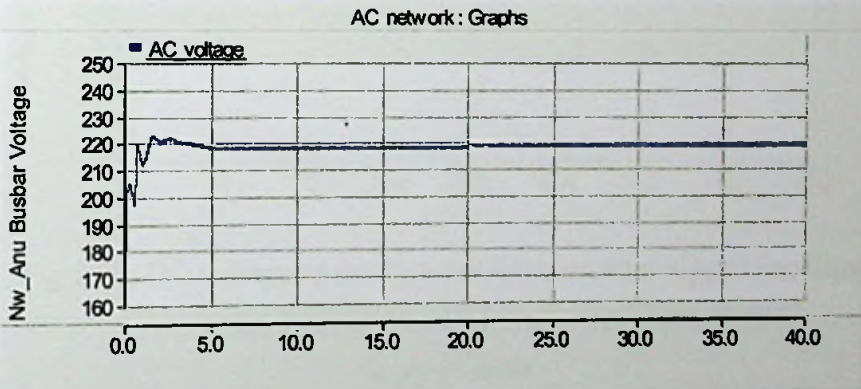


Fig 5.47: DC voltage curve for sudden AC load rejection

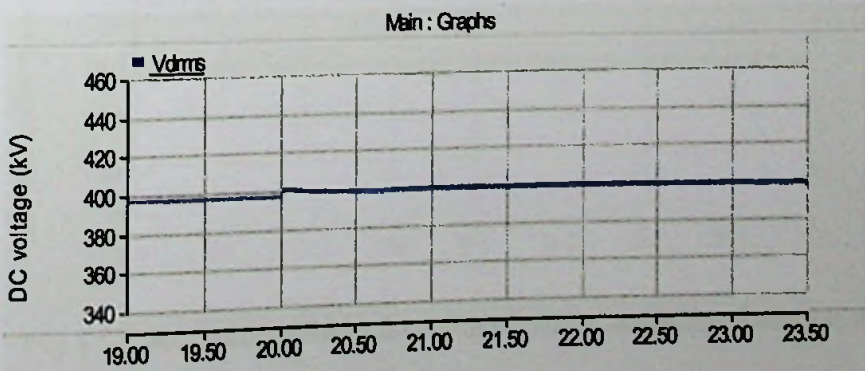


Fig 5.48: AC voltage curve for sudden AC load rejection

## 5. Transmission line tripped

New Anuradhaura-New Habarana transmission line trip was applied at 20 s. Simulated and obtained results are shown in figure 5.49, 5.50 and 5.51. As can be seen that DC power, DC voltage and AC voltage at the inverter terminal bus bar has increased. The result explanation is same as for the load rejection in AC network.

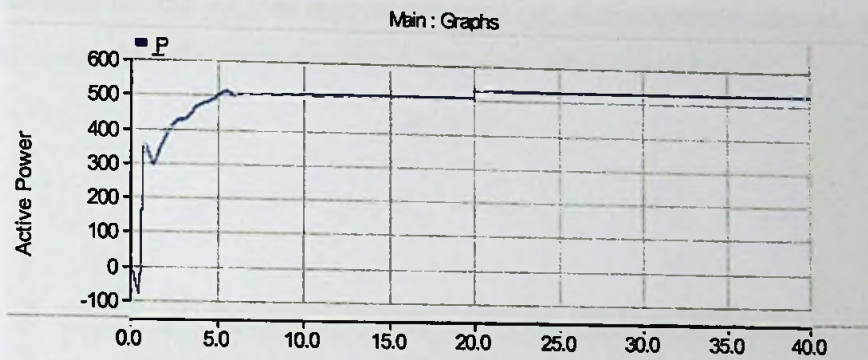


Fig 5.49: DC power curve for a transmission line tripped condition

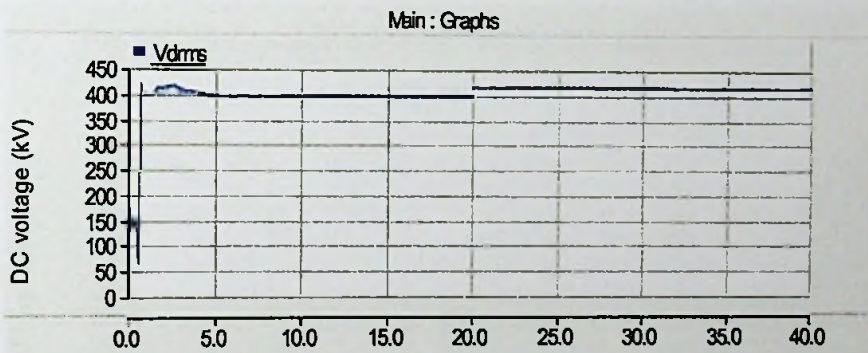


Fig 5.50: DC voltage curve for a transmission line tripped condition

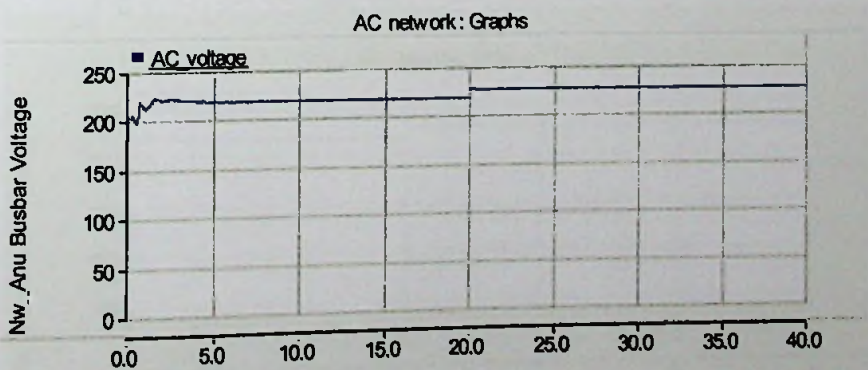


Fig 5.51: AC voltage curve for a transmission line tripped condition

## 6. Sudden DC load rejection

During the normal operation steady state condition, the 500 MW DC link tripped at 20 s and checked for the AC voltage and DC power responses in time domain. DC power becomes zero while AC bus voltage increases. The reason is that filters and the shunt capacitor were connected to the AC bus bar without disconnecting after the fault. The converter reactive power requirement reduces as DC active power becomes zero. The whole reactive power generated by the filters and the shunt capacitor caused for the AC voltage increment [21]. Consequently, the AC bus-bar voltage increased as DC power delivery to AC network reduced to zero.

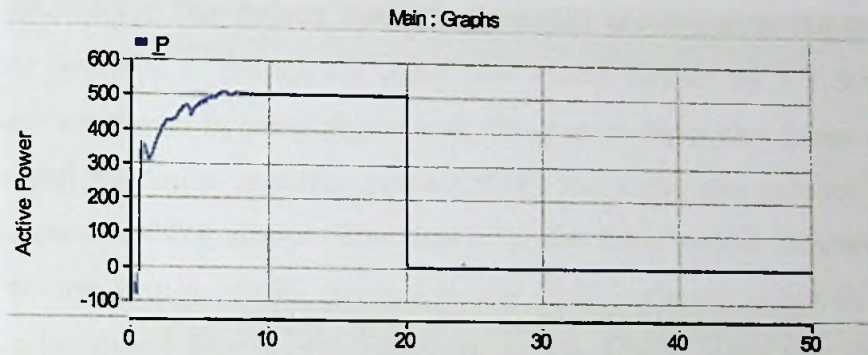


Fig 5.52: DC power curve for sudden DC load rejection

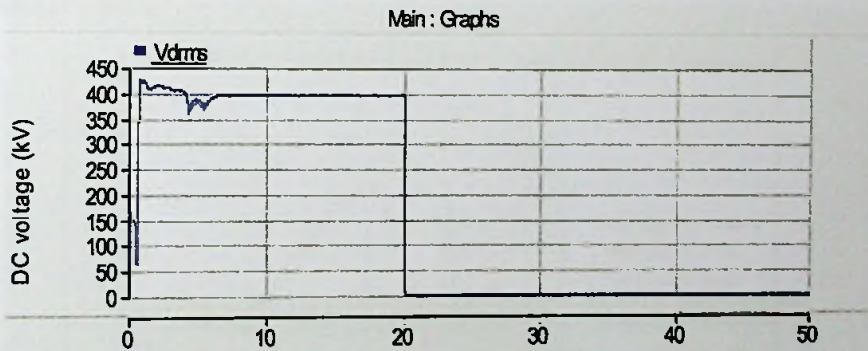


Fig 5.53: DC voltage curve for sudden DC load rejection

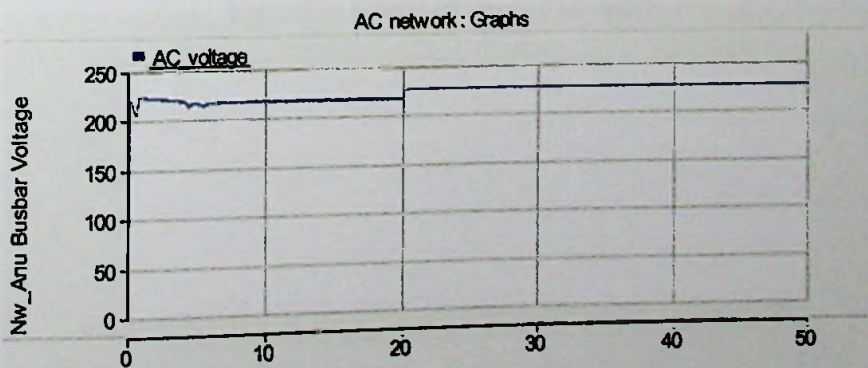


Fig 5.54: AC voltage curve for sudden DC load rejection

## 2. Exciter effect on the interaction

The Exciter effect was gained as fast exciter and slow exciter. To obtain the fast or slow effect, the voltage regulator gain and time constant were changed. The values were extracted from reference [49]. The responses of the exciter effect on MPC were analyzed.

- Exciter effect on DMPC

Fast to slower exciter parameters were used as [100, 0.15s], [100, 0.25 s] and [400, 0.25 s] respectively. The derived dynamic maximum power curves (DMPC) for steady state condition of the system under each exciter system for 3 x 300 MW power plants are shown in below figure 5.55. The results depict that fastest exciter has the largest maximum available power (MAP) and value gets reduced as the exciter system is getting slower. The reason is that faster exciter maintains the thevenin AC bus voltage ideally constant so that DMPC relevant to fast exciter is higher than the slower exciter [49]. Faster the exciter, DMPC curve gets closer to QMPC curve. The result is verified by the reference [49] explanation on fast/slow exciter effect on MPC.

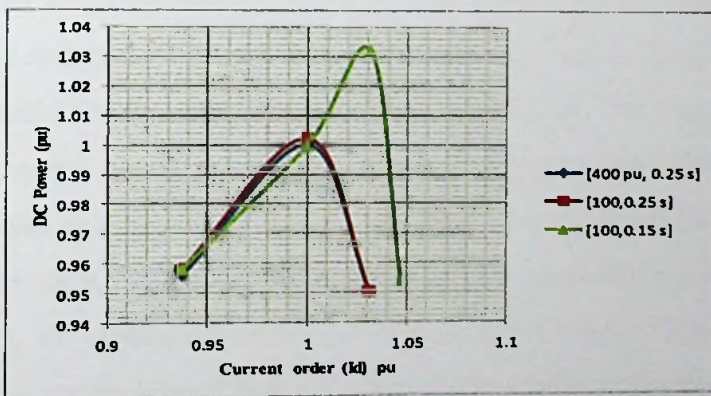


Fig 5.55: Effect of exciter on MPC



## Chapter 6

---

### Discussion

Objective of this thesis is to perform a stability analysis for the inverter side AC-DC interaction of the proposed India-Sri Lanka HVDC interconnection. To cater the objective, it was modeled the HVDC-HVAC detailed model on PSCAD/EMTDC software platform. The network was modeled for transient stability analysis. The definition of transient stability is applicable for HVDC-HVAC interaction as well. Therefore, the governor action for the AC generator was not included in to the detailed Sri Lankan network. As a consequence the inertial effect on the AC-DC interaction could not be studied in this thesis, which does effects on the strength of the HVAC system. Since line commutation converters require relatively strong AC voltage in order to commute, AC system strength is the major factor which needs more consideration for Current Source Converter transmission (CSC). Other than inertial effect, AC system impedance also affects the AC system strength. This thesis only focused upon the impact from AC system impedance on the AC-DC interaction.

This thesis used the basic control system for the rectifier and inverter transmission co-ordination. As per the objective of performing an asymptotic stability study for the proposed interconnection, this work did not add supplementary to the control system of HVDC transmission.

Modeling rectifier side Indian network as a thevenin's equivalent source is an issue that needs to consider. Before calculating thevenin's impedance components, some assumptions had to make due to less number of reference guides for the thevenin's equivalent source modeling.

There are research work which have done the stability studies of the AC-DC interaction. Reference [27] modeled AC network with generators in thevenin's equivalent sources behind its transient impedances and performed MPC analysis only in QMPC mode. This thesis has performed the DMPC analysis which provides the higher accuracy for the MPC analysis. Reference [52] modeled the network on a different platform and investigated the impact on AC network stability by HVDC transmission using different tools except the tools used in this thesis. Both this thesis work and reference [53] modeled the AC-DC model on PSCAD/EMTDC platform. Reference [53] has modeled a smaller power system than this thesis model and less comprehensive it is. It provides the time domain results for AC network internal faults simulations without further analysis. This thesis provides a wide analysis on each fault condition in terms of time domain analysis, maximum power curve and short circuit ratio tools.

According to the assumption of this thesis, at steady state operation, rectifier firing angle operates at  $20^{\circ}$  and inverter extinction angle is at  $18^{\circ}$  and Sri Lanka receives 500 MW at 400kV voltage from India. Steady state parameters for the simulation model were calculated based upon this assumption and modeled on PSCAD platform. However, in the modeled network, the rectifier operates at  $22^{\circ}$  and inverter at  $20^{\circ}$  (after the tuning for 400 kV ) and DC power delivers to Sri Lankan network at 500 MW under 400 kV DC voltage. The characteristic curve illustrated in this thesis assumed that inverter is operating on the Constant Extinction angle curve (CEA curve). However, according to the actual simulation result, there is a shift of inverter constant gamma operating curve downwards from the CEA curve. Therefore, the system does not operate exactly on the characteristic curve and there is a small shift from the assumption made in the thesis.

For quasi steady state condition, the maximum available power curve (MPC) illustrated in this thesis is lower than the actual power limit due to the change in the inverter gamma angle from the lower angle to a larger value. According to the definition of the MPC, the inverter must be operating at constant extinction angle mode which is the minimum gamma angle mode. It provides the maximum power that inverter can obtain by Maximum available power (MAP). If the converter operates in a larger angle than the minimum gamma angle in steady state, it provides reduced maximum power than the actual MAP. This is an issue that needs to be raised in this thesis results.



# Chapter 7

---

## Conclusion

This thesis main objective was to investigate the transient stability of the HVDC-HVAC interaction at Sri Lankan side of the proposed India-Sri Lanka interconnection. For that purpose, first it was modeled the proposed interconnection on PSCAD/EMTDC software platform. Then the results were analyzed quantitatively and qualitatively using three tools; Short circuit ratio, Maximum power curve and time domain analysis. The results were analyzed, verified and discussed with the aid of the references.

### 7.1. Main contribution of the thesis

The main contributions of the thesis are listed below.

- India-Sri Lanka HVDC interconnection was modeled in between detailed Sri Lankan network and thevenin equivalent Indian network on PSCAD/EMTDC software platform.
- All the system parameters were selected and calculated such that comply with the real world actual system condition.
- The accuracy of the modeled system was simulated and verified with the references.

- HVDC-HVAC interaction stability was analyzed and discussed the obtained results using the reference findings and mainly with the IEEE standards guide-reference [48].

## 7.2. Conclusions

The conclusions of the thesis can be summarized as below.

- From the maturity point of view or reliability point of view or converter losses point of view, the optimum converter technology that is suitable to model the proposed interconnection is CSC technology, although there are several operational drawbacks exist if it is not provided any supplementary control actions to eliminate those drawbacks.
- From the given algebraic and differential equations the HVDC-HVAC network could be modeled. The model accuracy was verified by the steady state time domain simulations. 500 MW DC power under rated 400 kV DC voltage was delivered from Indian power network to Sri Lankan power network. The steady state operating point rectifier firing angle was 20 degrees while the inverter extinction angle was 18 degrees.
- The inverter side AC terminal voltage has a huge impact on the AC-DC interaction. From the time domain simulations for inverter side AC faults it was emphasized. When the AC voltage single phase voltage was dropped that caused for commutation failures of the converters. This is one drawback of the CSC technology as it thoroughly depends upon the terminal voltage stiffness.
- This system was modeled with the basic DC control system without adding any supplementary control systems to stabilize the system under perturbed conditions. Therefore it can be said that; this modeled AC-DC interaction is asymptotic stable as it regain the pre-fault operating state after the fault is cleared as shown in inverter side AC faults time domain simulations.
- From the MPC curve and SCR value point of view, Sri Lankan network is a strong network in terms of the HVDC interconnection system strength

evaluation. Although Sri Lanka is an island the 220 kV and 132 kV power network is a strong network which has the strength to handle HVDC interconnection without losing the stability.

- However, there is a significant impact on the stability of the HVDC-HVAC interaction by the 300 MW coal power plants according to the simulation and calculation results.
- As the system impedance increases because of an AC system fault, AC busbar voltage drops and the DC power delivery reduces which impact on the power balance of the country.
- Therefore, it is necessary to take precaution actions to reduce the system impedance or keep stiff the inverter AC busbar voltage so that it does not affect the DC voltage and hence DC power delivery to AC system.
- If a fault causes for AC network impedance to be reduced, then that does not impact severely on DC power delivery. But the AC and DC busbar voltages increment due to impedance reduction can affect the insulations so that it is necessary to provide the necessary actions to keep the AC/DC voltages under the safety margins.
- All 3x 300 MW coal plants tripping affect to the DC power delivery such that, it reduces the DC power delivery by the characteristic control system. However, it does not cause to drop DC power delivery to zero. Therefore, it provides the security to the AC system although all 3 coal plants are not available.
- The exciter speed directly effects on the stability of HVAC-HVDC interaction as shown by the results because, the speed of the exciter effects on the AC busbar voltage stability. Faster the exciter, the DC power delivery capability increases as shown by the MPC and MPA derivations.
- The simulation results are more accurate by the DMPC derivations other than QMPC derivations because, the DMPC derivation allows AC voltage to be vary accordingly.

### 7.3. Future work

The system modeled in this thesis has a potential to simulated and analyze more perturbed conditions other than the ones done in this thesis. So that, it can analyze the stability behavior of HVDC-HVAC interaction under those perturbed conditions as well. From those results it can predict more thoroughly the behavior of the HVDC-HVAC interaction of the proposed interconnection. Other than that based on the findings of this thesis, the following topics are recommended for further research.

- The impact of exciters on the HVDC-HVAC stability needs to be studied thoroughly.
- Other than exciter, other generator parameters effect on the stability of HVDC-HVAC interaction are necessary to be studied thoroughly.
- The remedies those are necessary to take for pertaining stability of the interaction are necessary to simulate and analyze.
- QMPC for fast current order ramping is necessary to model and simulate. From that, it can analyze the automatic master control behavior impact on QMPC.

# References

- [1] S W A D N Wickramasinghe, "Tech. Prefeasibility for Developing a Transmission Syst Interconnection Between India & Sri Lanka," M.S thesis., Dept. Elect. Eng., Univ. of Moratuwa., 2006.
- [2] Asia Pacific Energy Research Centre, "Power Interconnection in the APEC Region", Asia Pacific Energy Research Centre, Institute of Energy Economics, Japan. ISBN: 4-931482-08-2, March 2000.
- [3] M. P. Bahrman, "HVDC Transmission Overview," Transmission and Distribution Conference and Exposition, Chicago, US, April 2008
- [4] "IEEE guide for planning DC links terminating at AC locations having low short circuit capacities", IEEE Std. 1204-1997, 26 June 1997
- [5] W. Long, S. Nilsson, "HVDC Transmission yesterday & Today," Power and Energy Magazine, IEEE, Volume:5, issue 2, March-April 2007
- [6] *ABB HVDC Reference Projects*, [online]. Available:  
<http://www04.abb.com/global/abbzh/abbzh251.nsf!OpenDatabase&db=/db/d b0003/db004333.nsf&v=9AAC910040&e=ge&m=100A&c=0853DA6A61867D0CC125750900328D6D>
- [7] WDAS Rodrigo et al, "Modeling and transient anal of HVDC bipolar link," Dep. Elect Eng, Univ Moratuwa, unpublished
- [8] A.J.M.I Jowsick. et al, "HVDC transmission line for interconnecting power grids in India and Sri Lanka," Dept. of Elect. & Electron. Eng., Univ. of Peradeniya, Peradeniya, Sri Lanka, Dec. 2009
- [9] M.P.Bahrman and B.K. Johnson, "The ABCs of HVDC Transmission technologies," Power and Energy Magazine, IEEE, Volume:5, issue 2, March-April 2007.
- [10] D. Melvold, IEEE DC and Flexible AC Transmission Subcommittee, "HVDC Projects listing," November 2006
- [11] A.G.R. Rendina et al, "The Italy-Greece HvdC Link," CIGRE, 21, rue d'Artois, F-75008 Paris, 2002



- [12] *List of HVDC projects* [online].  
Available:[https://en.wikipedia.org/wiki/List\\_of\\_HVDC\\_projects](https://en.wikipedia.org/wiki/List_of_HVDC_projects)
- [13] S. P. Teeuwesen, et al, "Dynamic Performance of the new 400 kV Storebaelt HVDC Project," Power systems conference and exposition, 2009, Seattle, WA, March 2009
- [14] FINGRID. (2009 February 08). "FENNO-SKAN HVDC Link" [online]:  
Available:<http://www.fingrid.fi/uploads/ConstructionSiteMap/attachments/esite.pdf>
- [15] FINGRID. "Evolving grid Fenno-Skan 2 HVDC link" [online]: Available:[http://www.fingrid.fi/en/news/News%20liitteet/Brochures/Trioton%20osoitteilla/fennoskan\\_esite\\_englanti\\_low.pdf](http://www.fingrid.fi/en/news/News%20liitteet/Brochures/Trioton%20osoitteilla/fennoskan_esite_englanti_low.pdf)
- [16] V.K. Sood, "HVDC and FACTS controllers," Boston, Kluwer Academic Publishers, 2004.
- [17] M.P. Bahrman, B.K. Johnson, "The ABCs of HVDC Transmission technologies," Power and Energy Magazine, IEEE, Volume: 5, issue 2, March-April 2007
- [18] N. Flourentzou, et al, "VSC-Based HVDC Power Transmission Systems: An Overview," Power Electronics, IEEE Transactions (volume: 24, issue: 3), February 2009.
- [19] "East Coast Transmission Network-Technical feasibility Stud," Crown Estate, Edinburgh, January 2008
- [20] Dr. L. Tang, "High Voltage DC technologies," ARPA-E Power Technology workshop, February 2010
- [21] S Rao, "EHV-AC & HVDC Transmission Eng & practice," 2nd ed. Delhi: Khanna Publisher, 1996.
- [22] P. Kundur, "Power System Stability and Control" McGraw Hill, Inc 1994
- [23] I. Norheim, "Suggested Methods for Preventing Core Saturation Instability in HVDC Transmission Systems," Norwegian University of Science and Technology, N-7491 Trondheim, Norway, February 2002
- [24] F. Yang et al, "An Approach to Select PI Parameters of HVDC Controllers," Power Engineering Society General Meeting, IEEE, Montreal, Que, 2006

- [25] D. Jovcic, "Control of high voltage DC and flexible AC transmission systems," M.Phil thesis, University of Auckland, New Zealand, December 1999
- [26] M.Szechtman, T.Wess, C.V.Thio, "1st Benchmark Model for HVDC control studies", CIGRE -WG 14.02., ELECTRA, No. 135, PP.54-73, April 1991
- [27] F.Wang and Y.Chen, "voltage /power stability study upon power system with multiple infeed configuration of HVDC links using quasi static modal analysis approach," M.S thesis, University of Technology, March 2006
- [28] X. Mao et al, " Selection of HVDC models for stability studies," Electric Utility Deregulation and Restructuring and Power Technologies, Nanjing, China, April 2008
- [29] A. L'Abbate, G. Fulli, "Modeling and Applicat of VSC-HVDC in the European transmission system", International Journal of Innovations in Energy Systems and Power ,Vol. 5 ,Issue 1, pp. 8-16, April 2010
- [30] H.L. Tayal et al, "Viability of Developing a Transmission System Interconnection between India and Sri Lanka," February 2002
- [31] D.Jovcic et al, "Analytical modeling of HVDC –HVAC systems," Power Delivery, IEEE Transactions ,volume:14, issue:2, April 1999
- [32] S. Jauria, "DC Power and Current Control Modes and Features", ABB power system, Technical Report, 1JNL100032-591 Rev-02.1999.
- [33] M. Anup, "Capacitor commutated converters for HVDC transmission system", M.S thesis, Concordia University, Montreal, Canada ,February 2002
- [34] M.A Laughton and M.G Say, "Electrical Engineer's reference book," London, Butterworth International Edition, 1990
- [35] N.G.Hingorani and M. F Burbery, "Simulation of AC System Impedance in HVDC System Studies," IEEE transnstonal on power apparatus and systems, volume, pas-89, No, 5/6, May/June 1970
- [36] O.S.D.De Silva et al, "Study on impact of wind power park integration on weak power systems: A case stud on Mannar wind park in Sri Lanka," Inform and Automation for sustainability, 7<sup>th</sup> international conference, December 2014

- [37] Applications of PSCAD® / EMTDCTM, Manitoba HVDC Research Centre Inc
- [38] K.U. Rao, "Comput techniques and models in power systems," New Delhi, I.K International Publishing House Pvt. Ltd, 2007
- [39] R.H. Miller, J. H. Malinowski, "Power system operation," 2008.
- [40] K.R Padiyar, "Power system dynamics," Hyderabad, BS publication, 2008
- [41] E. W. Kimbark Direct current transmission, Volume 1,
- [42] S Kamakshaiah; V Kamaraju, "HVDC transmission," New Delhi, Tata McGraw Hill Education (Pvt) Ltd, 2011.
- [43] "Tech. Specification of ACSR Conductor for Transmission Line" Gujarat Energy Transmission co-corporation Ltd, July 2008
- [44] Basslink Proposed interconnector linking the Tasmanian and Victorian electricity grids- Final Panel Report, Basslink Joint Advisory Panel, June 2002
- [45] CIGRE benchmark model –PSCAD/EMTDC
- [46] D. R. Northcott, S. Filizadeh, A. R. Chevretils, "Design of a Bidirectional Buck-Boost DC/DC Converter for a Series Hybrid Electric Vehicle Using PSCAD/EMTDC," 978-1-4244-2601-0/09/2009 IEEE
- [47] L. Zhang, "Modeling and Control of VSC-HVDC Links Connected to Weak AC Systems," Royal institute of technology, Stockholm 2010
- [48] "IEEE guide for planning DC links terminating at AC locations having low short circuit capacities", IEEE Std. 1204-1997, 26 June 1997
- [49] D. L. H. Aik, G. Anderson, "Impact of dynamic system modeling on the power stability of HVDC systems," IEEE Transactions on power delivery, Vol. 14, No. 4, October 1999
- [50] D.L.H. Aik, G. Anderson. "Influence of load characteristics on the power/voltage stability of HVDC systems, Part I: Basic equations and relationships", IEEE Transactions on power delivery, Vol. 13, No. 4, October 1998
- [51] D. L. H. Aik and G. Anderson, "Voltage and power stability of HVDC- Emerging issues and new analytical methodologies," Curitiba, Brazil, May 2000

[52] J. Paulinder, "Operation and control of HVDC links embedded in AC systems," Dept Elect Power Eng, Chalmers Univ of Technology, Göteborg, Sweden, 2003

[53] Z. Shuai et al, " Simulation studies of JeJu AC power system modeling by using PSCAD/EMTDC", IEEE T&D Asia, Seoul, 2009

